USGS
science for a changing world

Geochronologic, Isotopic, and Geochemical Data from Pre-Cretaceous Plutonic Rocks in the Lane Mountain Area, San Bernardino County, California

Open-File Report 2021–1094

U.S. Department of the Interior
U.S. Geological Survey

Cover. Photograph of Late Jurassic diorite outcrops in the Lane Mountain area, San Bernardino County, California. Locality of geochronology sample 17-LM-1749 for which a uranium-lead zircon age of 150.8 ± 2.3 mega-annum was obtained. U.S. Geological Survey photograph by Paul Stone.

Geochronologic, Isotopic, and Geochemical Data from Pre-Cretaceous Plutonic Rocks in the Lane Mountain Area, San Bernardino County, California

By Paul Stone, Howard J. Brown, M. Robinson Cecil, Robert J. Fleck, Jorge A. Vazquez, and John A. Fitzpatrick

Open-File Report 2021–1094

U.S. Department of the Interior
U.S. Geological Survey

U.S. Geological Survey, Reston, Virginia: 2021

For more information on the USGS—the Federal source for science about the Earth, its natural and living resources, natural hazards, and the environment—visit https://www.usgs.gov or call 1–888–ASK–USGS (1–888–275–8747).

For an overview of USGS information products, including maps, imagery, and publications, visit https://store.usgs.gov.

Suggested citation:
Stone, P., Brown, H.J., Cecil, M.R., Fleck, R.J., Vazquez, J.A., and Fitzpatrick, J.A., 2021, Geochronologic, isotopic, and geochemical data from pre-Cretaceous plutonic rocks in the Lane Mountain area, San Bernardino County, California: U.S. Geological Survey Open-File Report 2021–1094, 74 p., https://doi.org/10.3133/ofr20211094.

ISSN 2331-1258 (online)

Contents

Figures

Tables

Conversion Factors

International System of Units to U.S. customary units

Multiply	By	To obtain
	Length	
centimeter (cm)	0.3937	inch (in.)
millimeter (mm)	0.03937	inch (in.)
meter (m)	3.281	foot (ft)
kilometer (km)	0.6214	mile (mi)
kilometer (km)	0.5400	mile, nautical (nmi)
meter (m)	1.094	yard (yd)

Datum

Horizontal coordinate information is referenced to the North American Datum of 1927 (NAD27).

Abbreviations

ASI	aluminum saturation index
ICP-AES-MS	inductively coupled plasma atomic emission spectroscopy-mass spectrometry
Ma	mega-annum (a unit of time equivalent to one million years)
MALI	modified alkali-lime index
ppm	part per million
REE	rare-earth element
SHRIMP-RG	sensitive high-resolution ion microprobe-reverse geometry
Sr_i	initial $^{87}Sr/^{86}Sr$ ratio
TAS	total alkali-silica
TE	trace element
WDXRF	wavelength dispersive x-ray fluorescence

Chemical Symbols

Ag	Silver
Al	Aluminum
As	Arsenic
B	Boron
Ba	Barium
Be	Beryllium
Bi	Bismuth
Ca	Calcium
Cd	Cadmium
Ce	Cerium
Co	Cobalt
Cr	Chromium
Cs	Cesium
Cu	Copper
Dy	Dysprosium
Er	Erbium
Eu	Europium
Fe	Iron
Ga	Gallium
Gd	Gadolinium
Ge	Germanium
Hf	Hafnium
Ho	Holmium
In	Indium
K	Potassium
La	Lanthanum
Li	Lithium
Lu	Lutetium
Mg	Magnesium
Mn	Manganese
Mo	Molybdenum
Nb	Niobium
Nd	Neodymium
Ni	Nickel
O	Oxygen
P	Phosphorus
Pb	Lead
Pr	Praseodymium
Rb	Rubidium
S	Sulfur
Sb	Antimony
Sc	Scandium
Se	Selenium
Si	Silicon
Sm	Samarium
Sn	Tin
Sr	Strontium
Ta	Tantalum
Tb	Terbium
Te	Tellurium
Th	Thorium
Ti	Titanium
Tl	Thallium
Tm	Thulium
U	Uranium
V	Vanadium
W	Tungsten
Y	Yttrium
Yb	Ytterbium
Zn	Zinc
Zr	Zirconium

Geochronologic, Isotopic, and Geochemical Data from Pre-Cretaceous Plutonic Rocks in the Lane Mountain Area, San Bernardino County, California

By Paul Stone,[1] Howard J. Brown,[2] M. Robinson Cecil,[3] Robert J. Fleck,[1] Jorge A. Vazquez,[1] and John A. Fitzpatrick[1]

Abstract

Pre-Cretaceous, predominantly dioritic plutonic rocks in the Lane Mountain area, California, intrude metasedimentary and metavolcanic rocks considered part of the El Paso terrane. New geochronologic (uranium-lead zircon), geochemical, and isotopic data provide a reliable basis for dividing these pre-Cretaceous plutonic rocks into two mappable suites of Permian–Triassic and Late Jurassic ages. The 26 Permian–Triassic samples included in this report have a mean age of ~248 mega-annum (Ma), range in composition from monzodiorite to quartz monzonite and granodiorite, and have a mean initial $^{87}Sr/^{86}Sr$ ratio (Sr_i) of ~0.7045. The 22 Late Jurassic samples have a mean age of ~149 Ma, range in composition from gabbro to granite, and have a mean Sr_i of ~0.7055. Accurate mapping of these two plutonic suites and their detailed field relations with the associated metamorphic rocks is essential for resolving the geologic history and regional tectonic significance of the Lane Mountain area.

The sub-0.706 Sr_i values of both plutonic suites at Lane Mountain are consistent with previous suggestions that the El Paso terrane is allochthonous and did not develop on Precambrian continental lithosphere. Both suites are considered parts of northwest-trending magmatic arcs interpreted to have formed above east-dipping subduction zones along the evolving North American continental margin, and both arcs are interpreted to cross a major east-west-trending boundary between the El Paso terrane and rocks considered part of ancestral North America in the San Bernardino Mountains area to the south. The El Paso terrane thus appears to have been attached to the San Bernardino Mountains area at least since Permian–Triassic time, although the boundary probably has been modified by Cenozoic faulting.

Introduction

The Lane Mountain area is in the north-central Mojave Desert region about 20 kilometers (km) northeast of Barstow, California (fig. 1). In this geologically complex region, metasedimentary and metavolcanic rocks of offshore (eugeoclinal) lithologic character (McCulloh, 1952, 1960; Miller and Sutter, 1982; Carr and others, 1997) are associated with a variety of plutonic rocks, some of which are characterized by initial $^{87}Sr/^{86}Sr$ (Sr_i)[4] values <0.706 and other isotopic signatures that indicate little or no Precambrian continental (sialic) lithosphere in their magmatic source areas (Kistler, 1990; Miller and others, 1995). The eugeoclinal metasedimentary and metavolcanic rocks of this region comprise the El Paso terrane of Silberling and others (1987, 1992) (fig. 1), which some have interpreted as allochthonous because of its apparent juxtaposition against Paleozoic and early Mesozoic continental-shelf deposits to the east and south (Burchfiel and Davis, 1981; Miller and others, 1995). The associated low-Sr_i plutonic rocks form a narrow, northwest-trending belt that is surrounded by plutonic rocks with Sr_i>0.706 and is bisected and offset by the late Cenozoic, left-lateral Garlock Fault (Kistler and Ross, 1990) (fig. 2). The tectonic significance of the El Paso terrane and the associated low-Sr_i plutonic belt has not been firmly established.

To provide data for addressing this gap in understanding, we are conducting a multifaceted investigation of the Lane Mountain area that includes detailed geologic mapping, U-Pb zircon geochronology, Rb-Sr isotopic analysis, and geochemical analysis. Preliminary results of this investigation, focused primarily on the geologic mapping, have been presented elsewhere (Brown, 2016a, b; Brown and others, 2016, 2018). More recently, Stone and others (2019) presented geochronologic, isotopic, and geochemical data from 10 samples of igneous rocks analyzed in support of geologic mapping activities from 2014 to 2016. Here, we expand this database with new data from 44 additional samples of pre-Cretaceous plutonic rocks analyzed from 2017 to 2019. The expanded database provides information critical for distinguishing and mapping lithologically similar intrusive rock suites of Permian–Triassic and Late Jurassic ages across the Lane Mountain area.

[1]U.S. Geological Survey.

[2]Apple Valley, California.

[3]California State University Northridge.

[4]Chemical element symbols used in this paper are listed in the preface (p. viii).

Geographic Setting

The report area includes parts of the Lane Mountain, Williams Well, Paradise Range, and Coyote Lake 7.5-minute-quadrangles, which together comprise the area formerly covered by the Lane Mountain 15-minute quadrangle. The area encompasses bedrock uplands that extend northward and southeastward from Lane Mountain (fig. 3), including the northern part of the Calico Mountains. These uplands drain eastward and northward into a broad, alluvial valley that includes Coyote Dry Lake, which is about 15 km east of Lane Mountain. Access to the area is provided by Fort Irwin Road and a network of unpaved roads shown on the topographic quadrangle maps.

Previous Investigations and General Geologic Framework

The geology of the Lane Mountain 15-minute quadrangle was mapped by McCulloh (1952, 1960), who distinguished numerous units of pre-Tertiary metamorphic and plutonic rocks and of Tertiary volcanic and sedimentary rocks. Later analytical work added geochronologic, isotopic, and geochemical data that refined the framework of both the pre-Tertiary and Tertiary rocks (Burke and others, 1982; Miller and Sutter, 1982; Miller and Glazner, 1995; Miller and others, 1995; Singleton and Gans, 2008). A modified version of the map of McCulloh (1960) was published by Dibblee (2008).

A simplified version of McCulloh's (1960) map, together with updated age information from Brown and others (2018), Stone and others (2019), and presented herein, is shown in figure 3. Four major lithologic assemblages are shown: (1) metamorphosed and deformed sedimentary and volcanic rocks of Paleozoic and Mesozoic age; (2) mostly mafic to intermediate-composition plutonic rocks of Late Permian to Late Jurassic age; (3) felsic plutonic rocks of Late Cretaceous age; and (4) Tertiary volcanic and sedimentary rocks, including the Jackhammer and Pickhandle Formations of McCulloh (1952, 1960), that unconformably overlie the older rocks. Although the metamorphic suite, as a whole, is intruded by both the Cretaceous and the pre-Cretaceous plutonic rocks, detrital zircon data show that the maximum depositional ages of some metasedimentary rocks postdate the oldest rocks in the pre-Cretaceous plutonic assemblage (Brown and others, 2018; Stone and others, 2019). This relation complicates the geologic framework and indicates an intertwined history of sedimentation, magmatism, metamorphism, and deformation.

Purpose and Scope

The primary purpose of this study was to determine SHRIMP–RG (sensitive high-resolution ion microprobe–reverse geometry) U-Pb zircon crystallization ages for selected intrusive rock units in the Lane Mountain area. Stone and others (2019) established the existence of three major intrusive suites of Permian–Triassic, Late Jurassic, and Late Cretaceous ages in the Lane Mountain area. Subsequent mapping indicated the need for additional analytical data to confidently distinguish between the lithologically similar Permian–Triassic and Late Jurassic plutonic suites throughout the study area. To address this need, we report new SHRIMP-RG U-Pb zircon ages for 44 additional samples of pre-Cretaceous plutonic rocks from localities that extend across the study area (fig. 3; table 1). In addition, whole-rock geochemical analyses are presented for all 44 samples and whole-rock Rb-Sr isotopic data for 13 of those. Combined with data from the four samples analyzed by Stone and others (2019), these data provide information critical for mapping and interpreting the pre-Cretaceous intrusive rocks of the Lane Mountain area.

Most of the samples included in this report are from the informally named Larrea complex of McCulloh (1960). Two samples are from other informal units designated by McCulloh (1960): Daisy granodiorite (sample 14-LM-1) and pink biotite granite (sample 17-LM-1385). Several additional samples are from relatively small outcrop areas of plutonic rocks close to contacts with metasedimentary rocks and not shown by McCulloh (1960). We consider these outcrops to be unmapped parts of the Larrea complex.

Stone and others (2019) showed that the Larrea complex includes rocks of both Permian–Triassic and Late Jurassic ages, and that the Daisy granodiorite is Late Jurassic. The pink biotite granite unit, which had not been previously dated, is shown herein to be Late Jurassic as well.

Methods

U-Pb zircon analyses were carried out on the U.S. Geological Survey (USGS) SHRIMP–RG ion microprobe at Stanford University. Zircon crystals were separated from ~1–2 kilogram samples using standard processing techniques. Individual zircons from mineral separates were mounted in epoxy, polished, and coated with gold prior to analysis. Cathodoluminescence (CL) images were used to select relatively homogeneous spots within zoned zircons. Most zircons were analyzed at a single spot near the crystal rim. Analytical conditions for the SHRIMP–RG analyses were ~4–6 nano-ampere primary beam of negatively charged O_2 ions. Secondary ions were measured by peak hopping using a single electron multiplier collector. The mass spectrometer was tuned to a mass resolution of ~6,000, sufficient to resolve any significant interferences. Intensities of secondary ion peaks of Zr_2O^+, $^{204}Pb^+$, background, $^{206,207,208}Pb^+$, $^{238}U^+$, $^{232}Th^+$, and $^{238}U^{16}O^+$ were collected in five scans and corrected for collector deadtime. U/Pb ratios were calibrated to Temora-2 zircon using an age of 418.4 megaannum (Ma) (Mattinson, 2010) and employing the U/Pb–UO/U calibration typical for ion microprobe U-Pb geochronology (Williams, 1998). Uranium and thorium concentrations were calibrated to MAD-559 zircon (Coble and others, 2018). Analytical data reduction used the software programs Squid 2 version 2.51 and

Isoplot version 3.76 (Ludwig, 2009, 2012), which determined the weighted mean crystallization age of coherent groups of zircon spot analyses for each sample.

Because this study was designed to produce SHRIMP-RG data for many samples across the study area and distinguish between two age classes only, 10 zircons or fewer were analyzed for many samples and no trace element data were obtained in order to minimize the time and expense of analysis. Some samples were analyzed more than once, using additional zircons, to check the results of the initial SHRIMP-RG runs.

Whole-rock geochemical analyses were performed under contract to the U.S. Geological Survey using wavelength-dispersive X-ray fluorescence (WDXRF) and inductively coupled plasma atomic emission spectroscopy (ICP-AES). Graphic displays of the geochemical data were created in Microsoft Excel. All chemical symbols used in this report are explained in the preface (p. viii).

Determinations of Sr_i involved three steps. First, for each powdered, whole-rock sample, the isotopic ratio of $^{87}Sr/^{86}Sr$ was measured on a Finnigan MAT 261 solid source mass spectrometer at the USGS in Menlo Park, California, with methods consistent with those reported by Bayless and others (2004). That ratio and the Rb and Sr concentrations determined by ICP-AES geochemical analysis (see results section) were then used to calculate the $^{87}Rb/^{86}Sr$ isotopic ratio. Finally, both isotopic ratios and the U-Pb zircon age of the sample were used to calculate the Sr_i. This calculation used the ^{87}Rb decay constant 1.3971×10^{-11} following Rotenberg and others (2012). Based on the analytical methods involved, including the ICP-AES analyses of the rubidium and strontium concentrations, the uncertainty in the Sr_i values reported here is estimated to range from ~0.00002 to 0.0007, becoming greater with increasing Rb/Sr.

Analytical Results

Geochronology

Of the 44 plutonic rock samples analyzed on the SHRIMP-RG for this study, 25 yielded Late Permian to Middle Triassic ages and 19 yielded Late Jurassic ages (time scale of Gradstein and others, 2020). Including the four samples previously analyzed by Stone and others (2019), 26 Permian–Triassic and 22 Jurassic samples have been identified (tables 2–49, fig. 4). The Permian–Triassic sample ages range from ~258 to 237 Ma, averaging ~248±6 Ma; the Jurassic sample ages range from ~154 to 145 Ma, averaging ~149±4 Ma. The Jurassic suite includes sample 17-LM-1385 from the pink biotite granite unit of McCulloh (1960), which yielded an age of 150.8±1.8 Ma.

In all, 330 spots on 322 zircon crystals were analyzed from the Permian–Triassic samples, of which 48 spots were statistically rejected from the age determinations; 189 spots on 183 zircons were analyzed from the Jurassic samples, of which 21 spots were statistically rejected. A histogram of the 450 statistically acceptable spot ages illustrates the age distinction between the Permian–Triassic and the Jurassic suites (fig. 5).

Spots younger than the mean sample ages are interpreted as evidence of lead loss from the zircon crystals, as in Permian–Triassic sample 18-LM-2595 (table 37) and Jurassic sample 14-LM-490 (table 9). Rejected spots older than the mean sample age are interpreted to reflect inheritance from older rocks. Clear examples of inheritance are a Mesoproterozoic (~1104 Ma) zircon in Jurassic sample 14-LM-106 (table 5) and a Triassic (~234 Ma) zircon in Jurassic sample 15-LM-806 (table 11). Overall, however, little evidence of inheritance was found. Finally, a few spots were rejected because of large age errors caused by instrumentation problems during analysis, as in Permian–Triassic sample 19-LM-3063 (table 47).

The initial SHRIMP-RG runs of three samples (17-LM-2000, 18-LM-2595, 18-LM-2809) yielded dominantly Late Permian to Triassic ages for the individual zircon spots, but also a small number of Late Jurassic ages (tables 27, 37, 44). Subsequent SHRIMP-RG runs on these samples yielded a few additional Late Jurassic ages for zircons in samples 2000 and 2595, but none in sample 2809. The predominance of older ages points to the conclusion that these samples are part of the Permian–Triassic plutonic suite, with the younger ages representing Late Jurassic lead loss or recrystallization. The alternative interpretation would be that the samples are Jurassic, with the older ages representing large-scale inheritance. To further investigate this alternative, we performed additional SHRIMP-RG runs on several other samples from nearby localities that had yielded only Late Permian to Triassic zircon ages. None of these additional runs produced Jurassic zircon ages, effectively negating the possibility of a widespread and dominant population of inherited Late Permian to Triassic zircons in otherwise zircon-poor rocks of the Jurassic suite.

Of the 13 zircons in our sample set on which two different spots were analyzed, 11 were from samples 14-LM-43, 14-LM-154, and 14-LM-490 of Stone and others (2019). These spots (tables 4, 6, 9) did not indicate any systematic age differences that could be interpreted as evidence of multiple events, and there was no evidence of inherited zircon cores. One of the other two zircons on which two spots were analyzed was from Permian–Triassic sample 15-LM-802A (table 10); the second spot on this zircon was analyzed within a distinct overgrowth detected on the CL image. This spot yielded a substantially younger age (233±6 Ma) than the weighted mean age of the other five spots (248.4±3.6 Ma) and may represent a separate event that took place ~15 million years after initial crystallization of the zircon. The final zircon was from Permian–Triassic sample 18-LM-2809, on which three spots were analyzed. All three spots yielded similar Late Jurassic ages (table 44), demonstrating that this anomalous age applies to the entire crystal and not just the rim.

Zircon Uranium and Thorium Concentrations

Plots of uranium (U) and thorium (Th) concentrations in zircons analyzed on the SHRIMP-RG reveal differences between the Permian–Triassic and Jurassic suites (fig. 6). In zircons from

the Permian–Triassic suite, U concentrations (41–1,500 parts per million [ppm]) are somewhat higher than in most of the zircons from the Jurassic suite (29–913 ppm); Th concentrations also are generally higher in the Permian–Triassic suite (26–1,605 ppm) than in the Jurassic suite (15–481 ppm). Four zircon spots in the Jurassic suite, all from granite sample 17-LM-1385, have anomalously high concentrations of both U (2,687–3,676 ppm) and Th (1,407–3,318 ppm).

Th/U ratios in zircons from the Permian–Triassic suite range from 0.05 to 2.87; most (~68 percent) are between 0.5 and 1, but ~14 percent are less than 0.5 and ~18 percent are greater than 1. By contrast, Th/U ratios in zircons from the Jurassic suite are less variable, ranging from 0.16 to 1.19; most (~64 percent) are between 0.5 and 1, whereas ~34 percent are less than 0.5 and only 2 percent are greater than 1. The contrast in Th/U between the two suites is most pronounced above ~300 ppm U, where the Th concentrations in zircons from the Permian–Triassic suite are most variable (fig. 6). The Th/U ratios in our Jurassic suite are similar to those determined by Barth and others (2017) for late-Early to Middle Jurassic plutonic rocks in the Fort Irwin area 30 km northeast of Lane Mountain.

Whole-Rock Geochemistry

Tables 50–56 show whole-rock geochemical data for each dated sample included in this study, and table 57 shows normalized (volatile-free) WDXRF data. Note that one Jurassic sample (17-LM-2203) received two separate analyses, the results of which were averaged to produce a single set of values for use in the geochemical diagrams described herein.

Total alkali-silica (TAS) diagrams (Middlemost, 1994) provide a geochemical classification of the samples (fig. 7). Based on TAS, the Permian–Triassic suite includes monzodiorite, diorite, monzonite, quartz monzonite, and granodiorite. SiO_2 in the Permian–Triassic samples ranges from ~52.9 to 64.8 normalized weight percent and K_2O+Na_2O ranges from ~5.2 to 8.1 normalized weight percent. By contrast, the Jurassic suite has a broader compositional range that includes gabbro, gabbroic diorite, monzodiorite, diorite, monzonite, granodiorite, and granite. In the Jurassic samples, SiO_2 ranges from ~50.0 to 72.6 normalized weight percent and K_2O+Na_2O ranges from ~3.1 to 9.3 normalized weight percent. The Jurassic suite thus contains rocks that are either more mafic or more felsic than any in the Permian–Triassic suite, with the main compositional overlap between the two suites occurring in the diorite and monzodiorite fields of the TAS diagram. The Jurassic TAS diagram shows a gap between samples with ~61 and 68 percent SiO_2, suggesting that the suite could be bimodal. Additional sampling, however, would be necessary to confirm this suggestion.

Plots of the aluminum saturation index (ASI) show that the Permian–Triassic suite and most samples of the Jurassic suite are metaluminous, although the most siliceous Jurassic rocks are weakly peraluminous (fig. 8). The ASI plot of the Permian–Triassic samples shows less variation than that of the Jurassic suite. Plots of the modified alkali-lime index (MALI) show that both the Permian–Triassic and Jurassic suites are predominantly calc-alkalic (fig. 9). Most samples of both suites tend toward the calcic side of the calc-alkalic field and some plot within the calcic field, especially the least siliceous samples of the Jurassic suite (<54 percent SiO_2). One sample from each suite plots in the alkali-calcic field.

Harker diagrams (figs. 10, 11) show that increasing SiO_2 in both the Permian–Triassic and Jurassic suites correlates with decreasing TiO_2, MgO, Fe_2O_3, MnO, and CaO; Al_2O_3 is relatively constant. Overall, the Jurassic suite is less siliceous, more aluminous, and more calcic than the Permian–Triassic suite.

Harker diagrams for K_2O and Na_2O indicate a significant difference between the Permian–Triassic and Jurassic suites. The Jurassic plots show general increases in both K_2O and Na_2O with increasing SiO_2 (fig. 11). By contrast, the data points in each of the Permian–Triassic plots define an equidimensional pattern with a gap that divides the population into two parts. These gaps are between ~1.9 and 1.3 weight percent K_2O and between ~4.6 and 3.7 weight percent Na_2O (fig. 10). Most of the Permian–Triassic samples with relatively high K_2O also have relatively low Na_2O and vice-versa. This relation suggests that the samples have been affected by albitization, a form of sodium metasomatism that converts potassium feldspar to albite. A few of the Jurassic samples also show anomalously low K_2O (fig. 11). Widespread albitization of Jurassic plutons has been documented elsewhere in the Mojave Desert region, such as the Providence Mountains area 120 km east of Lane Mountain (Fox and Miller, 1990; Stone and others, 2017).

Most samples from both the Permian–Triassic and Jurassic suites plot in the volcanic-arc granites field on the Rb versus Y + Nb diagram of Pearce and others (1984) (fig. 12). A minor difference is that concentrations of Y + Nb exceed 30 ppm in all the Permian–Triassic samples but are less than 30 ppm in seven Jurassic samples. In addition, for both suites, the average Sr/Y ratio in samples with MgO between 2 and 4 normalized weight percent is ~20 (fig. 13), consistent with a crustal thickness of 20–30 km at the time of magmatic differentiation (Chapman and others, 2015; Chiaradia, 2015). Crustal thicknesses of this range are typical of modern continental slopes (Mooney and others, 1998). Both Sr/Y and MgO are more variable in the Jurassic suite than in the Permian–Triassic suite.

Spider plots of rare-earth elements (REE) and trace elements (TE) are similar between the Permian–Triassic and Jurassic suites (figs. 14, 15). The REE plots of both suites show a modest negative europium (Eu) anomaly, and the TE plots for both suites show negative anomalies for rubidium (Rb), niobium (Nb), phosphorus (P), zirconium (Zr), and titanium (Ti). Most elements on both plots are more variable in the Jurassic suite than in the Permian–Triassic suite.

Rb-Sr Isotopic Data

Based on isotopic analysis of four samples of pre-Cretaceous plutonic rocks in the Lane Mountain area, Stone and others (2019) showed that the Sr_i increased from ~0.704 in Late Permian-Early

Triassic sample 14-LM-43 (~253 Ma) to between 0.705 and 0.706 in Late Jurassic samples 14-LM-1, 14-LM-154, and 14-LM-490 (~151, 146, and 149 Ma, respectively). These results supported previous interpretations of very limited involvement of continental lithosphere in the generation of the Late Permian rocks and somewhat greater, although still limited, involvement of continental lithosphere in the generation of the Late Jurassic rocks (Miller and Glazner, 1995; Miller and others, 1995).

To further investigate this topic, we determined Sr_i for 13 additional samples of pre-Cretaceous plutonic rocks dated in this study, seven from the Permian–Triassic suite (for a total of eight) and six from the Jurassic suite (for a total of nine). The expanded dataset of 17 samples shows that Sr_i ranges from ~0.7037 to 0.7051 in the Permian–Triassic suite and from ~0.7047 to 0.7072 in the Jurassic suite (table 58; fig. 16). Despite the overlap, the mean Sr_i of samples from the Permian–Triassic suite (0.7045) is distinctly lower than that of samples from the Jurassic suite (0.7055). The expanded dataset thus remains consistent with the interpretation that the involvement of continental lithosphere in magma generation increased from Permian–Triassic to Late Jurassic time but remained limited. By contrast, four samples of Late Cretaceous (~72–85 Ma) plutonic rocks in the study area yielded Sr_i values of ~0.708–0.710 (fig. 16; Stone and others, 2019), indicating a substantial increase in continental lithospheric input to the magmatic source area by that time.

One Jurassic sample (17-LM-2191) from the southeast part of the map area (fig. 3) has anomalously high Sr_i compared to the other eight samples of the same age group, approaching the values of the Late Cretaceous rocks (table 58; fig. 16). The granitic rocks represented by this sample must have been derived from magma that had more input from continental lithosphere than other Jurassic rocks in the study area. Lithologically similar granite of presumed Jurassic age is widespread in the vicinity of sample 2191. Collection and analysis of more samples would be needed to test the importance of this isolated result.

Map Relations in the Lane Mountain Area

The geochronologic data presented here constrain the map extents of Permian–Triassic and Jurassic plutonic rocks in the Lane Mountain area (fig. 3). The Permian–Triassic suite is confined to the westernmost part of this area; all other outcrops of pre-Cretaceous plutonic rocks in the area represent the Jurassic suite. About 3 km north of Lane Mountain, the boundary between the two suites is between four Permian–Triassic localities (14-LM-16, 15-LM-802A, 15-LM-816, 19-LM-3160) and six Jurassic localities (14-LM-468, 14-LM-479, 15-LM-806, 15-LM-810, 17-LM-1656, 18-LM-2756). East of locality 14-LM-16, this generally northeast-trending boundary appears to be dextrally offset by a fault that separates localities 14-LM-479 and 19-LM-3160 (fig. 3). Roughly 1–3 km south of Lane Mountain, the boundary between the two suites is between six Permian–Triassic localities (17-LM-2113, 18-LM-2595, 18-LM-2604, 18-LM-2744, 18-LM-2997, 19-LM-3210) and five Jurassic localities (17-LM-2203, 18-LM-2594, 18-LM-2603, 18-LM-2607, 18-LM-2725). Our field observations suggest that this boundary coincides with a southeast-striking fault not mapped by McCulloh (1960).

North of Lane Mountain, our field observations indicate that the Permian–Triassic plutonic rocks are commonly faulted against the adjacent metamorphic rocks of the Carbide formation (McCulloh, 1960) to the east. Intrusive contacts, however, are recognized near locality 18-LM-3042 and near a group of localities farther south (17-LM-1992, 17-LM-2000, 17-LM-2001, 17-LM-2002, 18-LM-2809, 19-LM-3160). The Permian–Triassic plutonic rocks south of Lane Mountain clearly intrude the adjacent metamorphic rocks based on our field observations there. In both cases, only the two structurally lowest units of the Carbide formation (amphibolite unit Pca and quartzite unit Pcq_1) are demonstrably intruded by the Permian–Triassic suite. Detrital zircon data indicate that some of the structurally higher metasedimentary rocks in the area (including the Noble Well formation of McCulloh, 1960) are younger than the Permian–Triassic intrusive suite (Brown and others, 2018).

Permian–Triassic plutonic rocks within a few hundred meters of the metamorphic rocks are mostly monzonite, quartz monzonite, and granodiorite in composition. Farther away, the rocks are dioritic. The less mafic rocks were possibly contaminated by assimilation of country rock material during intrusion. The relatively high Sr_i values of Permian–Triassic samples 17-LM-1562 (granodiorite) and 17-LM-1688 (monzonite), both near the metamorphic rocks, could also be the result of assimilation.

Our field observations indicate that plutonic rocks of the Jurassic suite intrude many of the metamorphic rock units mapped by McCulloh (1960) and are likely younger than any metamorphic rocks in the area (fig. 3). In general, compositional variations in the Jurassic plutonic rocks appear random and are commonly abrupt. In the central part of the area, for example, the composition changes from granodiorite at locality 14-LM-1 to gabbro at nearby locality 14-LM-154 (fig. 3), and other bodies of granodiorite are present even closer to the latter. In the southeastern part of the area, Jurassic granitic rocks (represented by samples 17-LM-1835 and 17-LM-2191) are in sharp contact with diorite. Such variations suggest that the Jurassic suite formed by the coeval intrusion of complexly interdigitated magmas.

Near the western margin of the Jurassic suite, we have recognized a large body of mafic rocks (gabbroic diorite to gabbro) that is represented by four dated samples (15-LM-479, 15-LM-810, 17-LM-1656, 18-LM-2756) (fig. 3). This body lies beneath a previously unrecognized low-angle fault, the upper plate of which consists of less mafic dioritic rocks (including sample 14-LM-490) that intrude the Noble Well formation of McCulloh (1960). Our field observations indicate that the upper plate of this fault has an outcrop width of as much as 6 km, extending from the vicinity of locality 18-LM-2607 in the south to the vicinity of locality 17-LM-2128 in the north (fig. 3). The southern boundary of the upper plate appears to coincide with the previously noted fault between Permian-Triassic and Jurassic plutonic rocks south of Lane Mountain.

Regional Relations

Permian–Triassic and Late Jurassic plutonic rocks (and minor Late Jurassic volcanic rocks) approximately coeval with the rocks discussed in this report are scattered in the central Mojave Desert and adjacent areas to the north and south (fig. 17). Rocks of both age groups have been interpreted to represent segments of northwest-trending magmatic arcs emplaced above east-dipping subduction zones along the Cordilleran continental margin of southwestern North America (Barth and Wooden, 2006; Barth and others, 1997, 2008; Cecil and others, 2019).

Permian–Triassic Plutonic Rocks

Permian–Triassic plutonic rocks ranging in age from ~275 to ~240 Ma are documented in several widely scattered areas in addition to Lane Mountain (fig. 17). From north to south, these include the southeastern Sierra Nevada, El Paso Mountains, Fremont Peak, Opal Mountain, Black Mountain, Granite Mountains, and eastern Transverse Ranges (San Gabriel-San Bernardino-Pinto-Eagle Mountains) (Miller and others, 1995; Barth and others, 1997; Carr and others, 1997; Barth and Wooden, 2006; Stone and others, 2013; Saleeby and Dunne, 2015; Cecil and others, 2019). Prior to Cenozoic displacements on the San Andreas, Garlock, and other strike-slip faults, these outcrops formed a northwest-trending belt about 250 km long (Barth and Wooden, 2006). This belt is commonly interpreted to represent the initial pulse of Cordilleran arc magmatism after late Paleozoic truncation of the continental margin along a system of northwest-striking, left-lateral strike-slip (transform) faults (Barth and others, 1997; Saleeby and Dunne, 2015).

Permian–Triassic plutonic rocks in the San Bernardino Mountains area, including Black Mountain (fig. 17), intrude continental rocks that include Neoproterozoic to Paleozoic shallow-marine shelf strata of the Cordilleran miogeocline and the underlying crystalline basement (Stewart and Poole, 1975; Miller, 1981; Barth and Wooden, 2006; Stone and others, 2013). An enigmatic, east-west-trending boundary (fig. 17) separates these continental rocks from the eugeoclinal El Paso terrane to the north, which is intruded by the low-Sr_i Permian–Triassic plutons of the El Paso Mountains and Lane Mountain area (Miller and others, 1995; Cecil and others, 2019). This boundary was depicted as a concealed, terrane-bounding fault by Silberling and others (1987, 1992). The apparent continuity of the Permian–Triassic plutonic belt across this boundary suggests that the El Paso terrane was adjacent to the San Bernardino Mountains area by the time arc magmatism began (Walker and others, 2002), although the original boundary may have been modified by younger deformation (Martin and others, 1993).

The oldest known plutonic rocks of the Permian–Triassic suite are a ~274 Ma granite in the westernmost El Paso Mountains and a ~270 Ma granodiorite at Fremont Peak (fig. 17) (Cecil and others, 2019). These Middle Permian plutonic rocks have Sr_i >0.706 and other isotopic characteristics that suggest significant involvement of continental lithosphere in the generation of their parent magmas, in contrast to the less continental, Late Permian–Triassic plutonic rocks to the east. Cecil and others (2019) suggested that these high Sr_i values could have resulted from contractional tectonism and crustal thickening above the subduction zone at the onset of arc magmatism, as opposed to an extensional upper-plate regime during the Late Permian–Triassic time frame. Alternatively, a north-south-trending fault or terrane boundary could separate the two areas of contrasting isotopic signatures, although no direct evidence of such a feature has been identified.

Late Jurassic Plutonic Rocks

Like the Permian–Triassic plutons, Late Jurassic plutonic rocks ranging in age from ~155 to ~145 Ma are widely scattered in the area of figure 17. In addition to those at Lane Mountain, plutonic rocks of this age are known at Alvord Mountain and the Cronese Hills to the east, Iron Mountain, Black Mountain, and the Shadow Mountains to the south and southwest, and the San Bernardino, Pinto, and Eagle Mountains of the eastern Transverse Ranges (Miller and Sutter, 1982; Walker and others 1990; Martin and others, 2002; Miller and Walker, 2002; Barth and others, 2008, 2017). In addition, Late Jurassic volcanic rocks are known in the Sidewinder Mountain area (Schermer and others, 2002). Barth and others (2008) showed that the Late Jurassic magmatic arc developed outboard (west) of a more voluminous Middle Jurassic arc and the ~148 Ma Independence dike swarm.

The abundance of Late Jurassic plutonic rocks with Sr_i averaging ~0.7055 in the Lane Mountain area stands in contrast to the lack of such rocks in the El Paso Mountains (fig. 17). There, metasedimentary rocks of the El Paso terrane are intruded by the late Early Jurassic (~176 Ma) Laurel Mountain pluton with Sr_i ~0.708 (Miller and Glazner, 1995; Miller and others, 1995; Cecil and others, 2019). This Sr_i and other isotopic signatures indicate significant involvement of Precambrian continental lithosphere in the source magma of the Laurel Mountain pluton, which Miller and others (1995) interpreted to have resulted from pre-Laurel Mountain, east-directed thrusting of the El Paso terrane onto the continental margin. Whether or not this interpretation is valid, no comparable thrusting event appears to have affected the Lane Mountain area.

Lithosphere of the El Paso Terrane

Geochemical and isotopic properties of Permian–Triassic plutonic rocks in the El Paso Mountains led Cecil and others (2019) to interpret these rocks as part of a magmatic arc that developed "in a peri-allochthonous sliver of transitional (oceanic to attenuated continental) lithosphere capped by marine slope and rise facies of the passive margin." This interpretation is supported by the geochemical and isotopic data reported herein, including Sr/Y ratios that suggest a crustal thickness like that of modern continental slopes

(Mooney and others, 1998) at Lane Mountain from Permian–Triassic to Late Jurassic time. Kistler (1990) and Kistler and Ross (1990) had previously considered the El Paso terrane as part of their Panthalassan lithosphere, for which they found no evidence of a Precambrian continental basement. The increase in mean Sr_i from ~0.7045 in Permian–Triassic plutons to ~0.7055 in Late Jurassic plutons at Lane Mountain may indicate the introduction of subducted sedimentary material into the Late Jurassic magmatic source.

Summary

This report presents geochronologic, geochemical, and isotopic data from 48 samples of pre-Cretaceous plutonic rocks in the Lane Mountain area. Of these samples, 26 are of Permian–Triassic age (averaging ~248 Ma) and 22 are of Late Jurassic age (averaging ~149 Ma). Geochemically, the Permian–Triassic samples range from monzodiorite to quartz monzonite and granodiorite (~53–65 percent SiO_2), whereas the Late Jurassic samples range from gabbro to granite (~50–73 percent SiO_2). On average the Late Jurassic samples are less siliceous, more aluminous, and more calcic than the Permian–Triassic samples. The initial $^{87}Sr/^{86}Sr$ ratio (Sr_i) averages ~0.7045 for eight Permian–Triassic samples and ~0.7055 for nine Late Jurassic samples. These ratios indicate little Precambrian lithospheric material in the magmatic source area of the Permian–Triassic suite but more in that of the Late Jurassic suite, although still less than would be expected had the latter been generated in an area underlain by continental lithosphere.

The data reported herein provide a quantitative basis for dividing the pre-Cretaceous plutonic rocks of the Lane Mountain area into discrete, mappable units of Permian–Triassic and Late Jurassic age. As a result, metasedimentary and metavolcanic rocks intruded by, and thus older than, the Permian–Triassic plutonic rocks can be confidently distinguished from potentially younger units that are only intruded by Late Jurassic plutonic rocks. Metasedimentary and metavolcanic rocks at Lane Mountain are part of the El Paso terrane, which many consider to be allochthonous with respect to the Paleozoic continental margin.

Permian–Triassic and Late Jurassic plutonic rocks coeval with those at Lane Mountain are widely distributed in the central Mojave Desert, southeastern Sierra Nevada, and eastern Transverse Ranges. Both suites are interpreted as segments of northwest-trending magmatic arcs that developed above east-dipping subduction zones along the western margin of North America, and the Permian–Triassic suite is commonly interpreted to represent the initiation of arc magmatism after late Paleozoic truncation of the continental margin. The distinction between these two plutonic suites at Lane Mountain provides the type of information needed to address uncertainties regarding this hypothetical truncation event and the tectonic significance of the El Paso terrane.

Acknowledgments

This work was funded by the U.S. Geological Survey (USGS) National Cooperative Geologic Mapping Program and was conducted under the project leadership of David Miller and Andrew Cyr. Juliet Ryan-Davis and Nicole Thomas provided invaluable guidance and support as managers of the USGS mineral separation laboratory in Menlo Park. Geochronologic sample preparation and zircon separations were performed by Randy Woods, who also assisted with the SHRIMP-RG analyses. Marsha Lidzbarski helped with preparation of the zircon mounts. Brad Ito and Eric Angel provided electronics support of the SHRIMP-RG.

References Cited

Barth, A.P., Tosdal, R.M., Wooden, J.L., and Howard, K.A., 1997, Triassic plutonism in southern California—Southward younging of arc initiation along a truncated continental margin: Tectonics, v. 16, no. 2, p. 290–304.

Barth, A.P., and Wooden, J.L., 2006, Timing of magmatism following initial convergence at a passive margin, southwestern U.S. Cordillera, and ages of lower crustal magma sources: Journal of Geology, v. 114, p. 231–245.

Barth, A.P., Wooden, J.L., Howard, K.A., and Richards, J.L., 2008, Late Jurassic plutonism in the southwest U.S. Cordillera, *in* Wright, J.E., and Shervais, J.W., eds., Ophiolites, arcs, and batholiths—A tribute to Cliff Hopson: Geological Society of America Special Paper 438, p. 379–396, https://doi.org/10.1130/2008.2438(13).

Barth, A.P., Wooden, J.L., Miller, D.M., Howard, K.A., Fox, L.K., Schermer, E.R., and Jacobson, C.E., 2017, Regional and temporal variability of melts during a Cordilleran magma pulse—Age and chemical evolution of the Jurassic arc, eastern Mojave Desert, California: Geological Society of America Bulletin, v. 129, no. 3–4, p. 429–448, https://doi.org/10.1130/B31550.1.

Bayless, E.R., Bullen, T.D., and Fitzpatrick, J.A., 2004, Use of $^{87}Sr/^{86}Sr$ and $\delta^{11}B$ to identify slag-affected sediment in southern Lake Michigan: Environmental Science and Technology, v. 38, p. 1330–1337.

Boettcher, S.S., and Walker, J.D., 1993, Geologic evolution of Iron Mountain, central Mojave Desert, California: Tectonics, v. 12, p. 372–386.

Brown, H.J., 2016a, Detailed geologic map of the northern Calico Mountains and the Lane Mountain area, central Mojave Desert, California—part 1, the need for new mapping [abs.]: Geological Society of America Abstracts with Programs, v. 48, no. 4, https://doi.org/10.1130/abs/2016CD-271692.

Brown, H.J., 2016b, Detailed geologic map of the northern Calico Mountains and the Lane Mountain area, central Mojave Desert, California—part 2, stratigraphy and structure of Paleozoic, Mesozoic, and Cenozoic rocks [abs.]: Geological Society of America Abstracts with Programs, v. 48, no. 4, https://doi.org/10.1130/abs/2016CD-271693.

Brown, H.J., Stone, P., Cecil, M.R., and Fitzpatrick, J., 2018, New insights into the geology of the Lane Mountain and north Calico Mountains area, central Mojave Desert, California [abs.]: Geological Society of America Abstracts with Programs, v. 50, no. 5, https://doi.org/10.1130/abs/2018RM-311369.

Brown, H.J., Stone, P., Rosario, J., and Fitzpatrick, J., 2016, Detailed geologic map of the northern Calico Mountains and the Lane Mountain area, central Mojave Desert, California; part 3, preliminary digital geologic map [abs.]: Geological Society of America Abstracts with Programs, v. 48, no. 4, https://doi.org/10.1130/abs/2016CD-271694.

Burchfiel, B.C., and Davis, G.A., 1981, Mojave Desert and environs, chap. 9 *of* Ernst, W.G., ed., The geotectonic development of California, Rubey Volume 1: Englewood Cliffs, N.J., Prentice-Hall, p. 217–252.

Burke, D.B., Hillhouse, J.W., McKee, E.H., Miller, S.T., and Morton, J.L., 1982, Cenozoic rocks in the Barstow area of southern California—Stratigraphic relations, radiometric ages, and paleomagnetism: U.S. Geological Survey Bulletin 1529-E, p. E1–E16.

Carr, M.D., Christiansen, R.L., Poole, F.G., and Goodge, J.W., 1997, Bedrock geologic map of the El Paso Mountains in the Garlock and El Paso Peaks 7½' quadrangles, Kern County, California: U.S. Geological Survey Miscellaneous Investigations Series Map I-2389, scale 1:24,000, 9 p.

Cecil, M.R., Ferrer, M.A., Riggs, N.R., Marsaglia, K., Kylander-Clark, A., Ducea, M.N., and Stone, P., 2019, Early arc development recorded in Permian–Triassic plutons of the northern Mojave Desert region, California, USA: Geological Society of America Bulletin, v. 131, no. 5/6, p. 749–765, https://doi.org/10.1130/B31963.1.

Chapman, J.B., Ducea, M.N., DeCelles, P.G., and Profeta, L., 2015, Tracking changes in crustal thickness during orogenic evolution with Sr/Y; an example from the North American Cordillera: Geology, v. 43, no. 10, p. 919–922, https://doi.org/10.1130/G36996.1.

Chiaradia, M., 2015, Crustal thickness control on Sr/Y signatures of recent arc magmas; an Earth scale perspective: Scientific Reports, v. 5, no. 8115, 5 p., https://doi.org/10.1038/srep08115.

Coble, M.A., Vazquez, J.A., Barth, A.P., Wooden, J.L., Burns, D., Kylander-Clark, A., Jackson, S., and Vennari, C.E., 2018, Trace element characterisation of MAD-559 zircon reference material for ion microprobe analysis: Geostandards and Geoanalytical Research, v. 42, p. 481–497.

Dibblee, T.W., Jr., 2008, Geologic map of the Opal Mountain and Lane Mountain 15-minute quadrangles, San Bernardino County, California: Santa Barbara, Calif., Dibblee Geology Center Map DF-403, scale 1:62,500.

Fox, L.K., and Miller, D.M., 1990, Jurassic granitoids and related rocks of the southern Bristol Mountains, southern Providence Mountains, and Colton Hills, Mojave Desert, California, *in* Anderson, J.L., ed., The nature and origin of Cordilleran magmatism: Geological Society of America Memoir 174, p. 111–132.

Frost, B.R., Barnes, C.G., Collins, W.J., Arculus, R.J., Ellis, D.J., and Frost, C.D., 2001, A geochemical classification for granitic rocks: Journal of Petrology, v. 42, no. 11, p. 2033–2048.

Gradstein, F.M., Ogg, J.G., Schmitz, M.D., and Ogg, G.M., eds., 2020, Geologic time scale 2020: Cambridge, Mass., Elsevier, 1,357 p. (2 volumes).

Jennings, C.W., Strand, R.G., and Rogers, T.H., 1977, Geologic map of California: California Division of Mines and Geology, scale 1:750,000.

Kistler, R.W., 1990, Two different lithosphere types in the Sierra Nevada, California, *in* Anderson, J.L., ed., The nature and origin of Cordilleran magmatism: Geological Society of America Memoir 174, p. 271–281.

Kistler, R.W., and Ross, D.C., 1990, A strontium isotopic study of plutons and associated rocks of the southern Sierra Nevada and vicinity, California: U.S. Geological Survey Bulletin 1920, 20 p.

Ludwig, K., 2009, Squid 2, rev. 2.50, a user's manual: Berkeley Geochronology Center Special Publication 5, 110 p.

Ludwig, K., 2012, User's manual for Isoplot 3.75, a geochronological toolkit for Microsoft Excel: Berkeley Geochronology Center Special Publication 4, 75 p.

Martin, M.W., Glazner, A.F., Walker, J.D., and Schermer, E.L., 1993, Evidence for right-lateral transfer faulting accommodating en echelon Miocene extension, Mojave Desert, California: Geology, v. 21, p. 355–358.

Martin, M.W., Walker, J.D., and Fletcher, J.M., 2002, Timing of Middle to Late Jurassic ductile deformation and implications for paleotectonic setting, Shadow Mountains, western Mojave Desert, California, *in* Glazner, A.F., Walker, J.D., and Bartley, J.M., eds., Geologic evolution of the Mojave Desert and southwestern Basin and Range: Geological Society of America Memoir 195, p. 43–58.

Mattinson, J.M., 2010, Analysis of the relative decay constants of ^{235}U and ^{238}U by multi-step CA-TIMS measurements of closed-system natural zircon samples: Chemical Geology, v. 275, p. 186–198.

McCulloh, T.H., 1952, Geology of the southern half of the Lane Mountain quadrangle, California: Los Angeles, Calif., University of California, Ph.D. dissertation, 182 p.

McCulloh, T.H., 1960, Geologic map of the Lane Mountain quadrangle, California: U.S. Geological Survey Open-File Report 60–95, scale 1:48,000.

Middlemost, E.A.K., 1994, Naming materials in the magma/igneous rock system: Earth-Science Reviews, v. 37, p. 215–224.

Miller, E.L., 1981, Geology of the Victorville region, California: Geological Society of America Bulletin, part 2, v. 92, p. 554–608.

Miller, J.S., and Glazner, A.F., 1995, Jurassic plutonism and crustal evolution in the central Mojave Desert, California: Contributions to Mineralogy and Petrology, v. 118, p. 379–395.

Miller, J.S., Glazner, A.F., Walker, J.D., and Martin, M.W., 1995, Geochronologic and isotopic evidence for Triassic-Jurassic emplacement of the eugeoclinal allochthon in the Mojave Desert region, California: Geological Society of America Bulletin, v. 107, p. 1441–1457.

Miller, E.L., and Sutter, J.F., 1982, Structural geology and ^{40}Ar-^{39}Ar geochronology of the Goldstone-Lane Mountain area, Mojave Desert, California: Geological Society of America Bulletin, v. 93, p. 1191–1207.

Miller, J.S., and Walker, J.D., 2002, Mesozoic geologic evolution of Alvord Mountain, central Mojave Desert, California, *in* Glazner, A.F., Walker, J.D., and Bartley, J.M., eds., Geologic evolution of the Mojave Desert and southwestern Basin and Range: Geological Society of America Memoir 195, p. 59–77.

Mooney, W.D., Laski, G., and Masters, T.G., 1998, Crust 5.1; a global crustal model at 5° x 5°: Journal of Geophysical Research, v. 103, no. B1, p. 727–747.

Pearce, J.A., Harris, N.B.W., and Tindle, A.G., 1984, Trace element discrimination diagrams for the tectonic interpretation of granitic rocks: Journal of Petrology, v. 25, no. 4, p. 956–983.

Rotenberg, E., Davis, D.W., Amelin, Y., Ghosh, S., and Bergquist, B.A., 2012, Determination of the decay constant of ^{87}Rb by laboratory accumulation of ^{87}Sr: Geochimica et Cosmochimica Acta, v. 85, p. 41–57, https://doi.org/10.1016/j.gca.2012.01.016.

Saleeby, J., and Dunne, G., 2015, Temporal and tectonic relations of early Mesozoic arc magmatism, southern Sierra Nevada, California, *in* Anderson, T.H., Didenko, A.N., Johnson, C.L., Khanchuk, A.I., and MacDonald, J.H., Jr., eds., Late Jurassic margin of Laurasia—a record of faulting accommodating plate rotation: Geological Society of America Special Paper 513, p. 223–268, https://doi.org/10.1130/2015.2513(05).

Schermer, E.R., Busby, C.J., and Mattinson, J.M., 2002, Paleogeographic and tectonic implications of Jurassic sedimentary and volcanic sequences in the central Mojave Block, *in* Glazner, A.F., Walker, J.D., and Bartley, J.M., eds., Geologic evolution of the Mojave Desert and southwestern Basin and Range: Geological Society of America Memoir 195, p. 93–115.

Silberling, N.J., Jones, D.L., Blake, M.C., Jr., and Howell, D.G., 1987, Lithotectonic terranes of the western conterminous United States: U.S. Geological Survey Miscellaneous Field Studies Map MF-1874-C, scale 1:2,500,000, 20 p.

Silberling, N.J., Jones, D.L., Monger, J.W.H., and Coney, P.J., 1992, Lithotectonic terrane map of the North American Cordillera: U.S. Geological Survey Miscellaneous Investigations Series Map I-2176, scale 1:5,000,000.

Singleton, J.S., and Gans, P.B., 2008, Structural and stratigraphic evolution of the Calico Mountains; implications for early Miocene extension and Neogene transpression in the central Mojave Desert, California: Geosphere, v. 4, no. 3, p. 459–479, https://doi.org/10.1130/GES00143.1.

Stewart, J.H., and Poole, F.G., 1975, Extension of the Cordilleran miogeosynclinal belt to the San Andreas Fault, southern California: Geological Society of America Bulletin, v. 86, p. 205–212.

Stone, P., Barth, A.P., Wooden, J.L., Fohey-Breting, N.K., Vazquez, J.A., and Priest, S.S., 2013, Geochronologic and geochemical data from Mesozoic rocks in the Black Mountain area northeast of Victorville, San Bernardino County, California: U.S. Geological Survey Open-File Report 2013–1146, 31 p., https://doi.org/10.3133/ofr20131146.

Stone, P., Brown, H.J., Cecil, M.R., Fleck, R.L., Vazquez, J.A., Fitzpatrick, J.A., and Rosario, J.J., 2019, Geochronologic, isotopic, and geochemical data from igneous rocks in the Lane Mountain area, San Bernardino County, California: U.S. Geological Survey Open-File Report 2019–1070, 34 p, https://doi.org/10.3133/ofr20191070.

Stone, P., Miller, D.M., Stevens, C.H., Rosario, J.J., Vazquez, J.A., Wan, E., Priest, S.S., and Valin, Z.C., 2017, Geologic map of the Providence Mountains in parts of the Fountain Peak and adjacent 7.5’ quadrangles, San Bernardino County, California: U.S. Geological Survey Scientific Investigations Map 3376, scale 1:24,000, 52 p., https://doi.org/10.3133/sim3376.

Sun, S.-s., and McDonough, W.F., 1989, Chemical and isotopic systematics of oceanic basalts; implications for mantle composition and processes, *in* Saunders, A.D., and Norry, M.J., eds., Magmatism in the ocean basins: London, Geological Society Special Publication 42, p. 313–345.

U.S. Geological Survey and California Division of Mines, 1966, Geologic map of California: U.S. Geological Survey Miscellaneous Geological Investigations Map I-512, scale 1:2,500,000.

Walker, J.D., Martin, M.W., Bartley, J.M., and Coleman, J.S., 1990, Timing and kinematics of deformation in the Cronese Hills, California, and implications for Mesozoic structure of the southwestern Cordillera: Geology, v. 18, p. 554–557.

Walker, J.D., Martin, M.W., and Glazner, A.F., 2002, Late Paleozoic to Mesozoic development of the Mojave Desert and environs, *in* Glazner, A.F., Walker, J.D., and Bartley, J.M., eds., Geologic evolution of the Mojave Desert and southwestern Basin and Range: Geological Society of America Memoir 195, p. 1–18.

Williams, I.S., 1998, U-Th-Pb geochronology by ion microprobe: Reviews in Economic Geology, v. 7, p. 1–35.

Figures and Tables

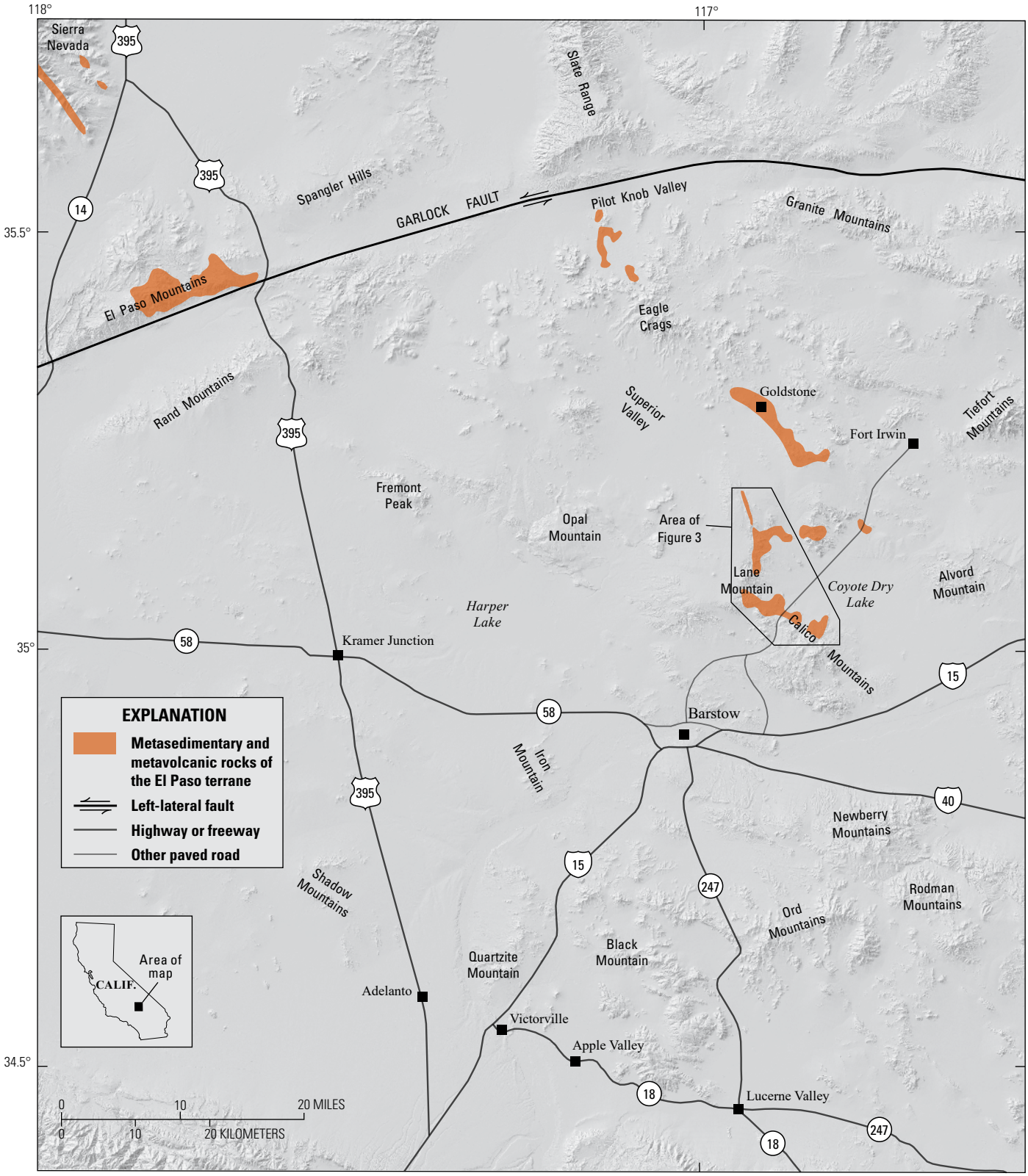

Digital elevation model base map from The National Map

Figure 1. Map of north-central Mojave Desert region showing outcrops of El Paso Terrane (modified from Jennings and others, 1977) and location of report area (fig. 3).

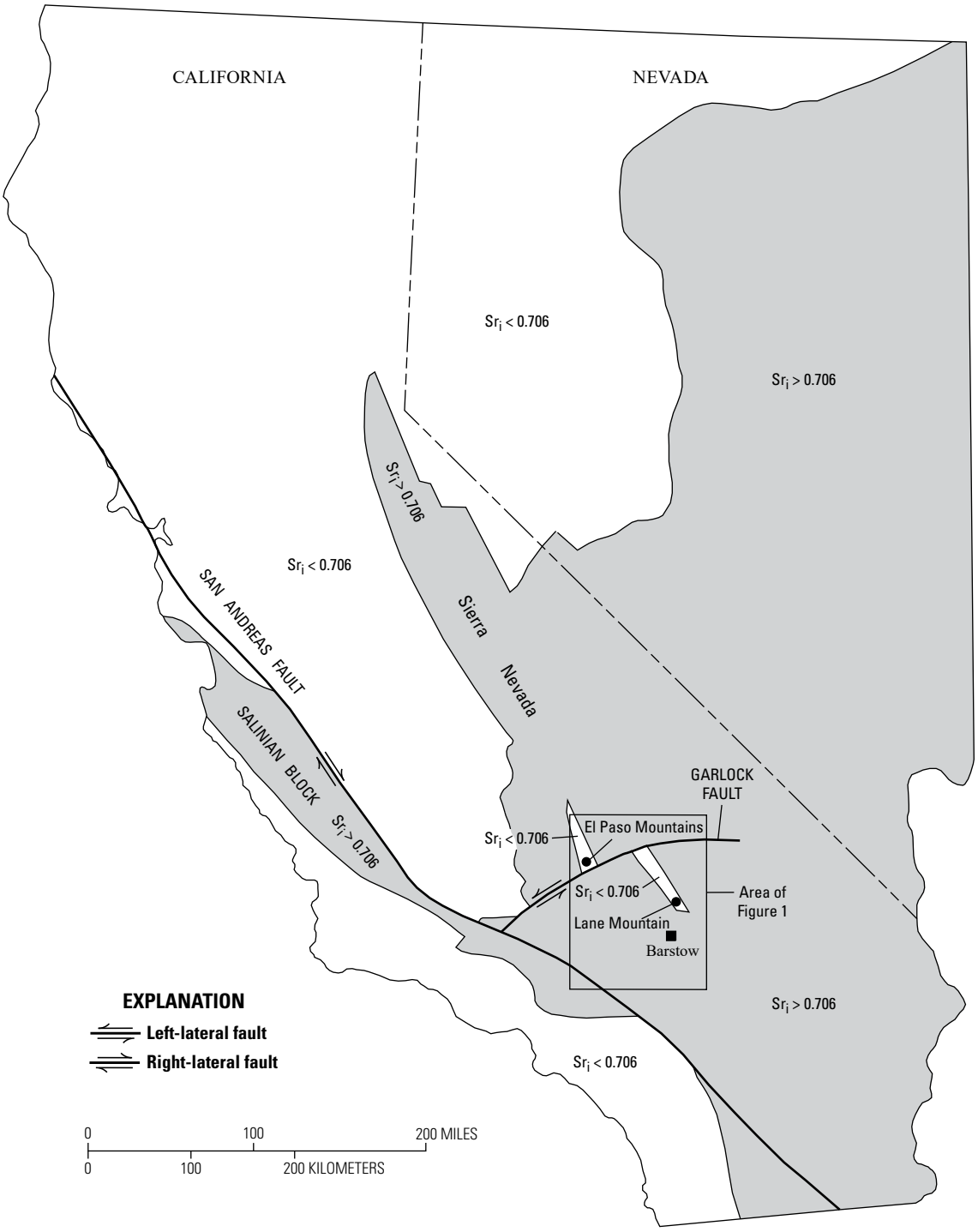

Figure 2. Map showing the initial $^{87}Sr/^{86}Sr$ ratio (Sr_i)=0.706 isopleth in California and Nevada (modified from Kistler and Ross, 1990). Shaded areas have Sr_i >0.706. Note narrow, northwest-trending zone of Sr_i <0.706 in the El Paso Mountains and Lane Mountain area. Box shows area of figure 1.

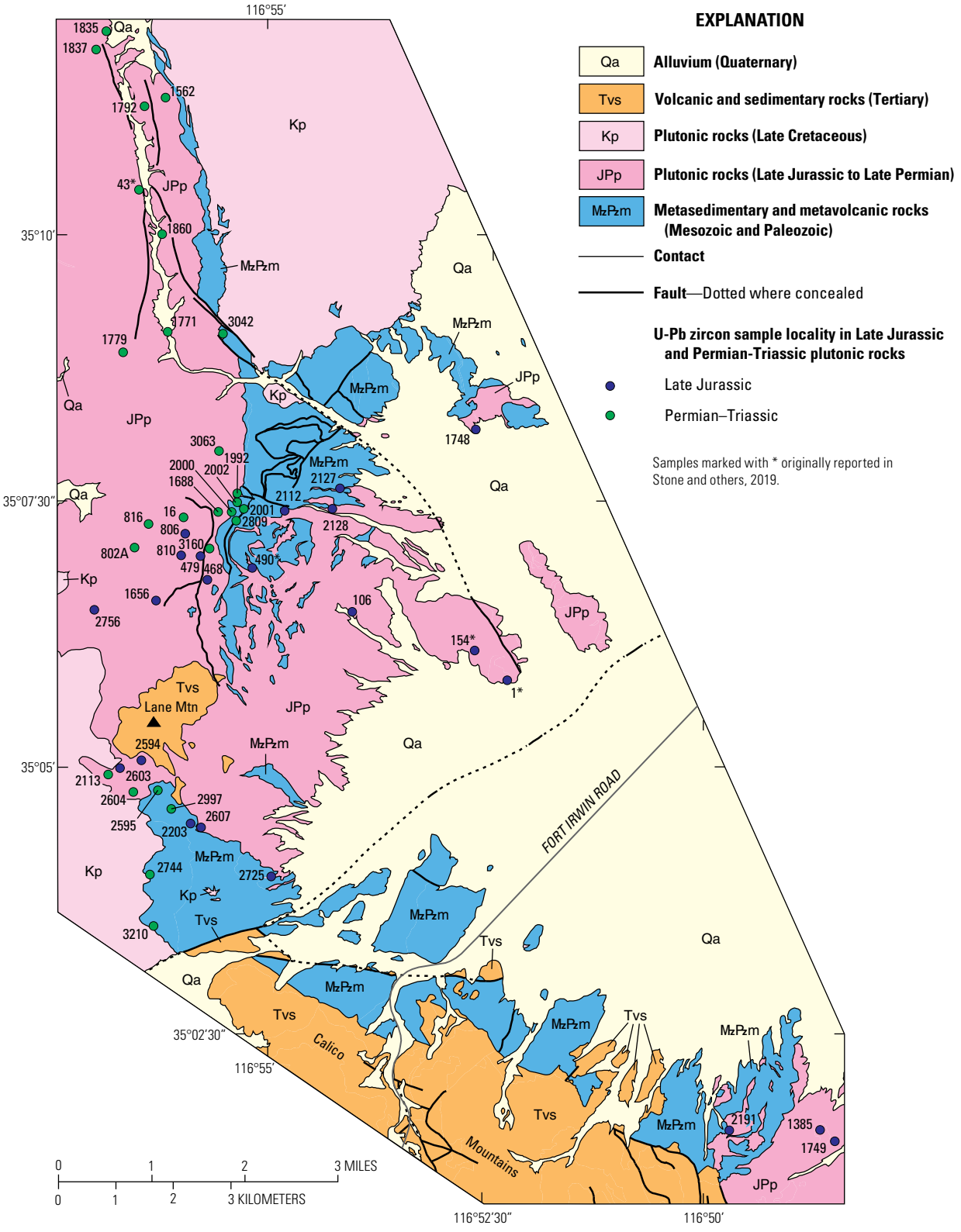

Figure 3. Map showing general geology of Lane Mountain area (modified from McCulloh, 1960) and locations and age groups of samples included in this report. Note abbreviated sample numbers; see table 1 for complete sample numbers.

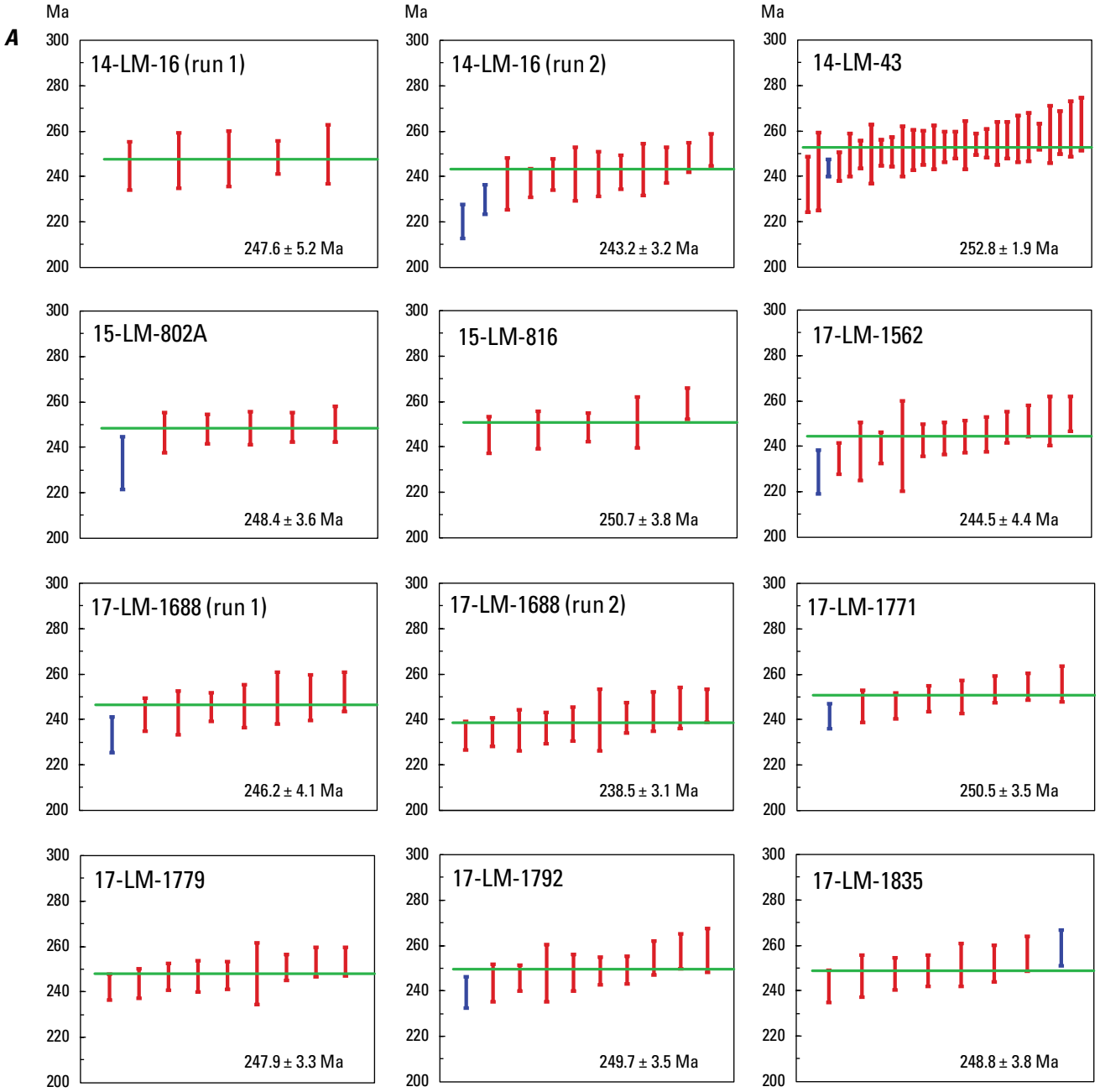

Figure 4. Isoplot diagrams showing weighted mean sensitive high resolution ion microprobe-reverse geometry (SHRIMP-RG) U-Pb zircon ages (green horizontal lines) of samples dated in this report. X-axis of each diagram is dimensionless; y-axis indicates numerical age in mega-annum (Ma). Vertical bars depict 2-sigma errors on $^{206}Pb^*/^{238}U$ ages of analyzed spots on zircon crystals; each bar represents a separate spot analysis. Red bars define coherent groups of spot analyses used for age determinations; blue bars represent spot analyses outside the statistical mean owing to inheritance from older rocks or presumed lead loss, which results in a younger age. Numerical age shown on each diagram includes the 1-sigma error. Samples analyzed more than once are denoted by (run 1), (run 2), and (run 3). Some samples contain older and (or) younger spot analyses outside the age limits of the diagrams; see tables 2–49 for complete dataset. *A–C*, Permian–Triassic samples (age range 200–300 Ma); *D–E*, Jurassic samples, (age range 100–200 Ma). *A*, Weighted mean age diagrams for Permian-Triassic samples 14-LM-16 through 17-LM-1835.

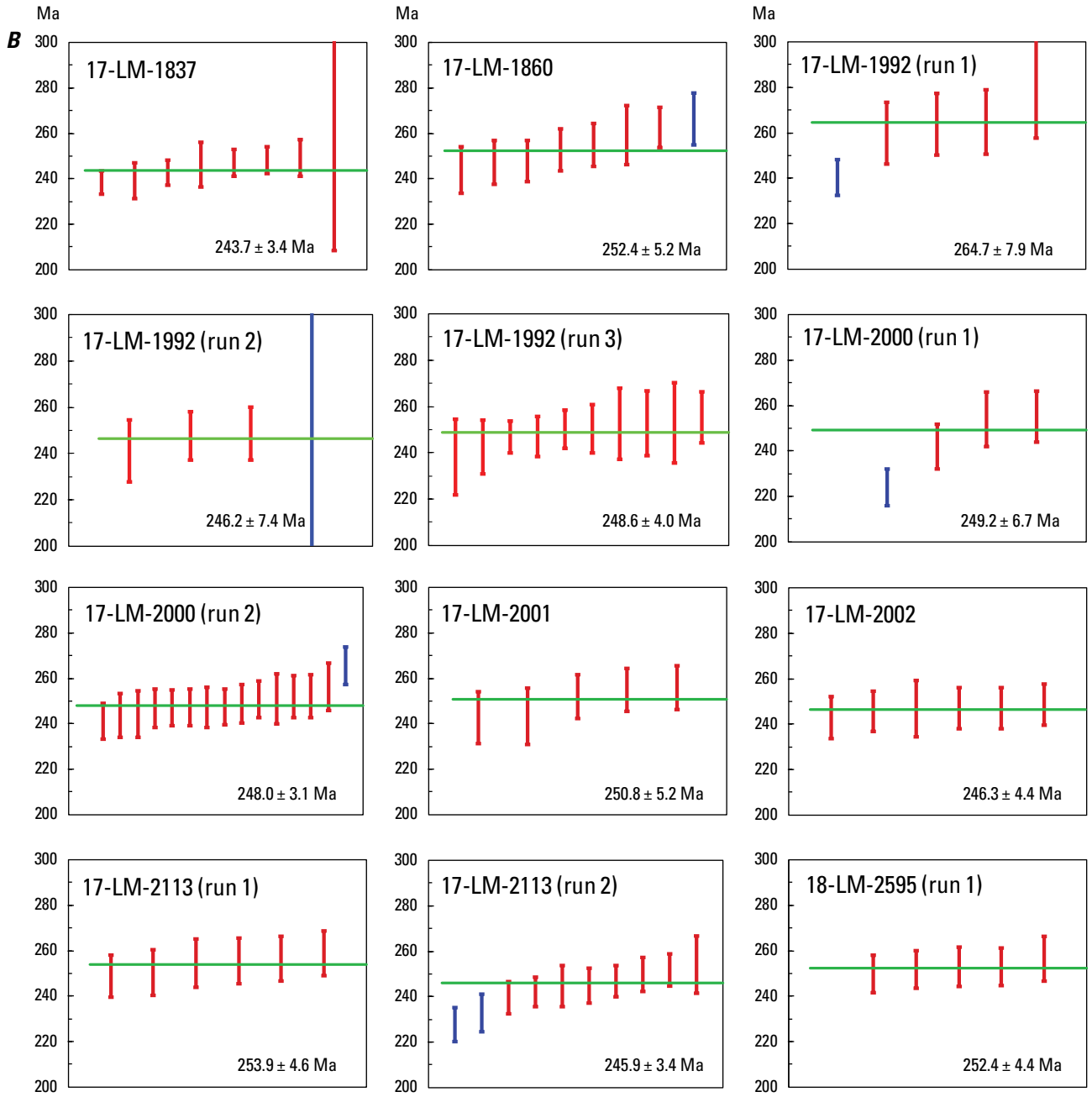

Figure 4. Isoplot diagrams showing weighted mean sensitive high resolution ion microprobe-reverse geometry (SHRIMP-RG) U-Pb zircon ages (green horizontal lines) of samples dated in this report (continued). *B*, Weighted mean age diagrams for Permian-Triassic samples 17-LM-1837 through 18-LM-2595 (run 1).

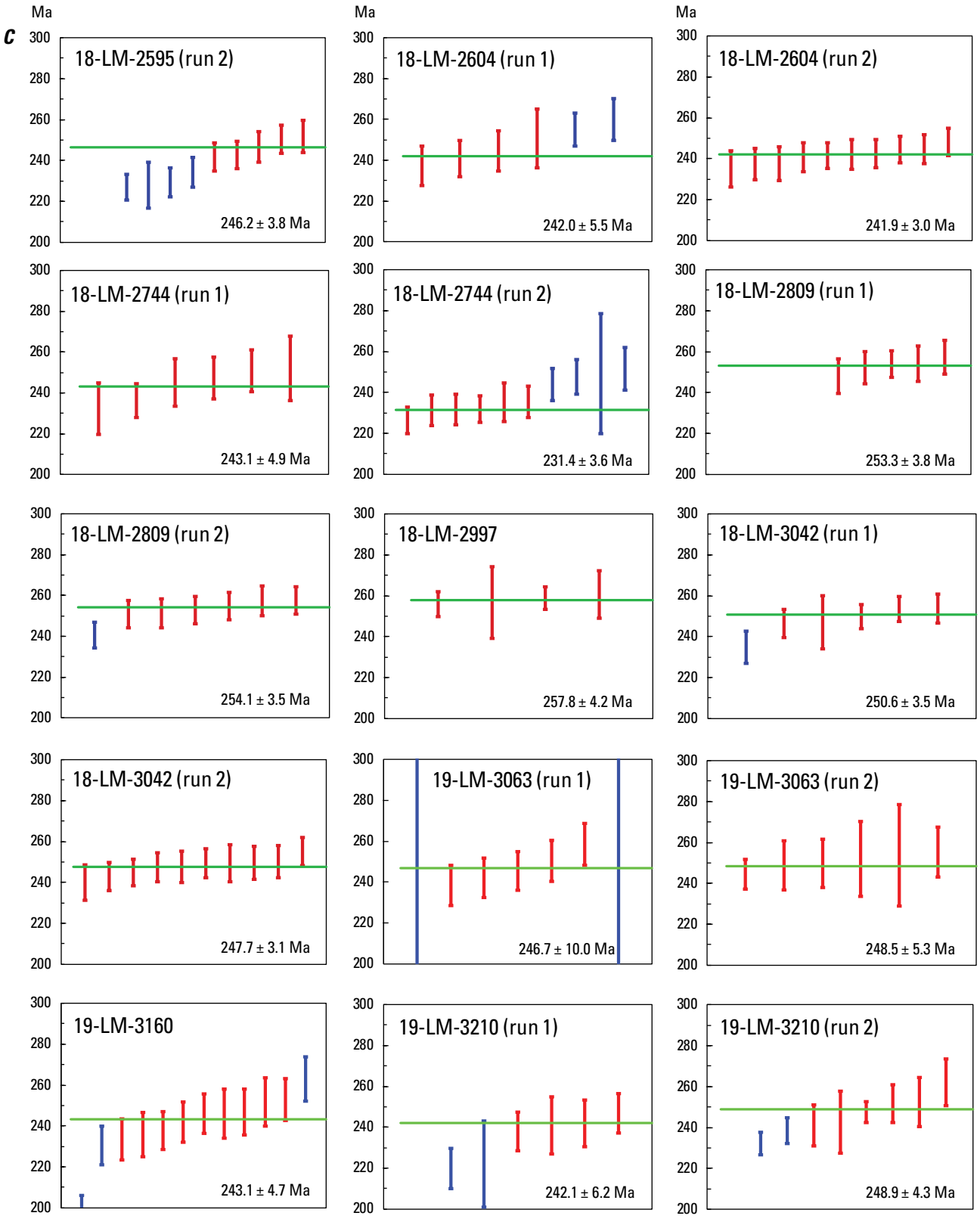

Figure 4. Isoplot diagrams showing weighted mean sensitive high resolution ion microprobe-reverse geometry (SHRIMP-RG) U-Pb zircon ages (green horizontal lines) of samples dated in this report (continued). *C*, Weighted mean age diagrams for Permian-Triassic samples 18-LM-2595 (run 2) through 19-LM-3210.

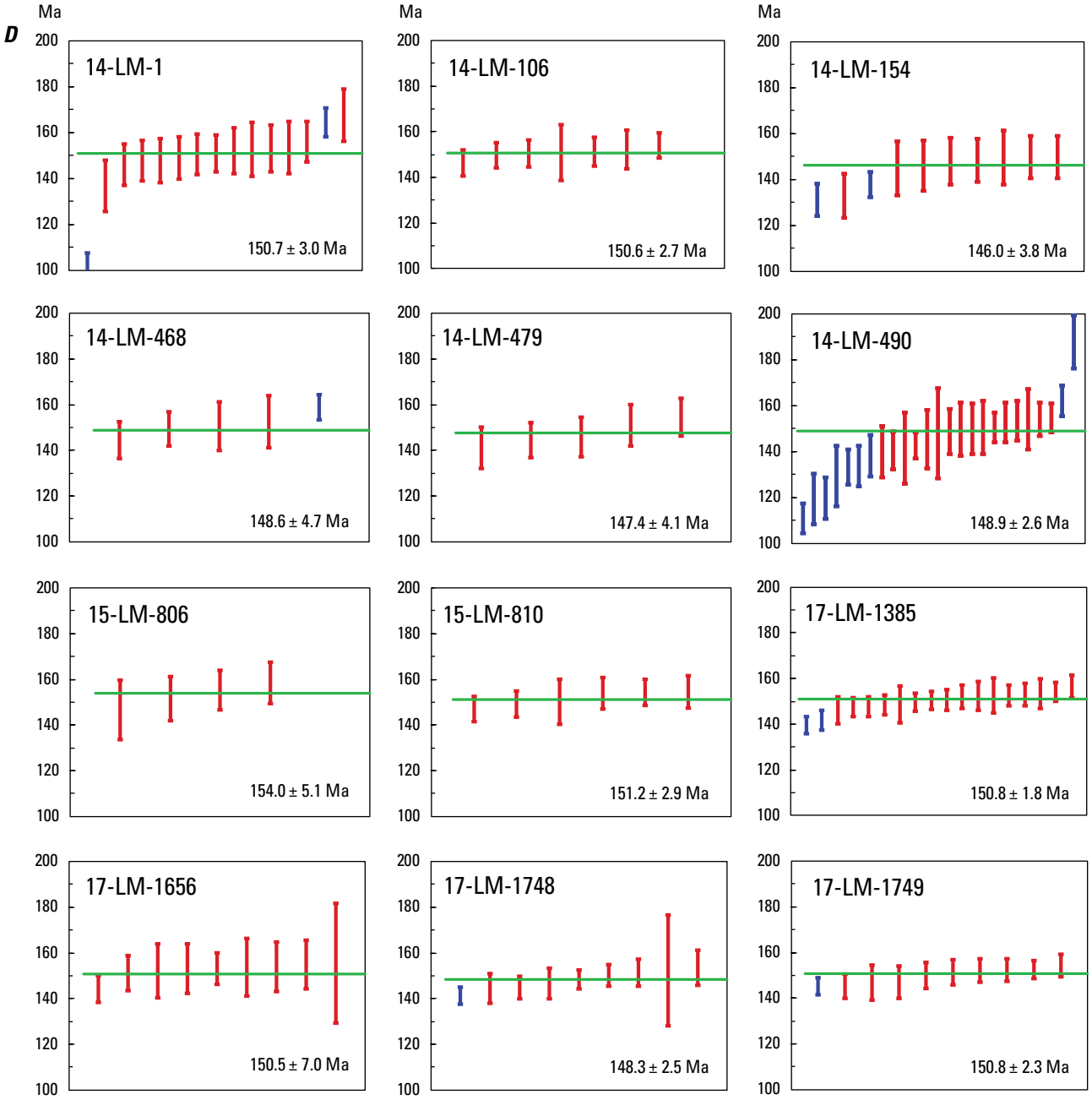

Figure 4. Isoplot diagrams showing weighted mean sensitive high resolution ion microprobe-reverse geometry (SHRIMP-RG) U-Pb zircon ages (green horizontal lines) of samples dated in this report (continued). *D*, Weighted mean age diagrams for Jurassic samples 14-LM-1 through 17-LM-1749.

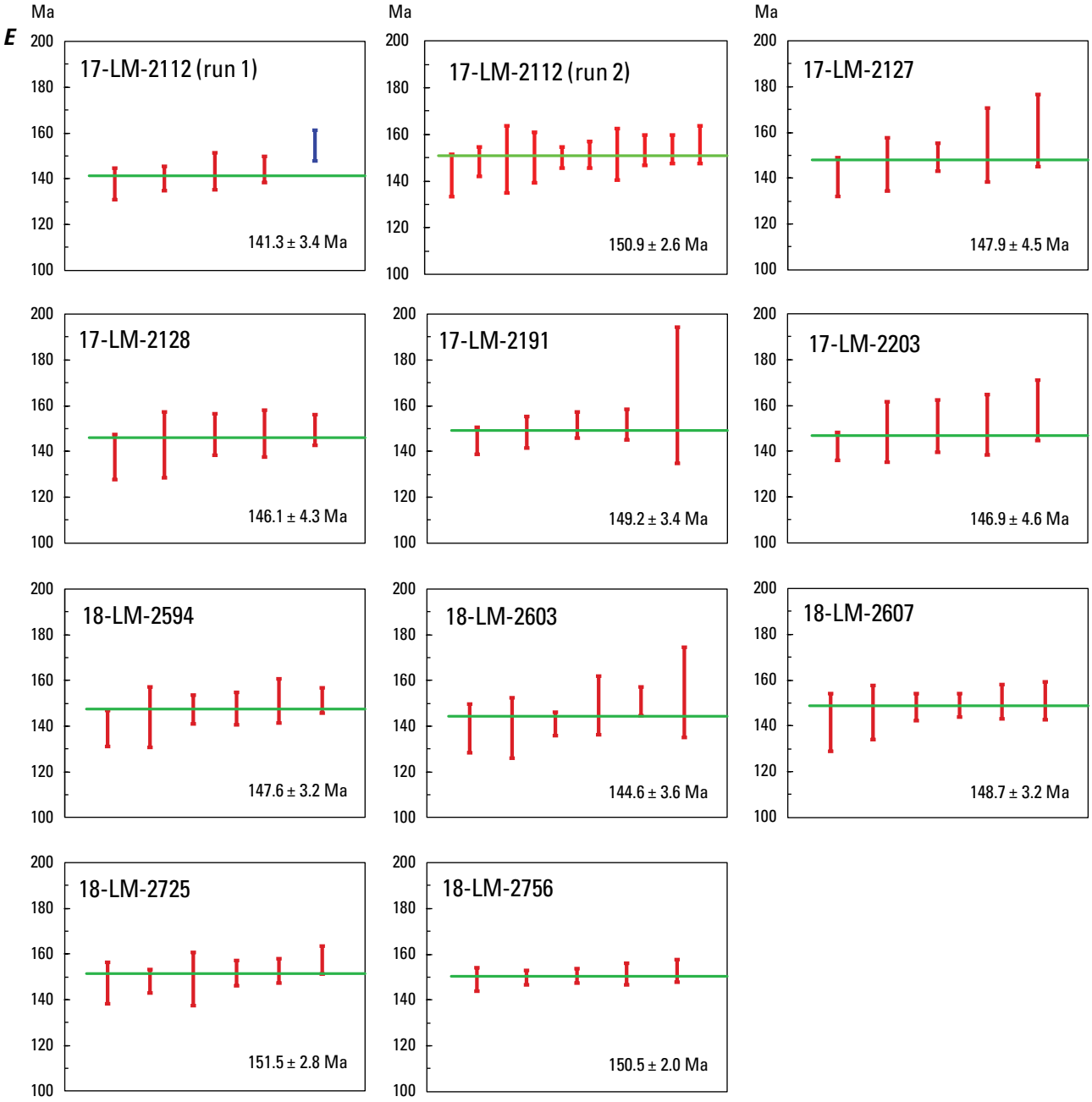

Figure 4. Isoplot diagrams showing weighted mean sensitive high resolution ion microprobe-reverse geometry (SHRIMP-RG) U-Pb zircon ages (green horizontal lines) of samples dated in this report (continued). *E*, Weighted mean age diagrams for Jurassic samples 17-LM-2112 through 18-LM-2756.

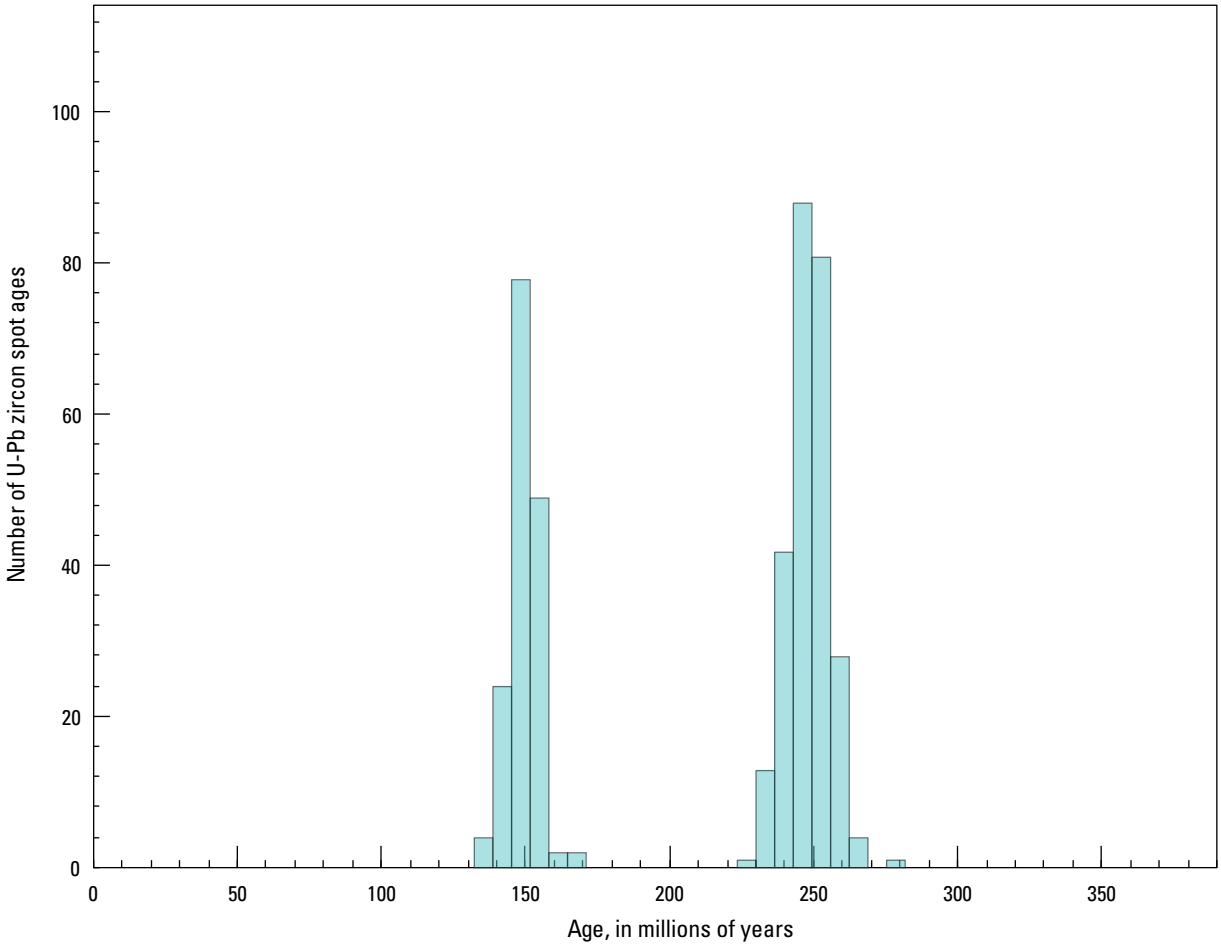

Figure 5. Histogram showing distribution of sensitive high resolution ion microprobe-reverse geometry (SHRIMP-RG) U-Pb zircon spot ages used to determine sample ages of Permian–Triassic and Jurassic rocks included in this report. See tables 2–49 for data.

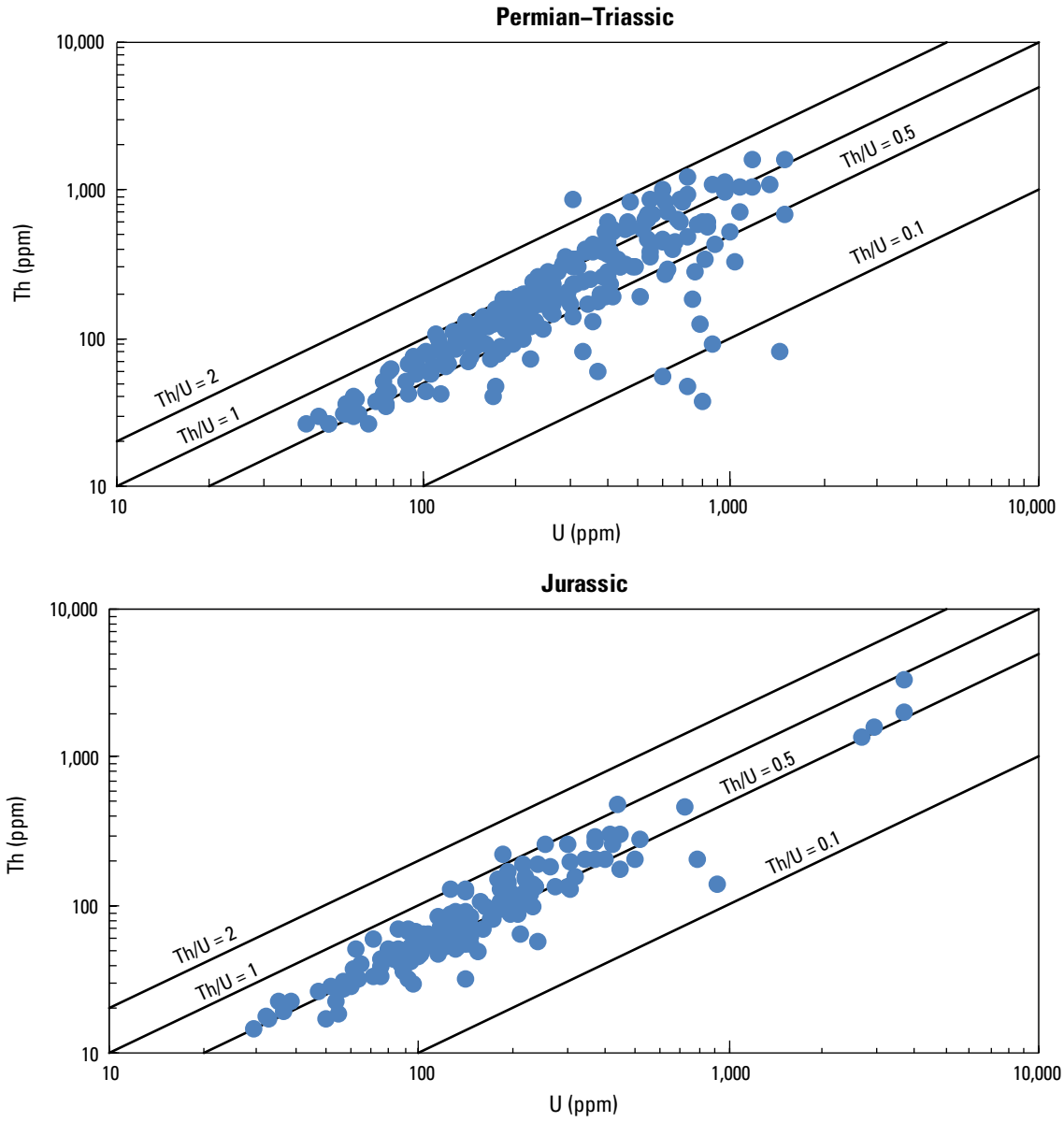

Figure 6. Diagrams showing thorium (Th) and uranium (U) concentrations in zircons analyzed by sensitive high resolution ion microprobe-reverse geometry (SHRIMP-RG) for this report. See tables 2–49 for data. Th/U, ratio of thorium to uranium; ppm, parts per million.

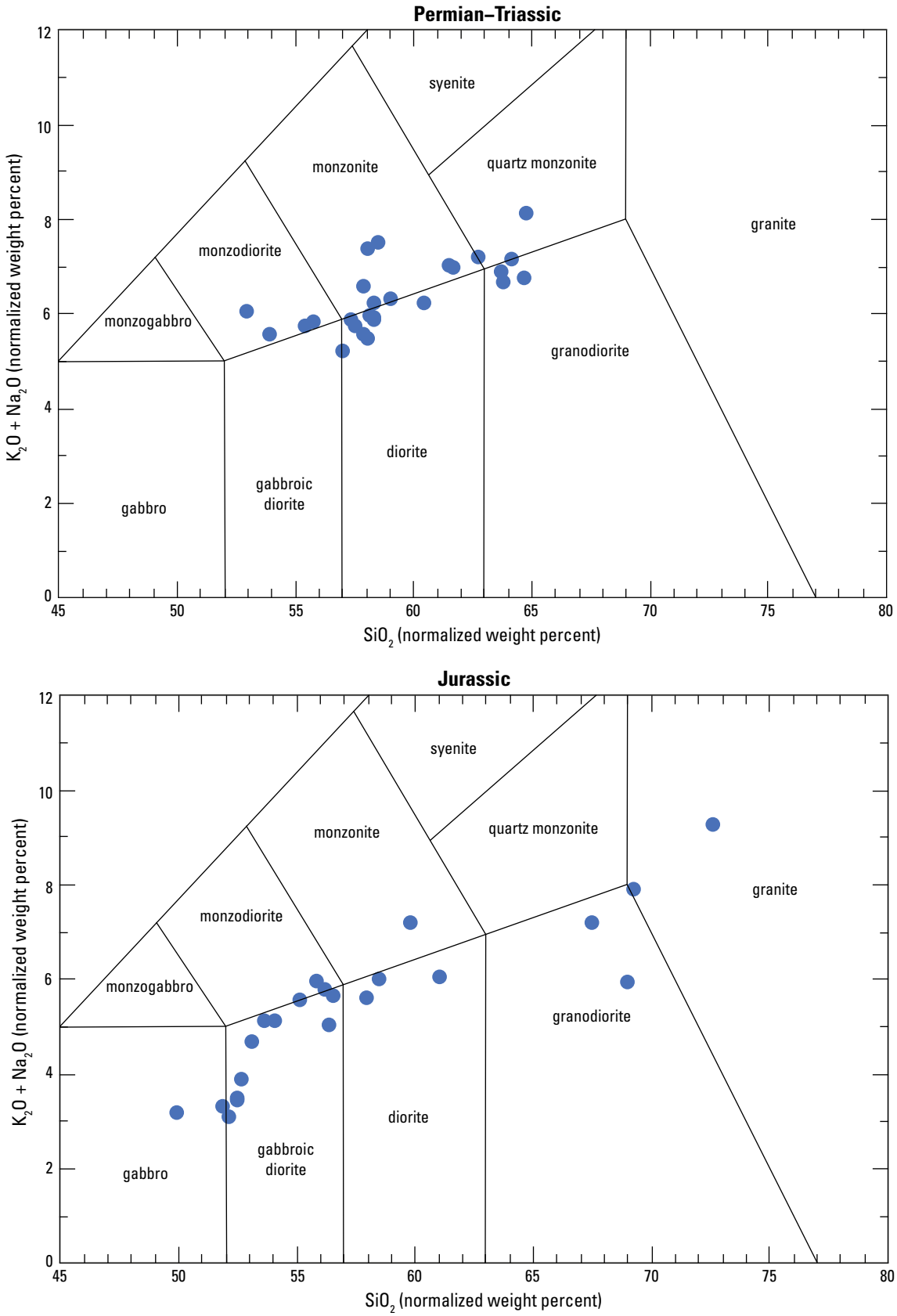

Figure 7. Modified total alkali-silica (TAS) diagrams showing the classification of samples included in this report. Plutonic rock names are from Middlemost (1994). Note the contrast between the compositionally expanded Jurassic suite and the less variable Permian–Triassic suite. Oxide values are in normalized weight percent (table 57).

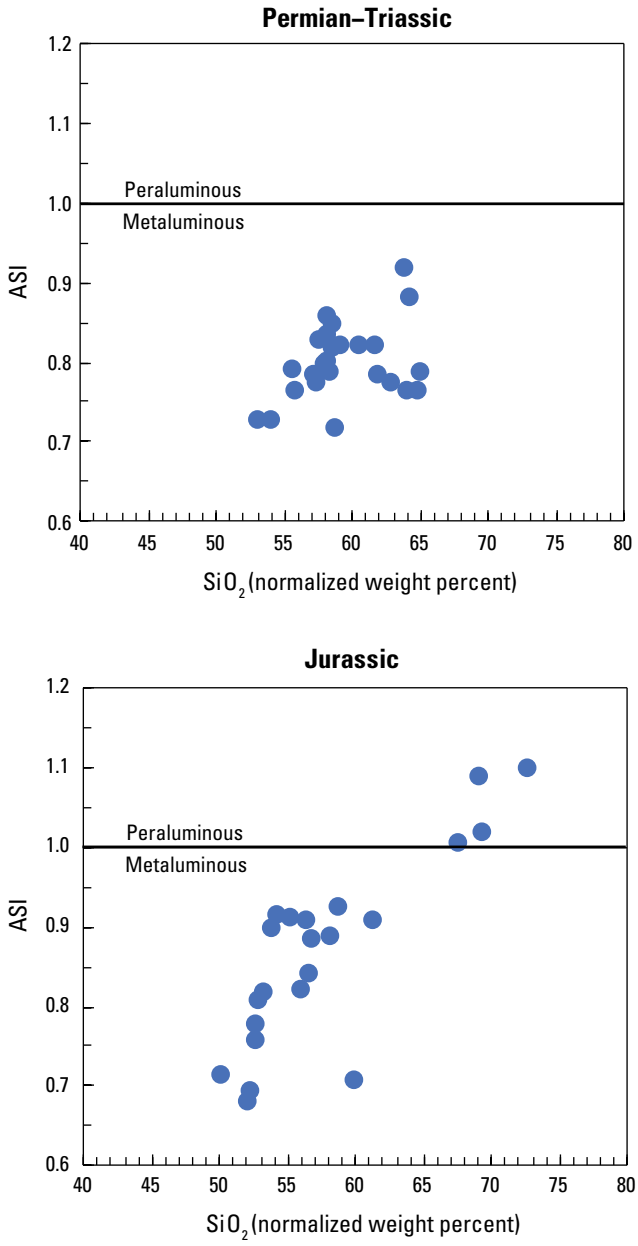

Figure 8. Diagrams showing the aluminum saturation index (ASI) (Frost and others, 2001) for samples included in this report. ASI is the molecular ratio Al/(Ca–1.67P+Na+K). The value of each element in this expression is calculated by dividing the normalized weight percent of the corresponding oxide (table 57) by the molecular weight of that oxide.

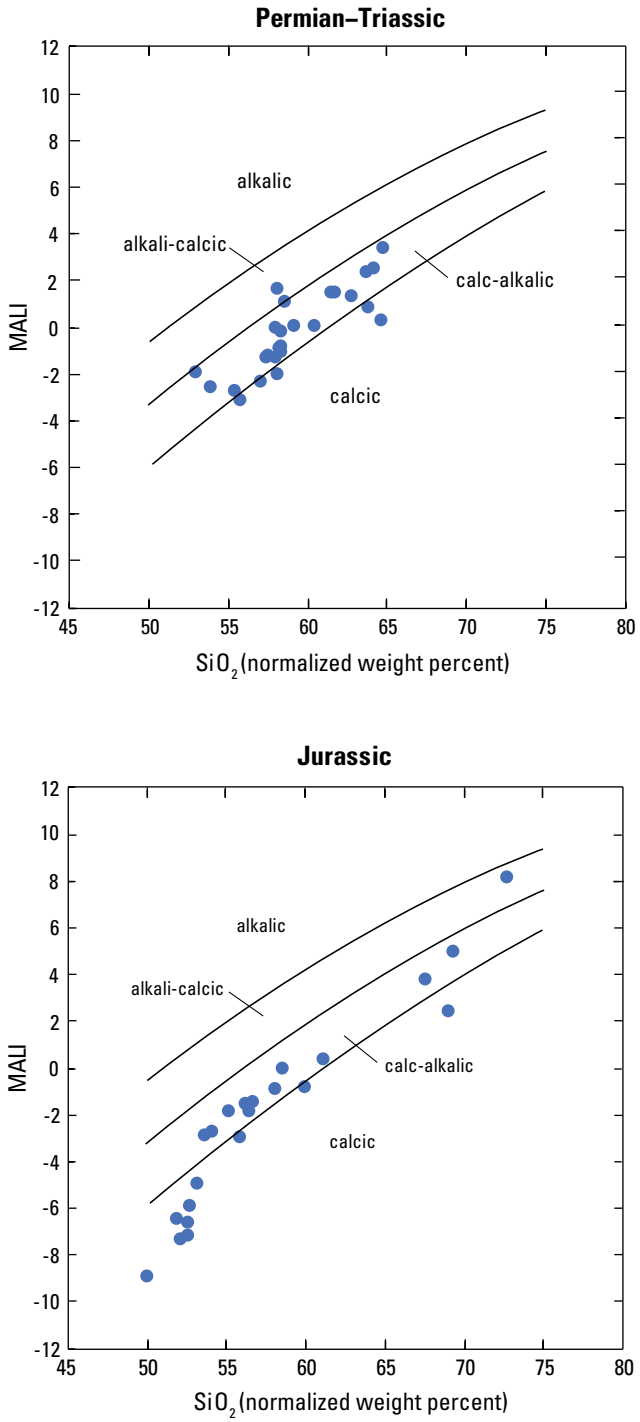

Figure 9. Diagrams showing the modified alkali-lime index (MALI) (Frost and others, 2001) for samples included in this report. MALI = $Na_2O + K_2O - CaO$. Oxide values are in normalized weight percent (table 57).

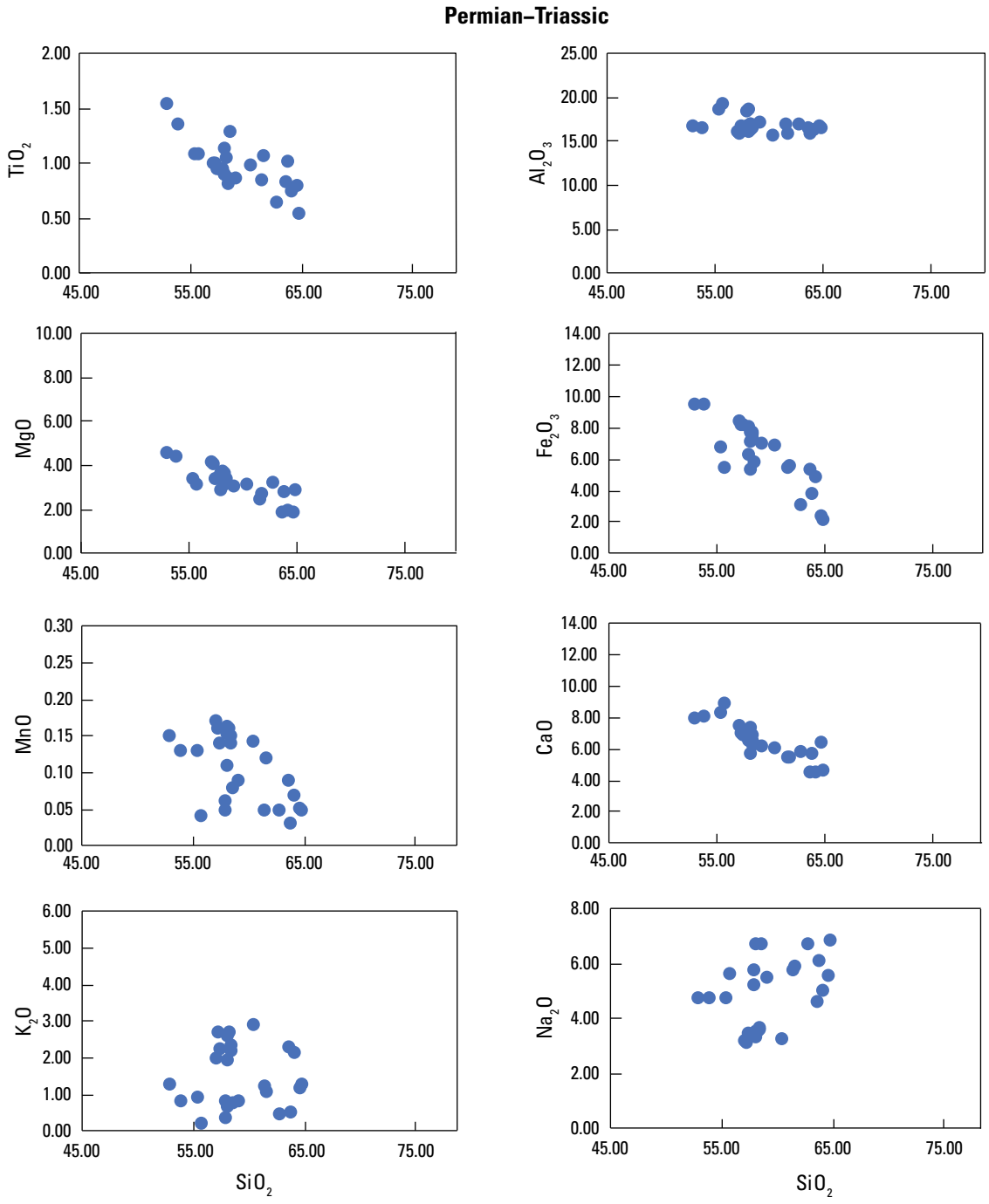

Figure 10. Harker diagrams showing variations in the abundances of selected oxides with respect to silica (SiO_2) in samples from Permian–Triassic plutonic rocks included in this report. Oxides are titanium (TiO_2), aluminum (Al_2O_3), magnesium (MgO), iron (Fe_2O_3), manganese (MnO), calcium (CaO), potassium (K_2O), and sodium (Na_2O). Oxide values are in normalized weight percent (table 57).

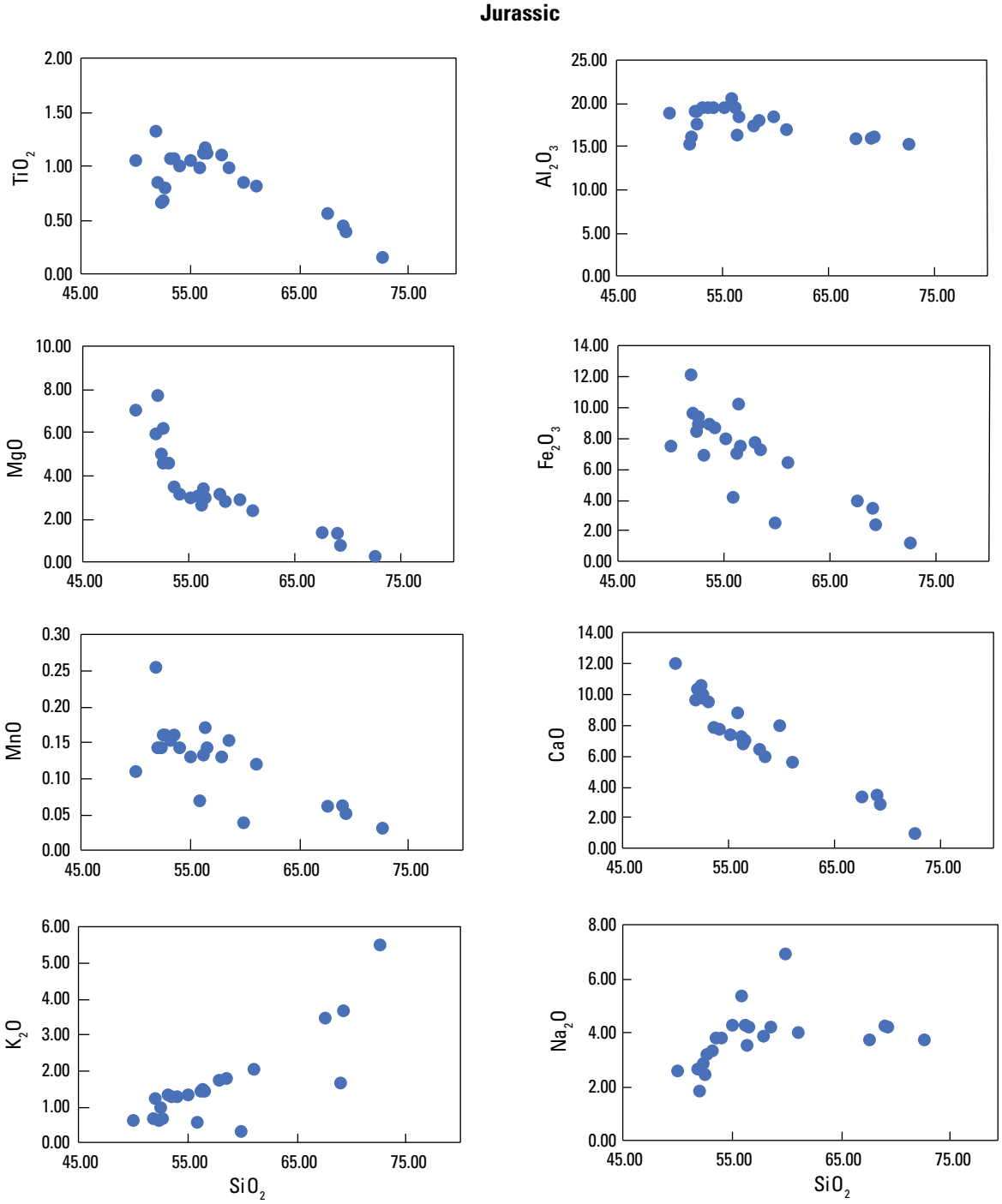

Figure 11. Harker diagrams showing variations in the abundances of selected oxides with respect to silica (SiO_2) in samples from Late Jurassic plutonic rocks included in this report. Oxides are titanium (TiO_2), aluminum (Al_2O_3), magnesium (MgO), iron (Fe_2O_3), manganese (MnO), calcium (CaO), potassium (K_2O), and sodium (Na_2O). Oxide values are in normalized weight percent (table 57).

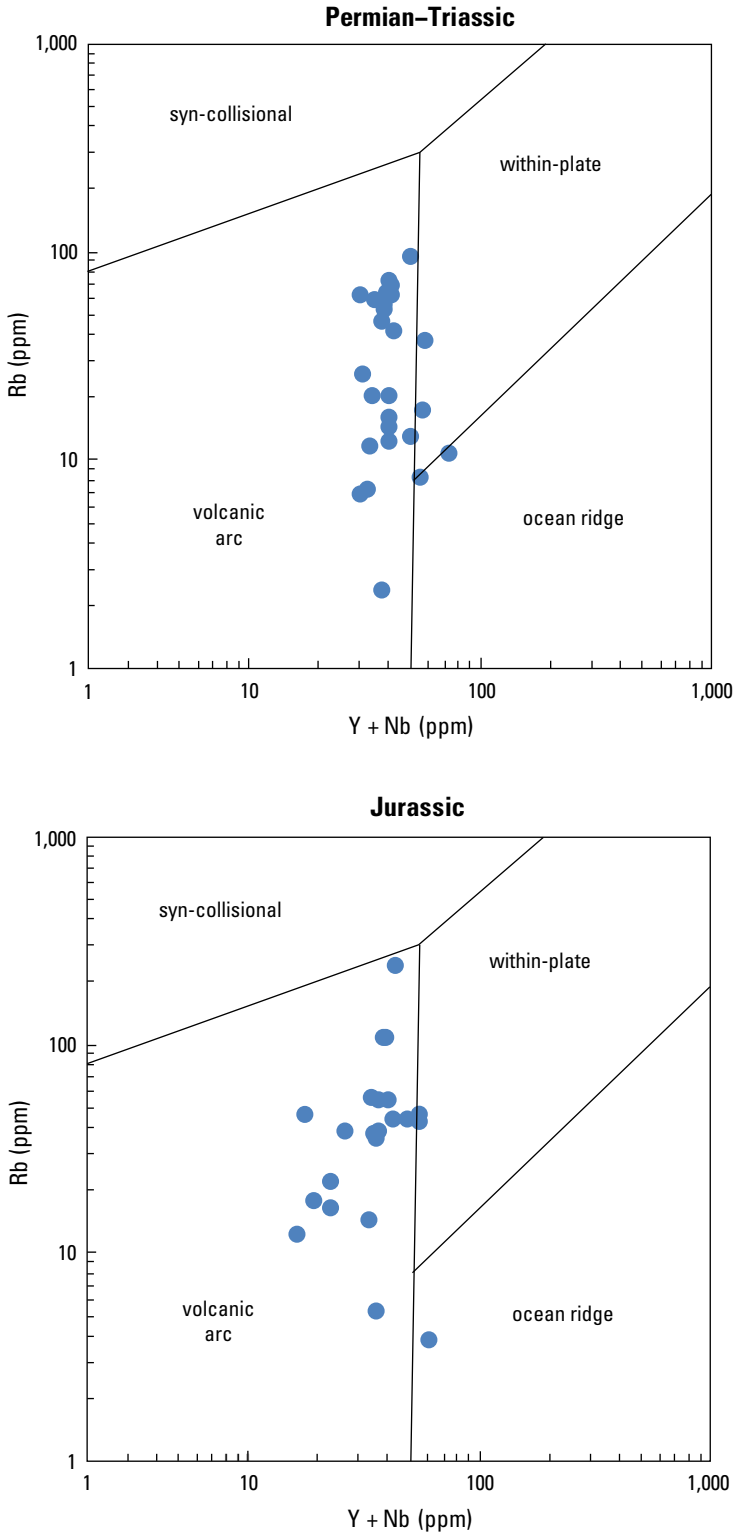

Figure 12. Diagrams showing Rb versus Y + Nb in samples included in this report, with their inferred intrusive settings (Pearce and others, 1984). Concentrations are in parts per million (ppm) (tables 50–55).

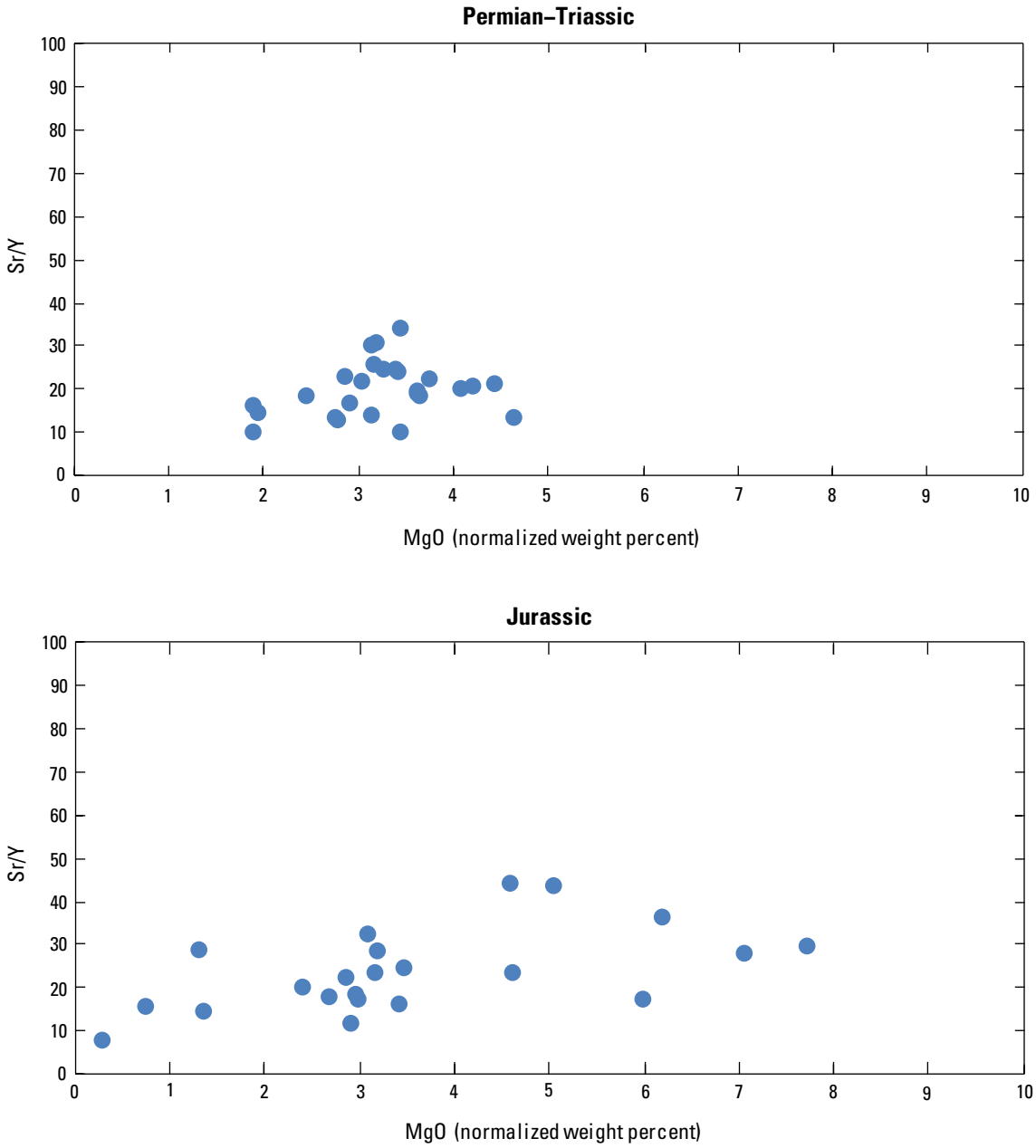

Figure 13. Diagrams showing Sr/Y versus MgO for samples included in this report. Concentrations of Sr and Y are in parts per million (tables 50–55); MgO is in normalized weight percent (table 57). For both suites, average Sr/Y ratio in samples with MgO between 2 and 4 normalized weight percent is ~20, consistent with a crustal thickness of 20–30 kilometers at the time of magmatic differentiation (Chapman and others, 2015; Chiaradia, 2015).

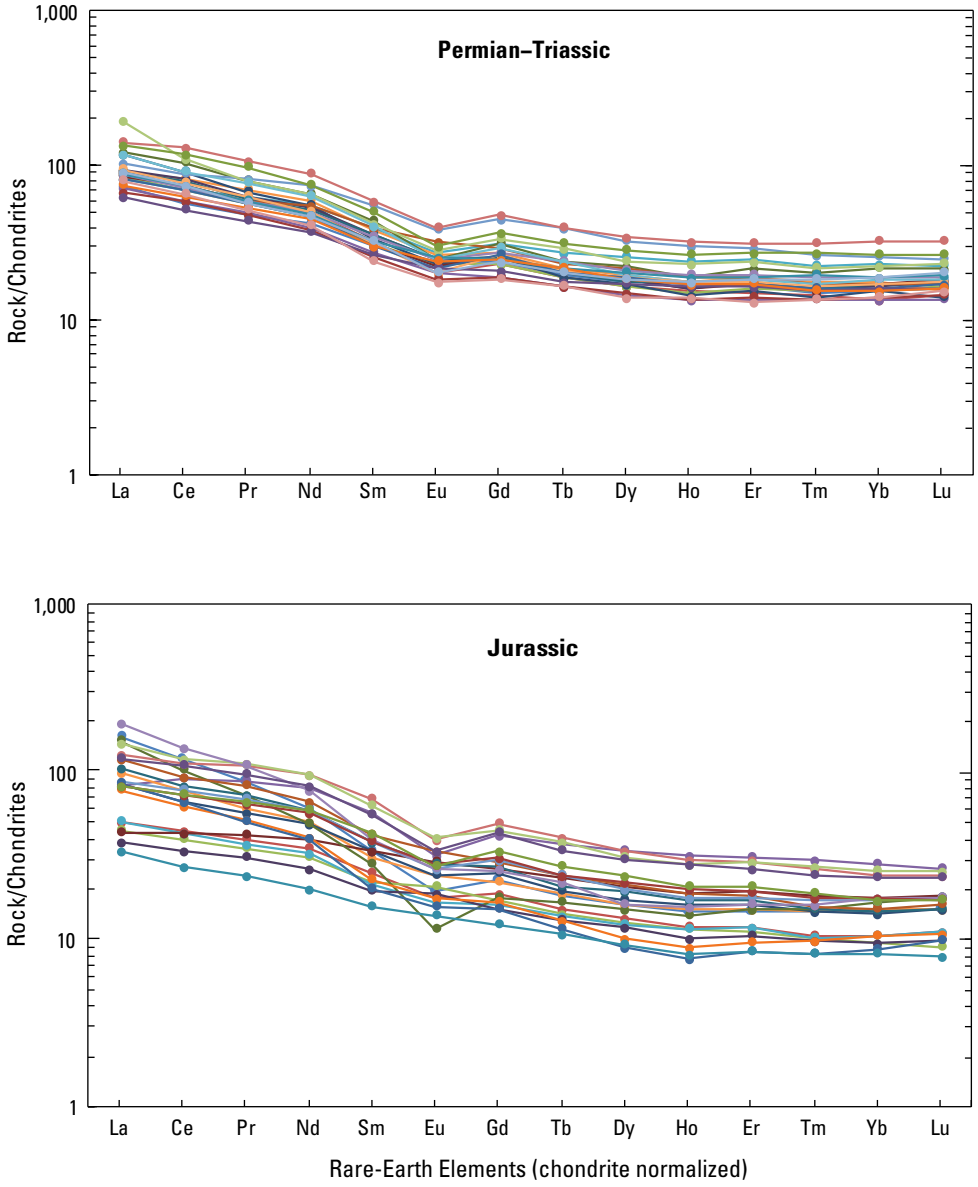

Figure 14. Diagrams showing rare earth element (REE) abundances normalized to chondrite values (Sun and McDonough, 1989) for samples included in this report. Y-axis indicates the relative abundances (in parts per million) of each element in the sampled rocks versus that in chondrites. See tables 50–55 for elemental concentrations.

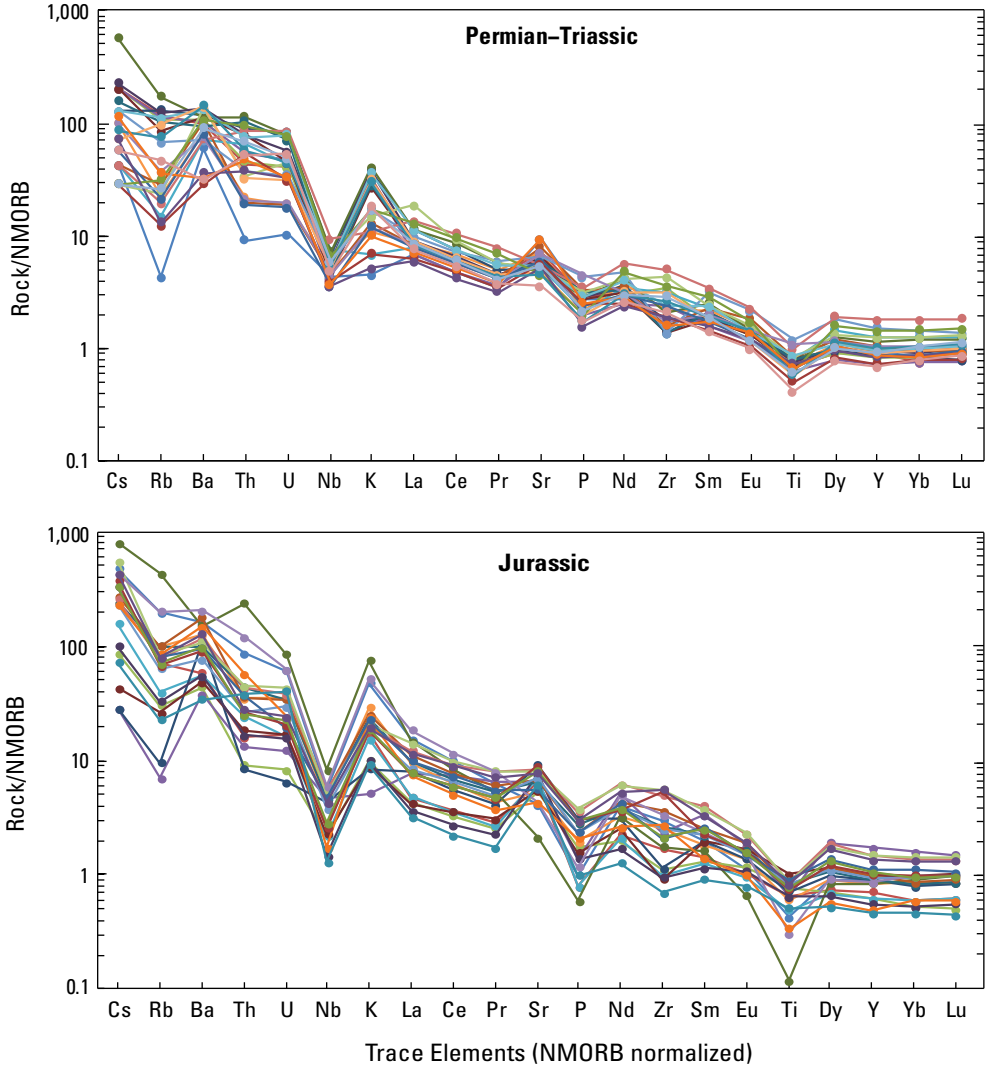

Figure 15. Diagrams showing trace element abundances normalized to normal midocean ridge basalt (NMORB) (Sun and McDonough, 1989) for samples included in this report. Y-axis indicates the relative abundances (in parts per million) of each element in the sampled rocks versus that in NMORB. See tables 50–55 for elemental concentrations.

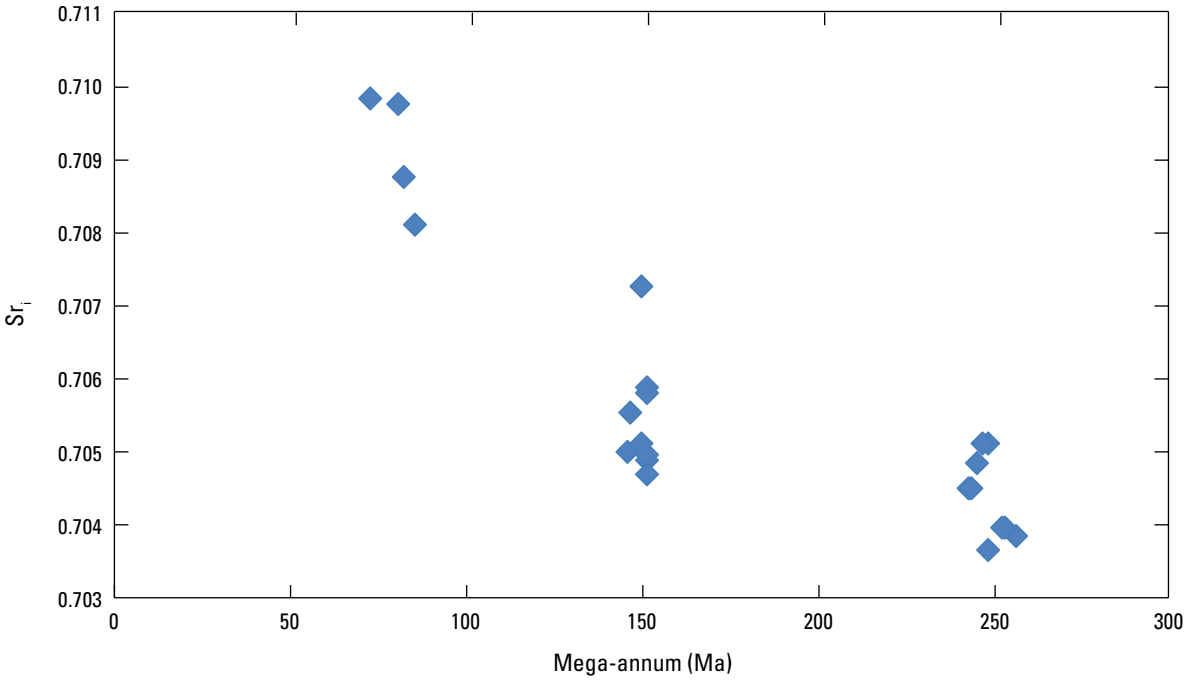

Figure 16. Diagram showing increase of $^{87}Sr/^{86}Sr$ ratio (Sr_i) with decreasing age of selected plutonic rock samples in the Lane Mountain area. This increase suggests an increasing involvement of Precambrian continental lithosphere in the generation of magmas through time. See table 58 for data.

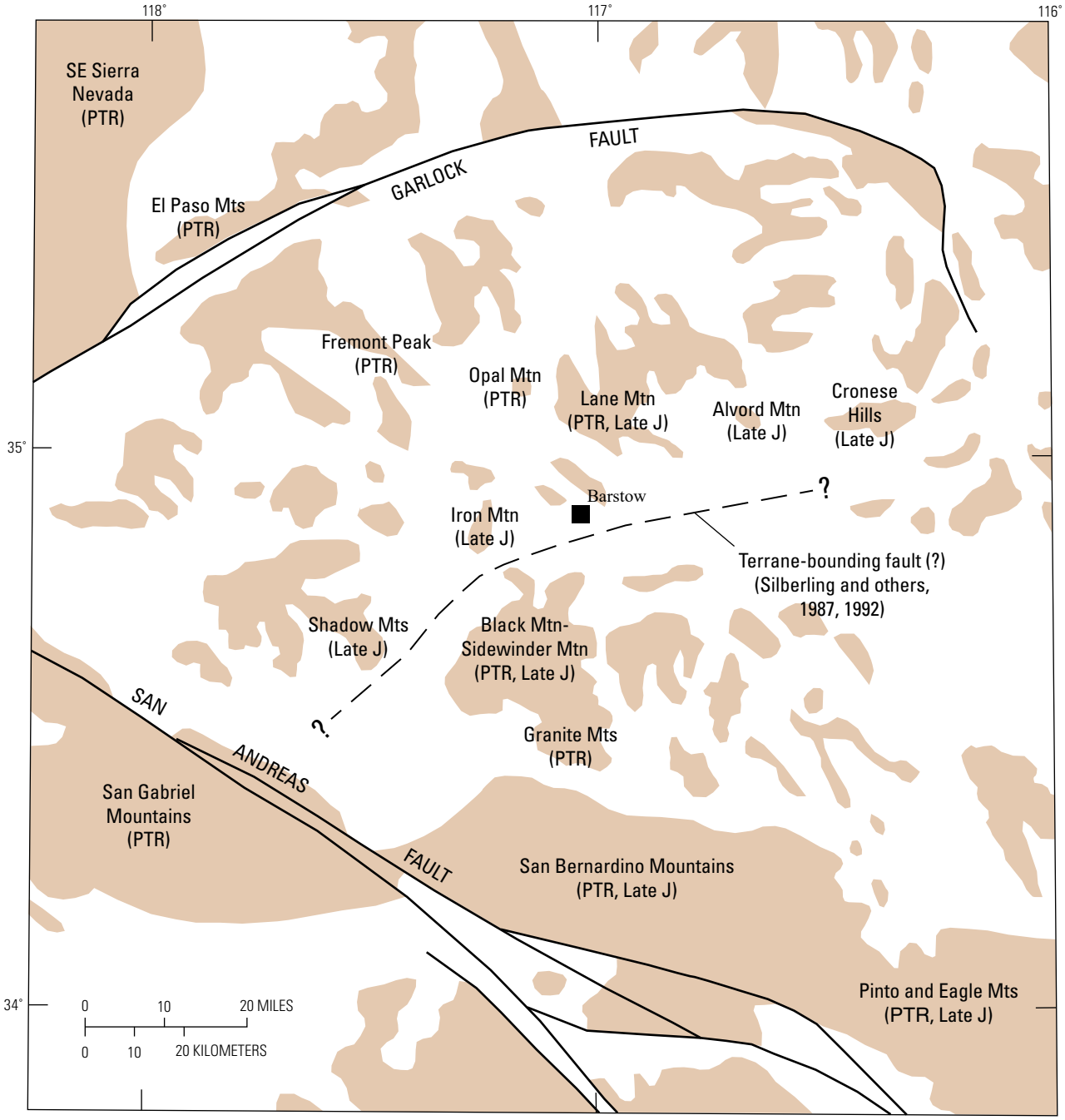

Figure 17. Map of Mojave Desert-San Bernardino Mountains region showing areas where plutonic rocks of Permian–Triassic (PTR) and Late Jurassic (Late J) ages are well documented, mainly by U-Pb zircon dating. Late Jurassic volcanic rocks also are included. Colored areas depict pre-Cenozoic bedrock outcrops (U.S. Geological Survey and California Division of Mines, 1966). Possible terrane-bounding fault (modified from Silberling and others, 1987, 1992) separates rocks of North American continental affinity to south from El Paso Terrane and other areas interpreted not to be underlain by thick continental lithosphere to north. See text for details and discussion.

Table 1. Location and basic lithologic, geochronologic, isotopic, and geochemical information for 48 plutonic rock samples studied for this report and the report of Stone and others (2019).

[Values for SiO_2 and K_2O+Na_2O are in normalized weight percent (volatile free). See tables 2–58 for detailed information. Abbreviations: avg., average; Ma, mega-annum; NAD27, North American Datum of 1927; Sri, initial $^{87}Sr/^{86}Sr$ ratio; wt. %, weight percent; —, no data]

Sample number	Latitude (°N) longitude (°W) (NAD27)	Map unit (fig. 3)	Unit of McCulloh (1960)	Lithology	Age (Ma)	Sr_i	SiO_2 (wt. %)	K_2O+Na_2O (wt. %)
14-LM-1*	35° 05’ 50.9” 116° 52’ 16.8”	JPp	Daisy granodiorite	Granodiorite	150.7±3.0	0.70590	67.50	7.21
14-LM-16	35° 07’ 20.0” 116° 55’ 59.0”	JPp	Larrea complex	Monzodiorite	244.7±4.4	—	55.71	5.85
14-LM-43*	35° 10’ 24.0” 116° 56’ 32.1”	JPp	Larrea complex	Diorite	252.8±1.9	0.70396	57.47	5.73
14-LM-106	35° 06’ 27.5” 116° 54’ 36.7”	JPp	Larrea complex	Gabbroic diorite	150.6±2.7	0.70490	52.10	3.08
14-LM-154*	35° 06’ 07.2” 116° 54’ 03.2”	JPp	Larrea complex	Gabbro	146.0±3.8	0.70553	49.96	3.17
14-LM-468	35° 06’ 44.5” 116° 55’ 42.6”	JPp	Larrea complex	Monzonite	148.6±4.7	—	59.84	7.21
14-LM-479	35° 06’ 57.9” 116° 55’ 47.3”	JPp	Larrea complex	Gabbroic diorite	147.4±4.1	—	52.51	3.44
14-LM-490*	35° 06’ 51.6” 116° 55’ 12.4”	JPp	Larrea complex	Diorite	148.9±2.6	0.70511	61.08	6.07
15-LM-802A	35° 07’ 02.5” 116° 56’ 32.5”	JPp	Larrea complex	Diorite	248.4±3.6	—	58.31	5.87
15-LM-806	35° 07’ 10.5” 116° 55’ 57.9”	JPp	Larrea complex	Monzodiorite	154.0±5.1	—	55.81	5.96
15-LM-810	35° 06’ 57.9” 116° 56’ 00.4”	JPp	Larrea complex	Gabbro	151.2±2.9	—	51.82	3.32
15-LM-816	35° 07’ 16.0” 116° 56’ 23.4”	JPp	Larrea complex	Diorite	250.7±3.8	—	58.32	5.94
17-LM-1385	35° 01’ 38.8” 116° 48’ 39.1”	JPp	Pink biotite granite	Granite	150.8±1.8	0.70495	72.59	9.28
17-LM-1562	35° 11’ 15.9” 116° 56’ 15.5”	JPp	Larrea complex	Granodiorite	244.5±4.4	0.70487	63.80	6.65
17-LM-1656	35° 06’ 32.3” 116° 56’ 17.4”	JPp	Larrea complex	Gabbroic diorite	150.5±7.0	0.70471	52.66	3.88
17-LM-1688	35° 07’ 32.3” 116° 55’ 35.8”	JPp	Larrea complex	Monzonite	241.7±5.2	0.70450	57.89	6.59
17-LM-1748	35° 08’ 12.0” 116° 52’ 40.1”	JPp	Larrea complex	Diorite	148.3±2.5	—	57.95	5.61
17-LM-1749	35° 01’ 33.0” 116° 48’ 28.1”	JPp	Larrea complex	Diorite	150.8±2.3	0.70582	58.48	6.01
17-LM-1771	35° 09’ 03.8” 116° 56’ 11.6”	JPp	Larrea complex	Monzonite	250.5±3.5	—	58.30	6.22
17-LM-1779	35° 08’ 51.8” 116° 56’ 42.2”	JPp	Larrea complex	Diorite	247.9±3.3	0.70366	58.04	5.46
17-LM-1792	35° 11’ 10.8” 116° 56’ 29.7”	JPp	Larrea complex	Diorite	249.7±3.5	—	60.39	6.21
17-LM-1835	35° 11’ 52.3” 116° 56’ 56.6”	JPp	Larrea complex	Diorite	248.8±3.8	—	57.30	5.87
17-LM-1837	35° 11’ 41.7” 116° 57’ 03.2”	JPp	Larrea complex	Diorite	243.7±3.4	—	57.01	5.21
17-LM-1860	35° 11’ 58.7” 116° 56’ 17.3”	JPp	Larrea complex	Monzodiorite	252.4±5.2	—	55.41	5.73

Table 1.—Continued

Sample number	Latitude (°N) longitude (°W) (NAD27)	Map unit (fig. 3)	Unit of McCulloh (1960)	Lithology	Age (Ma)	Sr_i	SiO_2 (wt. %)	K_2O+Na_2O (wt. %)
17-LM-1992	35° 07' 32.9" 116° 55' 22.6"	JPp	Larrea complex	Monzodiorite	252.0±9.5	0.70396	52.93	6.05
17-LM-2000	35° 07' 23.0" 116° 55' 26.3"	—	Larrea complex (unmapped)	Monzonite	248.2±4.0	—	58.49	7.53
17-LM-2001	35° 07' 24.8" 116° 55' 19.2"	JPp	Larrea complex	Monzonite	250.8±5.2	—	61.64	6.98
17-LM-2002	35° 07' 28.0" 116° 55' 22.4"	JPp	Larrea complex	Monzodiorite	246.3±4.4	—	53.87	5.58
17-LM-2112	35° 07' 23.8" 116° 54' 50.7"	JPp	Larrea complex	Gabbroic diorite	148.2±5.2	—	53.13	4.67
17-LM-2113	35° 04' 54.3" 116° 56' 48.0"	JPp	Larrea complex	Diorite	249.3±5.6	—	58.11	5.97
17-LM-2127	35° 07' 36.9" 116° 54' 13.0"	JPp	Larrea complex	Monzodiorite	147.9±4.5	—	56.15	5.77
17-LM-2128	35° 07' 25.3" 116° 54' 17.5"	JPp	Larrea complex	Gabbroic Diorite	146.1±4.3	—	56.57	5.67
17-LM-2191	35° 01' 38.7" 116° 49' 41.3"	JPp	Larrea complex	Granite	149.2±3.4	0.70725	69.25	7.91
17-LM-2203	35° 04' 27.1" 116° 55' 52.4"	—	Larrea complex (unmapped)	Granodiorite	146.9±4.6	—	68.97 (avg.)	5.92 (avg.)
18-LM-2594	35° 05' 03.2" 116° 56' 26.2"	JPp	Larrea complex	Gabbroic diorite	147.6±3.2	—	56.40	5.06
18-LM-2595	35° 04' 46.3" 116° 56' 14.6"	—	Larrea complex (unmapped)	Granodiorite	249.3±5.1	—	63.65	6.91
18-LM-2603	35° 04' 58.1" 116° 56' 41.2"	JPp	Larrea complex	Gabbroic diorite	144.6±3.6	0.70500	54.08	5.12
18-LM-2604	35° 04' 44.4" 116° 56' 31.3"	JPp	Larrea complex	Monzonite	241.9±3.9	—	59.04	6.33
18-LM-2607	35° 04' 25.0" 116° 55' 44.5"	JPp	Larrea complex	Gabbroic diorite	148.7±3.2	—	53.62	5.12
18-LM-2725	35° 03' 58.5" 116° 54' 56.2"	JPp	Larrea complex	Monzodiorite	151.5±2.8	—	55.12	5.57
18-LM-2744	35° 03' 58.0" 116° 56' 18.3"	—	Larrea complex (unmapped)	Quartz monzonite	237.3±7.3	—	62.72	7.21
18-LM-2756	35° 06' 27.3" 116° 56' 59.5"	JPp	Larrea complex	Gabbroic diorite	150.5±2.0	—	52.46	3.50
18-LM-2809	35° 07' 18.6" 116° 55' 23.1"	—	Larrea complex (unmapped)	Granodiorite	253.7±3.7	—	64.65	6.77
18-LM-2997	35° 04' 36.2" 116° 56' 05.1"	—	Larrea complex (unmapped)	Diorite	257.8±4.2	—	57.88	5.57
18-LM-3042	35° 09' 03.7" 116° 55' 33.8"	JPp	Larrea complex	Quartz monzonite	248.7±3.5	—	64.08	7.17
19-LM-3063	35° 07' 57.7" 116° 55' 35.9"	JPp	Larrea complex	Monzonite	247.7±7.8	0.70511	58.07	7.39
19-LM-3160	35° 07' 02.8" 116° 55' 41.3"	JPp	Larrea complex	Monzonite	243.1±4.7	0.70451	61.48	7.04
19-LM-3210	35° 03' 29.8" 116° 56' 16.3"	—	Larrea complex (unmapped)	Quartz monzonite	246.2±6.1	0.70512	64.75	8.14

*Indicates samples reported by Stone and others (2019).

Table 2. Sensitive high-resolution ion microprobe-reverse geometry (SHRIMP-RG) U-Pb zircon data for sample 14-LM-1, Lane Mountain area, California.

[Spot designation indicates sample number, crystal number, and spot number for each zircon analysis. Pb, lead; Pb_c, common lead; U, uranium; Th, thorium; ppm, part per million; Ma, mega-annum; MSWD, mean square weighted deviation; N, number of zircon spot analyses; %, percent; —, not applicable]

Sample 14-LM-1 (Stone and others, 2019)													
Spot	$^{204}Pb/^{206}Pb$	±%	$^{207}Pb/^{206}Pb$	±%	$^{208}Pb/^{206}Pb$	±%	$\%\ ^{206}Pb_c$	ppm U	ppm Th	Total $^{206}Pb/^{238}U$	±%	$^{206}Pb/^{238}U$ age ± error (Ma)	
1-01.1	—	—	0.0504	4.3	0.17	4.9	0.16	143	70	0.0237	2.6	151	4
1-02.1†	$6.1E^{-4}$	18	0.0621	2.2	0.12	3.7	1.77	1834	604	0.0158	3.9	100	4
1-03.1	$9.9E^{-4}$	38	0.0500	4.2	0.14	5.4	0.11	121	53	0.0240	3.8	153	6
1-04.1	$5.1E^{-4}$	58	0.0520	4.5	0.18	5.2	0.36	109	55	0.0239	3.3	152	5
1-05.1	$1.2E^{-4}$	100	0.0477	4.0	0.16	4.6	−0.17	149	71	0.0236	2.9	151	4
1-06.2†	$8.9E^{-4}$	33	0.0590	3.4	0.11	5.2	1.21	387	100	0.0261	1.9	164	3
1-07.2	$6.5E^{-4}$	45	0.0531	3.9	0.15	5.0	0.52	134	54	0.0230	3.1	146	4
1-08.2	$-5.7E^{-4}$	58	0.0559	4.7	0.15	11.9	0.87	100	46	0.0236	3.1	149	5
1-09.2	$3.9E^{-4}$	100	0.0740	6.1	0.26	6.6	3.09	140	88	0.0272	3.3	167	6
1-10.2	$1.6E^{-4}$	100	0.0531	4.3	0.17	5.0	0.51	123	56	0.0233	3.0	148	4
1-11.2	$6.0E^{-4}$	33	0.0546	2.8	0.18	5.3	0.73	301	135	0.0216	4.1	137	6
1-12.1	—	—	0.0486	3.6	0.24	3.5	−0.07	195	143	0.0240	3.4	153	5
1-13.1	$1.4E^{-3}$	32	0.0569	14.0	0.24	12.1	0.97	129	84	0.0247	2.6	156	4
1-14.1	$1.0E^{-3}$	35	0.0514	4.4	0.17	4.6	0.29	142	66	0.0242	3.8	153	6
1-15.1	$4.6E^{-4}$	50	0.0518	3.9	0.25	3.6	0.35	158	109	0.0233	3.3	148	5

†Spots were statistically rejected from mean age determinations.

Mean age of coherent group (N=13)	150.7 Ma
Age error (95% confidence, without error in standard)	2.7 Ma
MSWD	1.61
Probability of fit	0.08
Age error (95% confidence, with error in standard)	3.0 Ma
Final age and error (Ma)	150.7 ± 3.0 Ma

Table 3. Sensitive high-resolution ion microprobe-reverse geometry (SHRIMP-RG) U-Pb zircon data for sample 14-LM-16, Lane Mountain area, California.

[Spot designation indicates sample number, crystal number, and spot number for each zircon analysis. Pb, lead; Pb_c, common lead; U, uranium; Th, thorium; ppm, part per million; Ma, mega-annum; MSWD, mean square weighted deviation; N, number of zircon spot analyses; %, percent]

Sample 14-LM-16 (this report)													
Spot	$^{204}Pb/^{206}Pb$	±%	$^{207}Pb/^{206}Pb$	±%	$^{208}Pb/^{206}Pb$	±%	% $^{206}Pb_c$	ppm U	ppm Th	Total $^{206}Pb/^{238}U$	±%	$^{206}Pb/^{238}U$ age ± error (Ma)	
Run 1													
16-01.1	$5.7E^{-5}$	100	0.0530	2.7	0.186	4.2	0.232	150	92	0.0388	2.2	245	5
16-02.1	$2.8E^{-4}$	25	0.0541	1.5	0.413	1.5	0.360	462	604	0.0394	1.5	248	4
16-03.1	$1.4E^{-4}$	58	0.0515	5.3	0.142	7.0	0.038	209	100	0.0395	2.6	250	7
16-04.1	$5.2E^{-4}$	45	0.0496	3.9	0.208	5.4	−0.197	77	60	0.0390	2.5	247	6
16-05.1	$-9.3E^{-5}$	71	0.0535	2.5	0.212	3.6	0.289	184	117	0.0393	2.5	248	6
Run 2													
16-06.1	$1.8E^{-4}$	261	0.0504	5.4	0.276	3.3	−0.053	111	92	0.0363	1.4	230	3
16-07.1	$-8.5E^{-5}$	1158	0.0451	8.9	0.212	5.7	−0.747	46	29	0.0381	2.3	243	6
16-08.1	$-2.6E^{-4}$	310	0.0536	7.1	0.213	5.1	0.321	59	41	0.0384	1.5	242	4
16-09.1	$-1.2E^{-3}$	104	0.0412	9.8	0.220	6.1	−1.222	41	27	0.0376	2.4	241	6
16-10.1	$-1.4E^{-4}$	327	0.0538	5.1	0.296	3.5	0.352	109	106	0.0382	1.4	241	3
16-11.1	$1.2E^{-4}$	175	0.0544	3.4	0.368	1.9	0.412	252	286	0.0389	1.6	245	4
16-12.1†	$-5.7E^{-5}$	310	0.0518	3.3	0.137	4.9	0.156	286	112	0.0348	1.7	220	4
16-13.1	$6.0E^{-5}$	261	0.0502	3.2	0.946	1.1	−0.088	304	871	0.0374	1.3	237	3
16-14.1	$6.9E^{-5}$	275	0.0466	3.5	0.329	1.9	−0.572	273	279	0.0391	1.3	248	3
16-15.1	$6.8E^{-4}$	130	0.0453	7.5	0.222	4.9	−0.714	58	36	0.0378	2.0	241	5
16-16.1	$4.5E^{-4}$	136	0.0413	6.5	0.239	3.9	−1.249	89	68	0.0393	1.4	252	4
16-17.1	$-4.6E^{-5}$	1,226	0.0514	5.9	0.281	3.7	0.060	93	75	0.0374	2.4	237	6

†Spots were statistically rejected from mean age determinations.

Run 1	
Mean age of coherent group (N=5)	247.6 Ma
Age error (95% confidence, without error in standard)	4.6 Ma
MSWD	0.11
Probability of fit	0.98
Age error (95% confidence, with error in standard)	5.2 Ma
Run 2	
Mean age of coherent group (N=10)	243.2 Ma
Age error (95% confidence, without error in standard)	2.5 Ma
MSWD	1.58
Probability of fit	0.12
Age error (95% confidence, with error in standard)	3.2 Ma
Final age and error (statistical mean of both runs)	244.7 ± 4.4 Ma

Table 4. Sensitive high-resolution ion microprobe-reverse geometry (SHRIMP-RG) U-Pb zircon data for sample 14-LM-43, Lane Mountain area, California.

[Spot designation indicates sample number, crystal number, and spot number for each zircon analysis. Pb, lead; Pb_c, common lead; U, uranium; Th, thorium; ppm, part per million; Ma, mega-annum; MSWD, mean square weighted deviation; N, number of zircon spot analyses; %, percent; —, not applicable]

Sample 14-LM-43 (Stone and others, 2019)													
Spot	$^{204}Pb/^{206}Pb$	±%	$^{207}Pb/^{206}Pb$	±%	$^{208}Pb/^{206}Pb$	±%	% $^{206}Pb_c$	ppm U	ppm Th	Total $^{206}Pb/^{238}U$	±%	$^{206}Pb/^{238}U$ age ± error (Ma)	
43-01.1	$2.9E^{-5}$	58	0.0495	1.1	0.125	2.8	−0.217	757	281	0.0395	1.2	250	3
43-01.2	$1.2E^{-4}$	71	0.0508	2.7	0.188	2.2	−0.069	117	64	0.0405	2.0	256	5
43-02.1	$2.4E^{-4}$	38	0.0493	2.1	0.228	1.5	−0.220	204	141	0.0385	1.3	244	3
43-03.1	$-1.3E^{-4}$	58	0.0503	2.3	0.093	2.6	−0.076	171	47	0.0373	2.6	236	6
43-04.1	—	—	0.0503	4.0	0.218	1.7	−0.113	176	124	0.0394	1.9	249	5
43-05.1	$9.0E^{-5}$	58	0.0481	2.0	0.222	1.4	−0.408	242	169	0.0406	1.1	258	3
43-06.1	—	—	0.0483	2.9	0.258	1.8	−0.368	135	104	0.0395	1.3	251	3
43-07.1	$1.5E^{-4}$	50	0.0486	2.2	0.273	1.6	−0.330	184	152	0.0396	2.2	251	6
43-08.1	$-1.7E^{-5}$	71	0.0508	1.0	0.161	1.8	−0.051	880	437	0.0395	1.3	250	3
43-09.1	$2.5E^{-5}$	71	0.0510	1.2	0.141	1.1	−0.034	612	270	0.0399	1.5	253	4
43-09.2	$6.6E^{-5}$	41	0.0505	1.2	0.220	0.9	−0.098	659	451	0.0402	1.8	254	5
43-10.1	—	—	0.0509	2.3	0.225	1.6	−0.045	180	126	0.0398	1.8	252	5
43-11.1	$1.6E^{-4}$	45	0.0513	2.0	0.232	1.5	0.016	228	162	0.0395	2.7	250	7
43-12.1†	$1.2E^{-3}$	19	0.0532	2.3	0.237	3.0	0.258	169	114	0.0386	0.8	244	2
43-13.1	$9.1E^{-5}$	71	0.0505	4.4	0.144	5.1	−0.115	174	78	0.0407	2.1	257	5
43-14.1	—	—	0.0491	1.1	0.016	2.8	−0.278	802	37	0.0404	1.6	256	4
43-15.1	$2.0E^{-4}$	45	0.0503	5.3	0.246	1.6	−0.129	178	133	0.0399	1.9	253	5
43-16.1	$6.2E^{-5}$	71	0.0505	2.0	0.176	1.6	−0.118	219	119	0.0410	1.8	259	5
43-17.1	$2.3E^{-3}$	70	0.0836	13.9	0.264	9.6	4.061	206	109	0.0399	3.2	242	8
43-18.1	$8.9E^{-5}$	24	0.0515	0.8	0.153	0.7	0.010	1,500	671	0.0413	2.4	261	6
43-18.2	$6.6E^{-5}$	100	0.0459	3.0	0.127	2.8	−0.671	114	42	0.0399	0.9	254	2
43-19.1	$6.2E^{-5}$	38	0.0490	1.1	0.159	0.9	−0.289	997	514	0.0400	2.1	254	5
43-20.1	$1.5E^{-4}$	71	0.0527	3.0	0.194	2.4	0.155	105	62	0.0410	2.5	258	6
43-21.1	$3.3E^{-5}$	58	0.0505	2.5	0.091	1.3	−0.130	751	186	0.0416	2.2	263	6
43-21.2	$3.6E^{-5}$	100	0.0480	2.2	0.179	1.7	−0.413	222	120	0.0401	1.2	254	3
43-22.1	$3.3E^{-5}$	71	0.0514	1.4	0.124	1.4	0.010	502	190	0.0400	1.3	253	3
43-22.2	$2.6E^{-5}$	45	0.0504	0.8	0.018	2.0	−0.118	1,450	81	0.0401	1.2	254	3

†Spots were statistically rejected from mean age determinations.

Mean age of coherent group (N=26)	252.8 Ma
Age error (95% confidence, without error in standard)	1.5 Ma
MSWD	1.29
Probability of fit	0.15
Age error (95% confidence, with error in standard)	1.9 Ma
Final age and error (Ma)	252.8 ± 1.9 Ma

Table 5. Sensitive high-resolution ion microprobe-reverse geometry (SHRIMP-RG) U-Pb zircon data for sample 14-LM-106, Lane Mountain area, California.

[Spot designation indicates sample number, crystal number, and spot number for each zircon analysis. Pb, lead; Pb_c, common lead; U, uranium; Th, thorium; ppm, part per million; Ma, mega-annum; MSWD, mean square weighted deviation; N, number of zircon spot analyses; %, percent]

Sample 14-LM-106 (this report)													
Spot	$^{204}Pb/^{206}Pb$	±%	$^{207}Pb/^{206}Pb$	±%	$^{208}Pb/^{206}Pb$	±%	% $^{206}Pb_c$	ppm U	ppm Th	Total $^{206}Pb/^{238}U$	±%	$^{206}Pb/^{238}U$ age ± error (Ma)	
106-01.1	$2.2E^{-3}$	58	0.0653	12.5	0.251	9.8	2.033	71	33	0.0242	3.9	151	6
106-02.1	$1.3E^{-3}$	46	0.0564	4.2	0.174	7.1	0.927	207	101	0.0232	1.9	146	3
106-03.1	$3.9E^{-4}$	58	0.0508	5.6	0.262	9.0	0.222	412	312	0.0237	1.9	150	3
106-04.1	$9.2E^{-5}$	206	0.0505	7.5	0.209	4.3	0.177	425	297	0.0235	1.8	150	3
106-05.1†	$2.8E^{-5}$	206	0.0807	1.3	0.124	3.1	0.509	179	74	0.1878	1.9	1,104	21
106-06.1	$5.6E^{-4}$	54	0.0574	2.9	0.257	4.1	1.046	372	275	0.0240	2.1	151	3
106-07.1	$4.4E^{-4}$	82	0.0540	9.1	0.268	9.6	0.615	219	156	0.0243	1.6	154	3
106-08.1	$3.9E^{-4}$	93	0.0527	3.8	0.141	6.9	0.454	234	101	0.0240	2.8	152	4

†Spots were statistically rejected from mean age determinations.

Mean age of coherent group (N=7)	150.6 Ma
Age error (95% confidence, without error in standard)	2.4 Ma
MSWD	0.67
Probability of fit	0.67
Age error (95% confidence, with error in standard)	2.7 Ma
Final age and error (Ma)	150.6 ± 2.7 Ma

Table 6. Sensitive high-resolution ion microprobe-reverse geometry (SHRIMP-RG) U-Pb zircon data for sample 14-LM-154, Lane Mountain area, California.

[Spot designation indicates sample number, crystal number, and spot number for each zircon analysis. Pb, lead; Pb_c, common lead; U, uranium; Th, thorium; ppm, part per million; Ma, mega-annum; MSWD, mean square weighted deviation; N, number of zircon spot analyses; %, percent; —, not applicable]

Sample 14-LM-154 (Stone and others, 2019)													
Spot	$^{204}Pb/^{206}Pb$	±%	$^{207}Pb/^{206}Pb$	±%	$^{208}Pb/^{206}Pb$	±%	% $^{206}Pb_c$	ppm U	ppm Th	Total $^{206}Pb/^{238}U$	±%	$^{206}Pb/^{238}U$ age ± error (Ma)	
154-01.1†	$1.6E^{-3}$	41	0.0486	5.9	0.35	4.7	−0.02	120	101	0.0216	2.0	138	3
154-01.2†	$2.8E^{-4}$	41	0.0504	4.8	0.56	1.6	0.22	526	790	0.0206	2.7	131	4
154-02.1	$8.4E^{-4}$	58	0.0646	5.4	0.18	6.9	1.99	54	23	0.0212	3.7	133	5
154-02.2	$-3.8E^{-4}$	45	0.0476	3.2	0.21	3.2	−0.19	231	139	0.0234	3.9	150	6
154-03.2	$3.3E^{-5}$	100	0.0495	2.1	0.14	2.5	0.06	502	207	0.0235	3.1	150	5
154-04.1	$-3.8E^{-4}$	58	0.0520	4.0	0.17	8.5	0.38	133	61	0.0230	3.8	146	5
154-05.1	$6.4E^{-4}$	38	0.0562	3.2	0.16	4.0	0.90	210	89	0.0237	3.1	150	5
154-06.2	—	—	0.0482	2.7	0.22	2.7	−0.10	305	202	0.0227	4.1	145	6
154-07.1	$4.1E^{-5}$	100	0.0494	2.3	0.37	1.8	0.05	433	481	0.0232	3.5	148	5
154-07.2	$1.6E^{-4}$	71	0.0493	3.2	0.20	3.4	0.03	220	125	0.0233	3.2	148	5

†Spots were statistically rejected from mean age determinations.

Mean age of coherent group (N=8)	146.0 Ma
Age error (95% confidence, without error in standard)	3.6 Ma
MSWD	1.34
Probability of fit	0.22
Age error (95% confidence, with error in standard)	3.8 Ma
Final age and error	146.0 ± 3.8 Ma

Table 7. Sensitive high-resolution ion microprobe-reverse geometry (SHRIMP-RG) U-Pb zircon data for sample 14-LM-468, Lane Mountain area, California.

[Spot designation indicates sample number, crystal number, and spot number for each zircon analysis. Pb, lead; Pb_c, common lead; U, uranium; Th, thorium; ppm, part per million; Ma, mega-annum; MSWD, mean square weighted deviation; N, number of zircon spot analyses; %, percent]

Sample 14-LM-468 (this report)													
Spot	$^{204}Pb/^{206}Pb$	±%	$^{207}Pb/^{206}Pb$	±%	$^{208}Pb/^{206}Pb$	±%	% $^{206}Pb_c$	ppm U	ppm Th	Total $^{206}Pb/^{238}U$	±%	$^{206}Pb/^{238}U$ age ± error (Ma)	
468-01.1	$7.8E^{-4}$	41	0.0470	11.9	0.133	14.4	−0.260	109	57	0.0234	2.4	149	4
468-02.1	$-1.8E^{-4}$	100	0.0458	8.8	0.171	7.8	−0.400	78	44	0.0226	2.8	144	4
468-03.1	$5.7E^{-4}$	50	0.0522	8.9	0.177	6.7	0.391	97	52	0.0240	3.7	152	6
468-04.1	$9.2E^{-4}$	50	0.0469	5.8	0.161	16.6	−0.279	61	37	0.0236	3.5	151	5
468-05.1†	$-1.5E^{-4}$	100	0.0456	10.7	0.168	14.0	−0.457	95	51	0.0248	1.6	159	3

†Spots were statistically rejected from mean age determinations.

Mean age of coherent group (N=4)	148.6 Ma
Age error (95% confidence., without error in standard)	4.5 Ma
MSWD	0.56
Probability of fit	0.64
Age error (95% confidence, with error in standard)	4.7 Ma
Final age and error	148.6 ±4.7 Ma

Table 8. Sensitive high-resolution ion microprobe-reverse geometry (SHRIMP-RG) U-Pb zircon data for sample 14-LM-479, Lane Mountain area, California.

[Spot designation indicates sample number, crystal number, and spot number for each zircon analysis. Pb, lead; Pb_c, common lead; U, uranium; Th, thorium; ppm, part per million; Ma, mega-annum; MSWD, mean square weighted deviation; N, number of zircon spot analyses; %, percent]

Sample 14-LM-479 (this report)													
Spot	$^{204}Pb/^{206}Pb$	±%	$^{207}Pb/^{206}Pb$	±%	$^{208}Pb/^{206}Pb$	±%	% $^{206}Pb_c$	ppm U	ppm Th	Total $^{206}Pb/^{238}U$	±%	$^{206}Pb/^{238}U$ age ± error (Ma)	
479-01.1	$4.9E^{-4}$	71	0.0558	5.6	0.145	10.3	0.866	61	29	0.0223	3.2	141	5
479-02.1	$4.2E^{-4}$	58	0.0525	4.3	0.151	7.2	0.414	92	42	0.0243	2.7	154	4
479-03.1	$2.3E^{-4}$	71	0.0545	3.8	0.235	5.3	0.698	127	90	0.0228	2.7	145	4
479-04.1	$4.5E^{-4}$	58	0.0504	4.6	0.234	6.1	0.182	93	69	0.0229	2.9	146	4
479-05.1	$-7.3E^{-4}$	58	0.0467	10.3	0.169	19.2	−0.296	58	30	0.0236	3.0	151	5

Mean age of coherent group (N=5)	147.4 Ma
Age error (95% confidence, without error in standard)	3.8 Ma
MSWD	1.51
Probability of fit	0.20
Age error (95% confidence, with error in standard)	4.1 Ma
Final age and error	147.4 ± 4.1 Ma

Table 9. Sensitive high-resolution ion microprobe-reverse geometry (SHRIMP-RG) U-Pb zircon data for sample 14-LM-490, Lane Mountain area, California.

[Spot designation indicates sample number, crystal number, and spot number for each zircon analysis. Pb, lead; Pb_c, common lead; U, uranium; Th, thorium; ppm, part per million; Ma, mega-annum; MSWD, mean square weighted deviation; N, number of zircon spot analyses; %, percent; —, not applicable]

Sample 14-LM-490 (Stone and others, 2019)													
Spot	$^{204}Pb/^{206}Pb$	±%	$^{207}Pb/^{206}Pb$	±%	$^{208}Pb/^{206}Pb$	±%	% $^{206}Pb_c$	ppm U	ppm Th	Total $^{206}Pb/^{238}U$	±%	$^{206}Pb/^{238}U$ age ± error (Ma)	
490-01.1†	4.0E^{-3}	32	0.0536	7.0	0.25	7.1	0.68	227	164	0.0175	2.9	111	3
490-02.1†	4.4E^{-4}	71	0.0585	5.1	0.36	4.4	1.27	258	245	0.0189	4.6	119	5
490-02.2†	2.4E^{-3}	35	0.0593	5.8	0.27	5.9	1.34	86	66	0.0205	5.1	129	7
490-03.1†	—	—	0.0539	4.2	0.17	9.7	0.66	153	81	0.0210	2.9	133	4
490-03.2†	6.6E^{-3}	16	0.0519	4.4	0.17	5.2	0.43	403	129	0.0188	3.8	120	5
490-04.1†	4.2E^{-4}	71	0.0508	5.1	0.28	4.7	0.26	85	64	0.0210	3.3	133	4
490-04.2	1.4E^{-4}	50	0.0505	2.2	0.10	7.7	0.20	794	211	0.0221	2.9	141	4
490-05.1	1.5E^{-3}	35	0.0617	4.4	0.16	5.7	1.62	90	37	0.0225	5.5	141	8
490-06.1	1.4E^{-3}	38	0.0526	5.0	0.18	10.6	0.47	119	66	0.0220	4.0	140	6
490-07.1	1.3E^{-3}	38	0.0564	10.6	0.18	5.4	0.94	90	42	0.0230	4.4	145	6
490-08.1	8.7E^{-4}	45	0.0527	4.7	0.17	5.3	0.46	87	41	0.0234	3.3	149	5
490-09.1	−3.7E^{-4}	71	0.0546	4.6	0.17	5.6	0.71	98	46	0.0225	2.0	142	3
490-10.1	9.9E^{-4}	41	0.0525	4.5	0.24	4.4	0.43	97	68	0.0242	2.9	153	4
490-11.1	−2.0E^{-4}	100	0.0527	4.9	0.18	5.6	0.45	85	44	0.0241	2.8	153	4
490-12.1†	9.2E^{-4}	50	0.0528	5.6	0.10	9.0	0.37	182	44	0.0296	3.1	188	6
490-13.1†	1.8E^{-3}	35	0.0527	5.4	0.18	6.1	0.42	103	48	0.0255	2.0	162	3
490-14.1	2.2E^{-4}	100	0.0549	5.0	0.23	5.2	0.74	85	52	0.0237	3.9	150	6
490-15.1	1.3E^{-3}	38	0.0528	4.7	0.13	6.4	0.46	93	32	0.0244	2.0	154	3
490-16.1	5.8E^{-4}	58	0.0483	8.4	0.16	5.7	−0.09	94	42	0.0235	3.6	150	5
490-17.1	9.8E^{-4}	45	0.0507	5.0	0.18	5.5	0.20	84	44	0.0242	4.3	154	7
490-18.1	2.5E^{-3}	20	0.0701	20.2	0.16	19.7	2.65	155	50	0.0238	6.4	148	10
490-19.1	—	—	0.0540	5.5	0.27	5.3	0.62	62	52	0.0238	2.1	150	3
490-20.1	1.4E^{-3}	38	0.0521	4.9	0.22	5.1	0.38	80	51	0.0237	3.9	150	6
490-21.1	5.4E^{-4}	58	0.0518	4.8	0.26	4.4	0.38	100	67	0.0217	3.3	138	5
490-22.1	6.0E^{-4}	58	0.0535	4.9	0.23	5.1	0.54	97	64	0.0243	2.4	154	4

†Spots were statistically rejected from mean age determinations.

Mean age of coherent group (N=16)	148.9 Ma
Age error (95% confidence, without error in standard)	2.2 Ma
MSWD	1.40
Probability of fit	0.14
Age error (95% confidence, with error in standard)	2.6 Ma
Final age and error	148.9 ± 2.6 Ma

Table 10. Sensitive high-resolution ion microprobe-reverse geometry (SHRIMP-RG) U-Pb zircon data for sample 15-LM-802A, Lane Mountain area, California.

[Spot designation indicates sample number, crystal number, and spot number for each zircon analysis. Pb, lead; Pb_c, common lead; U, uranium; Th, thorium; ppm, part per million; Ma, mega-annum; MSWD, mean square weighted deviation; N, number of zircon spot analyses; %, percent; —, not applicable]

Sample 14-LM-802A (this report)													
Spot	$^{204}Pb/^{206}Pb$	±%	$^{207}Pb/^{206}Pb$	±%	$^{208}Pb/^{206}Pb$	±%	% $^{206}Pb_c$	ppm U	ppm Th	Total $^{206}Pb/^{238}U$	±%	$^{206}Pb/^{238}U$ age ± error (Ma)	
802A-01.1	$-5.5E^{-4}$	58	0.0533	4.7	0.169	5.6	0.259	69	37	0.0394	0.71	249	3
802A-02.1	$3.0E^{-5}$	100	0.0523	1.9	0.230	1.9	0.145	398	262	0.0393	0.27	248	4
802A-03.1	—	—	0.0517	4.6	0.175	5.3	0.067	76	43	0.0390	0.67	246	5
802A-04.1	$3.5E^{-4}$	71	0.0557	4.4	0.233	4.6	0.566	74	51	0.0394	2.45	248	3
802A-04.2	$7.5E^{-4}$	32	0.0699	11.6	0.211	7.0	2.377	173	86	0.0377	0.47	233	6
802A-05.1	$1.1E^{-4}$	100	0.0524	3.6	0.246	3.5	0.148	112	85	0.0396	0.48	250	4

Mean age of coherent group (N=5)	248.4 Ma
Age error (95% confidence, without error in standard)	3.2 Ma
MSWD	0.10
Probability of fit	0.98
Age error (95% confidence, with error in standard)	3.6 Ma
Final age and error	248.4 ± 3.6 Ma

Table 11. Sensitive high-resolution ion microprobe-reverse geometry (SHRIMP-RG) U-Pb zircon data for sample 15-LM-806, Lane Mountain area, California.

[Spot designation indicates sample number, crystal number, and spot number for each zircon analysis. Pb, lead; Pb_c, common lead; U, uranium; Th, thorium; ppm, part per million; Ma, mega-annum; MSWD, mean square weighted deviation; N, number of zircon spot analyses; %, percent]

Sample 15-LM-806 (this report)													
Spot	$^{204}Pb/^{206}Pb$	±%	$^{207}Pb/^{206}Pb$	±%	$^{208}Pb/^{206}Pb$	±%	% $^{206}Pb_c$	ppm U	ppm Th	Total $^{206}Pb/^{238}U$	±%	$^{206}Pb/^{238}U$ age ± error (Ma)	
806-01.1	$3.0E^{-3}$	35	0.0481	13.8	0.106	30.4	−0.124	37	19	0.0238	3.1	152	5
806-02.1†	$1.4E^{-4}$	100	0.0501	13.6	0.155	7.4	−0.101	61	30	0.0369	3.0	234	7
806-03.1	$-5.3E^{-4}$	71	0.0462	10.8	0.146	10.2	−0.353	57	32	0.0229	4.4	147	7
806-04.1	$9.3E^{-4}$	58	0.0415	16.0	0.186	9.8	−0.978	47	27	0.0246	2.7	158	4
806-05.1	$5.2E^{-4}$	58	0.0511	10.9	0.262	12.1	0.245	71	60	0.0244	2.7	155	4

†Spots were statistically rejected from mean age determinations.

Mean age of coherent group (N=4)	154.0 Ma
Age error (95% confidence, without error in standard)	4.8 Ma
MSWD	0.87
Probability of fit	0.45
Age error (95% confidence, with error in standard)	5.1 Ma
Final age and error	154.0 ± 5.1 Ma

Table 12. Sensitive high-resolution ion microprobe-reverse geometry (SHRIMP-RG) U-Pb zircon data for sample 15-LM-810, Lane Mountain area, California.

[Spot designation indicates sample number, crystal number, and spot number for each zircon analysis. Pb, lead; Pb_c, common lead; U, uranium; Th, thorium; ppm, part per million; Ma, mega-annum; MSWD, mean square weighted deviation; N, number of zircon spot analyses; %, percent]

Sample 15-LM-810 (this report)													
Spot	$^{204}Pb/^{206}Pb$	±%	$^{207}Pb/^{206}Pb$	±%	$^{208}Pb/^{206}Pb$	±%	% $^{206}Pb_c$	ppm U	ppm Th	Total $^{206}Pb/^{238}U$	±%	$^{206}Pb/^{238}U$ age ± error (Ma)	
810-01.1	$1.8E^{-3}$	50	0.045	8.1	0.129	8.4	−0.460	50	18	0.0241	2.2	154	3
810-02.1	$8.7E^{-4}$	35	0.047	3.9	0.097	4.7	−0.232	212	66	0.0234	1.9	149	3
810-03.1	$-2.5E^{-4}$	100	0.050	5.9	0.163	5.6	0.110	88	44	0.0236	3.3	150	5
810-04.1	$5.2E^{-4}$	41	0.048	3.4	0.156	3.4	−0.089	275	134	0.0231	1.9	147	3
810-05.1	$1.1E^{-3}$	41	0.052	4.9	0.153	9.8	0.392	114	48	0.0243	2.3	154	4
810-06.1	$9.0E^{-5}$	100	0.051	3.4	0.079	4.6	0.267	243	58	0.0243	1.9	154	3

Mean age of coherent group (N=6)	151.2 Ma
Age error (95% confidence, without error in standard)	2.6 Ma
MSWD	1.08
Probability of fit	0.37
Age error (95% confidence, with error in standard)	2.9 Ma
Final age and error	151.2 ± 2.9 Ma

Table 13. Sensitive high-resolution ion microprobe-reverse geometry (SHRIMP-RG) U-Pb zircon data for sample 15-LM-816, Lane Mountain area, California.

[Spot designation indicates sample number, crystal number, and spot number for each zircon analysis. Pb, lead; Pb_c, common lead; U, uranium; Th, thorium; ppm, part per million; Ma, mega-annum; MSWD, mean square weighted deviation; N, number of zircon spot analyses; %, percent; —, not applicable]

Sample 15-LM-816 (this report)													
Spot	$^{204}Pb/^{206}Pb$	±%	$^{207}Pb/^{206}Pb$	±%	$^{208}Pb/^{206}Pb$	±%	% $^{206}Pb_c$	ppm U	ppm Th	Total $^{206}Pb/^{238}U$	±%	$^{206}Pb/^{238}U$ age ± error (Ma)	
816-01.1	—	—	0.0502	2.6	0.249	2.5	−0.120	238	174	0.0393	1.3	249	3
816-02.1	$9.3E^{-5}$	100	0.0515	3.4	0.227	3.4	0.039	127	86	0.0391	1.7	247	4
816-03.1	—	—	0.0527	3.1	0.278	2.9	0.179	148	115	0.0397	2.3	251	6
816-04.1	—	—	0.0512	2.3	0.243	2.2	−0.023	270	193	0.0410	1.3	259	3
816-05.1	$-2.6E^{-4}$	71	0.0569	3.9	0.230	4.1	0.727	94	66	0.0391	1.6	245	4

Mean age of coherent group (N=5)	250.7 Ma
Age error (95% confidence, without error in standard)	3.4 Ma
MSWD	2.23
Probability of fit	0.06
Age error (95% confidence, with error in standard)	3.8
Final age and error	250.7 ± 3.8 Ma

Table 14. Sensitive high-resolution ion microprobe-reverse geometry (SHRIMP-RG) U-Pb zircon data for sample 17-LM-1385, Lane Mountain area, California.

[Spot designation indicates sample number, crystal number, and spot number for each zircon analysis. Pb, lead; Pb_c, common lead; U, uranium; Th, thorium; ppm, part per million; Ma, mega-annum; MSWD, mean square weighted deviation; N, number of zircon spot analyses; %, percent; —, not applicable]

Sample 17-LM-1385 (this report)													
Spot	$^{204}Pb/^{206}Pb$	±%	$^{207}Pb/^{206}Pb$	±%	$^{208}Pb/^{206}Pb$	±%	$\%\ ^{206}Pb_c$	ppm U	ppm Th	Total $^{206}Pb/^{238}U$	±%	$^{206}Pb/^{238}U$ age ± error (Ma)	
1385-01.1	$-2.8E^{-4}$	100	0.0410	6.8	0.137	7.7	−1.013	95	50	0.0236	1.6	152	2
1385-02.1	$-8.0E^{-4}$	50	0.0510	5.1	0.290	4.5	0.253	193	173	0.0234	2.7	149	4
1385-03.1	$-1.4E^{-5}$	71	0.0499	0.9	0.308	0.8	0.107	3,676	3,318	0.0236	1.4	150	2
1385-04.1	$2.1E^{-4}$	58	0.0477	3.0	0.225	3.0	−0.168	445	308	0.0231	1.4	147	2
1385-05.1	$4.4E^{-4}$	45	0.0484	5.4	0.195	3.6	−0.091	200	120	0.0241	2.1	153	3
1385-06.1	$7.3E^{-4}$	50	0.0443	5.1	0.195	5.2	−0.597	106	66	0.0238	2.1	153	3
1385-07.1	$1.5E^{-4}$	100	0.0501	4.3	0.131	5.7	0.140	146	56	0.0232	1.5	148	2
1385-08.1	—	—	0.0487	3.6	0.145	4.3	−0.044	305	132	0.0233	1.4	148	2
1385-09.1†	$2.7E^{-4}$	22	0.0525	1.2	0.229	1.3	0.452	2,101	1,436	0.0223	1.5	142	2
1385-10.1	$3.2E^{-4}$	50	0.0483	3.2	0.180	4.0	−0.104	239	134	0.0240	1.7	153	3
1385-11.1	—	—	0.0496	0.9	0.183	1.1	0.068	2,924	1,648	0.0236	1.5	151	2
1385-12.1	$1.6E^{-4}$	19	0.0519	0.8	0.196	0.9	0.356	3,648	2,015	0.0235	1.4	150	2
1385-13.1	$-1.1E^{-4}$	100	0.0477	4.0	0.138	5.0	−0.177	131	52	0.0239	2.5	153	4
1385-14.1	—	—	0.0534	4.5	0.174	5.9	0.545	397	209	0.0241	1.5	153	2
1385-15.1	$6.9E^{-5}$	71	0.0481	3.9	0.185	2.3	−0.133	521	280	0.0245	1.6	157	3
1385-16.1	$-2.4E^{-4}$	71	0.0477	4.2	0.233	3.8	−0.154	182	129	0.0229	2.0	146	3
1385-17.1†	$1.2E^{-3}$	6	0.0710	0.6	0.326	0.6	2.789	5,372	4,680	0.0225	1.4	140	2
1385-18.1	$3.9E^{-5}$	41	0.0494	0.9	0.179	1.0	0.027	2,687	1,407	0.0242	1.4	154	2

†Spots were statistically rejected from mean age determinations.

Mean age of coherent group (N=16)	150.8 Ma
Age error (95% confidence, without error in standard)	1.2 Ma
MSWD	1.29
Probability of fit	0.20
Age error (95% confidence, with error in standard)	1.8 Ma
Final age and error	150.8 ± 1.8 Ma

Table 15. Sensitive high-resolution ion microprobe-reverse geometry (SHRIMP-RG) U-Pb zircon data for sample 17-LM-1562, Lane Mountain area, California.

[Spot designation indicates sample number, crystal number, and spot number for each zircon analysis. Pb, lead; Pb_c, common lead; U, uranium; Th, thorium; ppm, part per million; Ma, mega-annum; MSWD, mean square weighted deviation; N, number of zircon spot analyses; %, percent; —, not applicable]

Sample 17-LM-1562 (this report)													
Spot	$^{204}Pb/^{206}Pb$	±%	$^{207}Pb/^{206}Pb$	±%	$^{208}Pb/^{206}Pb$	±%	% $^{206}Pb_c$	ppm U	ppm Th	Total $^{206}Pb/^{238}U$	±%	$^{206}Pb/^{238}U$ age ± error (Ma)	
1562-01.1	$6.7E^{-5}$	71	0.0511	2.0	0.388	3.1	0.010	338	392	0.0383	1.5	243	4
1562-02.1†	$1.9E^{-4}$	58	0.0541	2.7	0.075	12.7	0.419	297	66	0.0362	2.1	229	5
1562-03.1	$9.6E^{-5}$	100	0.0511	3.5	0.217	3.6	0.030	294	203	0.0371	1.5	235	3
1562-04.1	$-5.2E^{-5}$	71	0.0520	1.8	0.338	1.5	0.093	520	545	0.0398	1.4	251	3
1562-05.1	$3.0E^{-4}$	58	0.0540	8.1	0.316	3.1	0.380	170	156	0.0377	2.7	238	6
1562-06.1	—	—	0.0517	4.9	0.314	2.1	0.078	264	257	0.0386	1.4	244	4
1562-07.1	$3.9E^{-4}$	41	0.0540	4.6	0.385	2.3	0.371	308	339	0.0386	1.4	243	4
1562-08.1	$8.5E^{-4}$	50	0.0522	5.2	0.181	5.8	0.149	55	31	0.0380	4.2	240	10
1562-09.1	$6.1E^{-4}$	41	0.0542	6.2	0.292	3.2	0.386	112	98	0.0389	1.5	245	4
1562-10.1	$8.1E^{-5}$	50	0.0521	1.6	0.421	2.1	0.106	537	675	0.0403	1.5	254	4
1562-11.1	$-7.2E^{-5}$	100	0.0508	3.0	0.108	4.3	−0.026	356	129	0.0378	1.4	239	3
1562-12.1	$7.3E^{-5}$	71	0.0531	2.1	0.332	1.8	0.244	305	304	0.0394	1.4	248	3
1562-13.1	$5.6E^{-4}$	50	0.0481	4.3	0.249	4.0	−0.391	102	81	0.0396	2.2	251	5

†Spots were statistically rejected from mean age determinations.

Mean age of coherent group (N=12)	244.5 Ma
Age error (95% confidence, without error in standard)	3.8 Ma
MSWD	2.31
Probability of fit	0.01
Age error (95% confidence, with error in standard)	4.4 Ma
Final age and error	244.5 ± 4.4 Ma

Table 16. Sensitive high-resolution ion microprobe-reverse geometry (SHRIMP-RG) U-Pb zircon data for sample 17-LM-1656, Lane Mountain area, California.

[Spot designation indicates sample number, crystal number, and spot number for each zircon analysis. Pb, lead; Pb_c, common lead; U, uranium; Th, thorium; ppm, part per million; Ma, mega-annum; MSWD, mean square weighted deviation; N, number of zircon spot analyses; %, percent]

Sample 17-LM-1656 (this report)													
Spot	$^{204}Pb/^{206}Pb$	±%	$^{207}Pb/^{206}Pb$	±%	$^{208}Pb/^{206}Pb$	±%	% $^{206}Pb_c$	ppm U	ppm Th	Total $^{206}Pb/^{238}U$	±%	$^{206}Pb/^{238}U$ age ± error (Ma)	
1656-01.1	$2.5E^{-4}$	71	0.0201	321.6	0.161	6.6	−3.654	124	62	0.0235	3.3	155	13
1656-02.1	$2.3E^{-4}$	45	0.0479	2.5	0.190	3.7	−0.138	341	205	0.0226	2.0	144	3
1656-03.1	$-3.3E^{-4}$	71	0.0417	5.7	0.092	10.4	−0.939	96	30	0.0239	4.1	154	6
1656-04.1	$-1.1E^{-4}$	100	0.0481	4.4	0.073	9.3	−0.126	141	32	0.0240	3.6	153	5
1656-05.1	$1.2E^{-4}$	45	0.0487	1.8	0.222	4.4	−0.060	724	465	0.0240	2.3	153	3
1656-06.1	$2.6E^{-4}$	71	0.0468	4.7	0.145	7.1	−0.293	134	66	0.0236	2.6	151	4
1656-07.1	$3.4E^{-4}$	50	0.0477	3.4	0.193	5.0	−0.187	221	120	0.0241	3.5	154	5
1656-08.1	$5.9E^{-5}$	100	0.0609	27.5	0.162	4.6	1.480	320	161	0.0242	3.3	152	6
1656-09.1	$5.2E^{-4}$	41	0.0481	3.9	0.172	5.4	−0.128	229	119	0.0243	3.5	155	5

Mean age of coherent group (N=9)	150.5 Ma
Age error (95% confidence, without error in standard)	3.0 Ma
MSWD	0.86
Probability of fit	0.55
Age error (95% confidence, with error in standard)	7.0 Ma
Final age and error	150.5 ± 7.0 Ma

Table 17. Sensitive high-resolution ion microprobe-reverse geometry (SHRIMP-RG) U-Pb zircon data for sample 17-LM-1688, Lane Mountain area, California.

[Spot designation indicates sample number, crystal number, and spot number for each zircon analysis. Pb, lead; Pb_c, common lead; U, uranium; Th, thorium; ppm, part per million; Ma, mega-annum; MSWD, mean square weighted deviation; N, number of zircon spot analyses; %, percent; —, not applicable]

Sample 17-LM-1688 (this report)													
Spot	$^{204}Pb/^{206}Pb$	±%	$^{207}Pb/^{206}Pb$	±%	$^{208}Pb/^{206}Pb$	±%	% $^{206}Pb_c$	ppm U	ppm Th	Total $^{206}Pb/^{238}U$	±%	$^{206}Pb/^{238}U$ age ± error (Ma)	
Run 1													
1688-02.1	$9.2E^{-5}$	58	0.0511	1.9	0.318	2.3	−0.006	313	304	0.0389	1.9	246	5
1688-03.1	$-9.1E^{-5}$	71	0.0507	2.4	0.295	3.0	−0.042	236	220	0.0384	2.0	243	5
1688-04.1	$2.0E^{-4}$	45	0.0523	2.3	0.277	3.0	0.162	265	228	0.0383	1.5	242	4
1688-05.1†	$7.8E^{-5}$	45	0.0504	1.4	0.348	1.6	−0.050	727	770	0.0368	1.7	233	4
1688-06.1	—	100	0.0491	2.5	0.273	3.1	−0.263	231	192	0.0393	2.3	249	6
1688-07.1	—	—	0.0522	3.4	0.210	14.2	0.136	136	95	0.0389	1.3	246	3
1688-08.1	$9.4E^{-5}$	71	0.0500	5.5	0.285	3.1	−0.151	230	206	0.0394	2.0	250	5
1688-09.1	—	—	0.0514	1.3	0.542	2.4	0.013	716	1,200	0.0399	1.8	252	4
Run 2													
1688-10.1	$-2.9E^{-4}$	344	0.0495	7.9	0.167	6.1	−0.184	55	31	0.0375	1.5	238	4
1688-11.1	$-2.2E^{-5}$	1,352	0.0543	4.0	0.177	3.2	0.434	191	109	0.0370	1.4	233	3
1688-12.1	$-2.1E^{-5}$	1,226	0.0517	3.9	0.305	2.4	0.094	190	176	0.0372	1.9	235	5
1688-13.1	$-9.8E^{-6}$	1,291	0.0514	2.7	0.373	2.6	0.034	396	442	0.0389	1.5	246	4
1688-14.1	$5.0E^{-5}$	288	0.0502	2.9	0.325	1.6	−0.105	382	379	0.0384	1.8	243	4
1688-15.1	$5.2E^{-5}$	261	0.0481	3.1	0.229	2.0	−0.348	382	258	0.0369	1.3	234	3
1688-16.1	$-6.5E^{-5}$	183	0.0517	2.7	0.410	1.4	0.082	414	518	0.0381	1.4	241	3
1688-17.1	$-1.7E^{-4}$	99	0.0503	3.3	0.406	1.7	−0.103	291	357	0.0387	1.9	245	5
1688-18.1	$-2.5E^{-4}$	183	0.0560	5.2	0.190	4.0	0.641	106	63	0.0376	1.4	236	3
1688-19.1	$-1.3E^{-4}$	173	0.0534	6.2	0.333	2.2	0.304	225	242	0.0380	2.8	240	7

†Spots were statistically rejected from mean age determinations.

Run 1

Mean age of coherent group (N=7)	246.2 Ma
Age error (95% confidence, without error in standard)	3.2 Ma
MSWD	0.71
Probability of fit	0.64
Age error (95% confidence, with error in standard)	4.1 Ma

Run 2

Mean age of coherent group (N=10)	238.5 Ma
Age error (95% confidence, without error in standard)	2.4 Ma
MSWD	1.56
Probability of fit	0.12
Age error (95% confidence, with error in standard)	3.1 Ma
Final age and error (statistical mean of both runs)	241.7 ± 5.2 Ma

Table 18. Sensitive high-resolution ion microprobe-reverse geometry (SHRIMP-RG) U-Pb zircon data for sample 17-LM-1748, Lane Mountain area, California.

[Spot designation indicates sample number, crystal number, and spot number for each zircon analysis. Pb, lead; Pb_c, common lead; U, uranium; Th, thorium; ppm, part per million; Ma, mega-annum; MSWD, mean square weighted deviation; N, number of zircon spot analyses; %, percent]

Sample 17-LM-1748 (this report)													
Spot	$^{204}Pb/^{206}Pb$	±%	$^{207}Pb/^{206}Pb$	±%	$^{208}Pb/^{206}Pb$	±%	% $^{206}Pb_c$	ppm U	ppm Th	Total $^{206}Pb/^{238}U$	±%	$^{206}Pb/^{238}U$ age ± error (Ma)	
1748-01.1	$-1.2E^{-3}$	45	0.0474	5.9	0.132	10.2	−0.208	75	33	0.0232	1.4	148	2
1748-02.1	$6.8E^{-4}$	50	0.0450	4.8	0.168	16.7	−0.516	106	57	0.0236	2.0	151	3
1748-03.1	$4.6E^{-4}$	58	0.0481	4.6	0.227	11.6	−0.123	115	84	0.0235	1.6	150	2
1748-04.1	$-1.6E^{-4}$	100	0.0449	4.8	0.162	7.7	−0.537	104	54	0.0240	2.5	153	4
1748-05.1†	$4.2E^{-4}$	58	0.0520	4.2	0.159	7.3	0.394	129	67	0.0222	1.3	141	2
1748-06.1	$3.4E^{-4}$	50	0.0515	3.5	0.285	4.4	0.318	217	192	0.0231	2.2	147	3
1748-07.1	$9.8E^{-5}$	45	0.0488	1.8	0.065	45.7	−0.037	913	144	0.0239	8.0	152	12
1748-08.1	$-3.8E^{-4}$	58	0.0482	4.1	0.242	5.5	−0.094	140	92	0.0227	1.7	145	3
1748-09.1	$2.6E^{-4}$	71	0.0494	8.7	0.166	11.9	0.050	128	63	0.0227	2.2	144	3

†Spots were statistically rejected from mean age determinations.

Mean age of coherent group (N=8)	148.3 Ma
Age error (95% confidence, without error in standard)	2.1 Ma
MSWD	1.01
Probability of fit	0.42
Age error (95% confidence, with error in standard)	2.5 Ma
Final age and error	148.3 ± 2.5 Ma

Table 19. Sensitive high-resolution ion microprobe-reverse geometry (SHRIMP-RG) U-Pb zircon data for sample 17-LM-1749, Lane Mountain area, California.

[Spot designation indicates sample number, crystal number, and spot number for each zircon analysis. Pb, lead; Pb_c, common lead; U, uranium; Th, thorium; ppm, part per million; Ma, mega-annum; MSWD, mean square weighted deviation; N, number of zircon spot analyses; %, percent; —, not applicable]

Sample 17-LM-1749 (this report)													
Spot	$^{204}Pb/^{206}Pb$	±%	$^{207}Pb/^{206}Pb$	±%	$^{208}Pb/^{206}Pb$	±%	% $^{206}Pb_c$	ppm U	ppm Th	Total $^{206}Pb/^{238}U$	±%	$^{206}Pb/^{238}U$ age ± error (Ma)	
1749-01.1	$8.7E^{-5}$	100	0.0524	3.2	0.141	5.8	0.424	192	98	0.0232	2.4	147	3
1749-02.1	$2.8E^{-4}$	58	0.0463	3.6	0.143	6.0	−0.350	196	88	0.0238	1.7	152	3
1749-03.1	—	—	0.0493	3.7	0.169	10.1	0.047	169	81	0.0228	1.8	145	3
1749-04.1	$-1.3E^{-4}$	100	0.0468	4.2	0.166	6.5	−0.286	141	66	0.0238	1.6	152	2
1749-05.1	$-2.6E^{-4}$	71	0.0472	4.2	0.138	7.2	−0.245	147	63	0.0241	1.6	154	2
1749-06.1	—	—	0.0452	4.5	0.156	7.3	−0.493	120	57	0.0238	1.3	152	2
1749-07.1	$3.0E^{-4}$	71	0.0458	4.6	0.216	11.0	−0.413	117	74	0.0237	1.8	151	3
1749-08.1†	$4.3E^{-4}$	50	0.0465	8.5	0.140	6.6	−0.316	172	83	0.0227	1.2	145	2
1749-09.1	$1.3E^{-4}$	100	0.0503	7.7	0.116	7.9	0.154	142	55	0.0236	1.9	150	3
1749-10.1	$1.9E^{-3}$	26	0.0617	13.0	0.195	6.1	1.590	143	64	0.0234	2.4	147	4

†Spots were statistically rejected from mean age determinations.

Mean age of coherent group (N=9)	150.8 Ma
Age error (95% confidence, without error in standard)	1.8 Ma
MSWD	1.27
Probability of fit	0.25
Age error (95% confidence, with error in standard)	2.3 Ma
Final age and error	150.8 ± 2.3 Ma

Table 20. Sensitive high-resolution ion microprobe-reverse geometry (SHRIMP-RG) U-Pb zircon data for sample 17-LM-1771, Lane Mountain area, California.

[Spot designation indicates sample number, crystal number, and spot number for each zircon analysis. Pb, lead; Pb_c, common lead; U, uranium; Th, thorium; ppm, part per million; Ma, mega-annum; MSWD, mean square weighted deviation; N, number of zircon spot analyses; %, percent; —, not applicable]

Sample 17-LM-1771 (this report)													
Spot	$^{204}Pb/^{206}Pb$	±%	$^{207}Pb/^{206}Pb$	±%	$^{208}Pb/^{206}Pb$	±%	% $^{206}Pb_c$	ppm U	ppm Th	Total $^{206}Pb/^{238}U$	±%	$^{206}Pb/^{238}U$ age ± error (Ma)	
1771-01.1	$-5.3E^{-5}$	100	0.0504	2.6	0.240	3.6	−0.095	196	149	0.0389	1.2	246	3
1771-02.1†	$-3.0E^{-5}$	100	0.0522	1.9	0.200	5.1	0.145	339	215	0.0382	1.1	242	3
1771-03.1	$1.3E^{-4}$	45	0.0491	1.8	0.253	4.1	−0.260	416	313	0.0395	1.5	250	4
1771-04.1	$3.8E^{-5}$	58	0.0519	1.2	0.213	1.8	0.076	844	555	0.0401	1.2	253	3
1771-05.1	—	—	0.0506	2.3	0.204	3.3	−0.094	256	151	0.0402	1.2	255	3
1771-06.1	$6.3E^{-5}$	58	0.0507	2.8	0.207	2.4	−0.088	488	299	0.0404	1.6	256	4
1771-07.1	$1.7E^{-4}$	45	0.0514	4.9	0.232	6.7	0.029	306	232	0.0389	1.4	246	4
1771-08.1	$6.4E^{-5}$	71	0.0509	2.0	0.253	2.7	−0.043	329	237	0.0394	1.1	249	3

†Spots were statistically rejected from mean age determinations.

Mean age of coherent group (N=7)	250.5 Ma
Age error (95% confidence, without error in standard)	2.4 Ma
MSWD	1.47
Probability of fit	0.18
Age error (95% confidence, with error in standard)	3.5 Ma
Final age and error	250.5 ± 3.5 Ma

Table 21. Sensitive high-resolution ion microprobe-reverse geometry (SHRIMP-RG) U-Pb zircon data for sample 17-LM-1779, Lane Mountain area, California.

[Spot designation indicates sample number, crystal number, and spot number for each zircon analysis. Pb, lead; Pb_c, common lead; U, uranium; Th, thorium; ppm, part per million; Ma, mega-annum; MSWD, mean square weighted deviation; N, number of zircon spot analyses; %, percent; —, not applicable]

Sample 17-LM-1779 (this report)													
Spot	$^{204}Pb/^{206}Pb$	±%	$^{207}Pb/^{206}Pb$	±%	$^{208}Pb/^{206}Pb$	±%	% $^{206}Pb_c$	ppm U	ppm Th	Total $^{206}Pb/^{238}U$	±%	$^{206}Pb/^{238}U$ age ± error (Ma)	
1779-01.1	$7.9E^{-5}$	100	0.0503	3.2	0.276	4.0	−0.120	133	108	0.0400	1.2	253	3
1779-02.1	$2.0E^{-4}$	58	0.0508	2.9	0.226	4.1	−0.068	152	115	0.0400	1.3	253	3
1779-03.1	$-8.0E^{-5}$	71	0.0508	4.1	0.241	3.1	−0.032	262	193	0.0385	1.3	244	3
1779-04.1	$1.0E^{-4}$	71	0.0481	2.6	0.235	3.5	−0.375	195	153	0.0389	1.2	247	3
1779-05.1	$2.5E^{-5}$	100	0.0521	1.8	0.183	2.8	0.110	403	234	0.0397	1.1	251	3
1779-06.1	$8.5E^{-4}$	41	0.0505	4.3	0.138	7.5	−0.085	76	34	0.0392	2.7	248	7
1779-07.1	$2.0E^{-4}$	58	0.0509	2.9	0.274	3.7	−0.033	158	134	0.0391	1.3	247	3
1779-08.1	—	—	0.0518	2.7	0.263	3.6	0.099	176	146	0.0383	1.2	242	3
1779-09.1	$9.5E^{-4}$	41	0.0542	4.3	0.115	8.6	0.383	66	27	0.0392	1.4	247	3

Mean age of coherent group (N=9)	247.9 Ma
Age error (95% confidence, without error in standard)	2.2 Ma
MSWD	1.60
Probability of fit	0.12
Age error (95% confidence, with error in standard)	3.3 Ma
Final age and error	247.9 ± 3.3

Table 22. Sensitive high-resolution ion microprobe-reverse geometry (SHRIMP-RG) U-Pb zircon data for sample 17-LM-1792, Lane Mountain area, California.

[Spot designation indicates sample number, crystal number, and spot number for each zircon analysis. Pb, lead; Pb_c, common lead; U, uranium; Th, thorium; ppm, part per million; Ma, mega-annum; MSWD, mean square weighted deviation; N, number of zircon spot analyses; %, percent]

Sample 17-LM-1792 (this report)													
Spot	$^{204}Pb/^{206}Pb$	±%	$^{207}Pb/^{206}Pb$	±%	$^{208}Pb/^{206}Pb$	±%	% $^{206}Pb_c$	ppm U	ppm Th	Total $^{206}Pb/^{238}U$	±%	$^{206}Pb/^{238}U$ age ± error (Ma)	
1792-01.1	$8.1E^{-5}$	45	0.0520	1.4	0.209	2.1	0.073	650	398	0.0408	1.5	257	4
1792-02.1	$1.1E^{-4}$	71	0.0533	2.5	0.256	3.4	0.266	184	142	0.0394	1.2	249	3
1792-03.1	$1.7E^{-4}$	58	0.0510	2.6	0.146	4.7	−0.007	197	90	0.0385	1.7	243	4
1792-04.1	$-1.2E^{-4}$	71	0.0517	2.8	0.256	3.7	0.060	168	131	0.0394	1.2	249	3
1792-05.1	$-1.5E^{-5}$	100	0.0521	1.3	0.276	1.7	0.100	686	600	0.0403	1.5	254	4
1792-06.1	$-1.6E^{-4}$	50	0.0498	2.2	0.224	3.1	−0.163	276	190	0.0388	1.2	246	3
1792-07.1	$-5.5E^{-5}$	100	0.0505	2.6	0.176	4.1	−0.081	215	120	0.0391	2.5	248	6
1792-08.1	$2.2E^{-5}$	100	0.0498	3.7	0.213	2.4	−0.203	480	306	0.0407	1.9	258	5
1792-09.1	$1.4E^{-4}$	58	0.0536	2.6	0.183	3.9	0.304	231	130	0.0393	1.6	248	4
1792-10.1†	$1.4E^{-5}$	100	0.0544	1.5	0.203	2.0	0.429	722	462	0.0380	1.4	239	3

†Spots were statistically rejected from mean age determinations.

Mean age of coherent group (N=9)	249.7 Ma
Age error (95% confidence, without error in standard)	2.4 Ma
MSWD	1.64
Probability of fit	0.11
Age error (95% confidence, with error in standard)	3.5 Ma
Final age and error	249.7 ± 3.5

Table 23. Sensitive high-resolution ion microprobe-reverse geometry (SHRIMP-RG) U-Pb zircon data for sample 17-LM-1835, Lane Mountain area, California.

[Spot designation indicates sample number, crystal number, and spot number for each zircon analysis. Pb, lead; Pb_c, common lead; U, uranium; Th, thorium; ppm, part per million; Ma, mega-annum; MSWD, mean square weighted deviation; N, number of zircon spot analyses; %, percent; —, not applicable]

Sample 17-LM-1835 (this report)													
Spot	$^{204}Pb/^{206}Pb$	±%	$^{207}Pb/^{206}Pb$	±%	$^{208}Pb/^{206}Pb$	±%	% $^{206}Pb_c$	ppm U	ppm Th	Total $^{206}Pb/^{238}U$	±%	$^{206}Pb/^{238}U$ age ± error (Ma)	
1835-01.1	$6.0E^{-5}$	50	0.0510	1.4	0.219	2.0	−0.027	724	479	0.0391	1.4	247	3
1835-02.1†	$2.0E^{-5}$	71	0.0522	1.1	0.165	1.8	0.103	1,053	513	0.0410	1.5	259	4
1835-03.1	$3.0E^{-4}$	41	0.0515	2.5	0.255	3.3	0.059	215	165	0.0383	1.5	242	4
1835-04.1	$7.1E^{-5}$	58	0.0521	1.7	0.228	4.1	0.112	433	308	0.0394	1.4	249	3
1835-05.1	$-1.1E^{-4}$	71	0.0568	2.5	0.246	3.5	0.703	208	150	0.0392	1.9	246	5
1835-06.1	$-4.7E^{-5}$	100	0.0520	2.4	0.253	3.2	0.094	219	171	0.0399	1.6	252	4
1835-07.1	—	—	0.0520	1.8	0.230	2.5	0.093	393	279	0.0398	1.9	251	5
1835-08.1	$8.4E^{-5}$	58	0.0504	1.9	0.148	3.2	−0.115	370	177	0.0405	1.5	256	4

†Spots were statistically rejected from mean age determinations.

Mean age of coherent group (N=7)	248.8 Ma
Age error (95% confidence, without error in standard)	2.9 Ma
MSWD	1.46
Probability of fit	0.19
Age error (95% confidence, with error in standard)	3.8 Ma
Final age and error	248.8 ± 3.8 Ma

Table 24. Sensitive high-resolution ion microprobe-reverse geometry (SHRIMP-RG) U-Pb zircon data for sample 17-LM-1837, Lane Mountain area, California.

[Spot designation indicates sample number, crystal number, and spot number for each zircon analysis. Pb, lead; Pb_c, common lead; U, uranium; Th, thorium; ppm, part per million; Ma, mega-annum; MSWD, mean square weighted deviation; N, number of zircon spot analyses; %, percent]

Sample 17-LM-1837 (this report)													
Spot	$^{204}Pb/^{206}Pb$	±%	$^{207}Pb/^{206}Pb$	±%	$^{208}Pb/^{206}Pb$	±%	$\%\ ^{206}Pb_c$	ppm U	ppm Th	Total $^{206}Pb/^{238}U$	±%	$^{206}Pb/^{238}U$ age ± error (Ma)	
1837-01.1	$2.0E^{-4}$	58	0.0513	2.9	0.135	12.4	0.019	164	71	0.0391	1.2	247	3
1837-02.1	$-1.5E^{-4}$	71	0.0495	3.2	0.243	4.2	−0.218	142	115	0.0393	1.6	249	4
1837-03.1	$-1.1E^{-4}$	71	0.0503	2.6	0.226	7.2	−0.090	198	145	0.0378	1.6	239	4
1837-04.1	$1.5E^{-4}$	41	0.0535	1.7	0.219	2.5	0.310	433	301	0.0385	1.1	243	3
1837-05.1	$-6.1E^{-5}$	100	0.0488	2.8	0.251	3.7	−0.294	168	123	0.0391	1.2	248	3
1837-06.1	$-7.6E^{-5}$	100	0.0510	3.1	0.261	4.1	−0.021	136	109	0.0389	2.0	246	5
1837-07.1	$-5.4E^{-5}$	100	0.0527	2.5	0.249	3.5	0.167	185	137	0.0407	9.5	257	24
1837-08.1	$1.3E^{-3}$	35	0.0553	4.2	0.249	5.9	0.543	179	123	0.0378	1.1	238	3

Mean age of coherent group (N=8)	243.7 Ma
Age error (95% confidence, without error in standard)	2.4 Ma
MSWD	1.69
Probability of fit	0.11
Age error (95% confidence, with error in standard)	3.4 Ma
Final age and error	243.7 ± 3.4 Ma

Table 25. Sensitive high-resolution ion microprobe-reverse geometry (SHRIMP-RG) U-Pb zircon data for sample 17-LM-1860, Lane Mountain area, California.

[Spot designation indicates sample number, crystal number, and spot number for each zircon analysis. Pb, lead; Pb_c, common lead; U, uranium; Th, thorium; ppm, part per million; Ma, mega-annum; MSWD, mean square weighted deviation; N, number of zircon spot analyses; %, percent; —, not applicable]

Sample 17-LM-1860 (this report)													
Spot	$^{204}Pb/^{206}Pb$	±%	$^{207}Pb/^{206}Pb$	±%	$^{208}Pb/^{206}Pb$	±%	$\%\ ^{206}Pb_c$	ppm U	ppm Th	Total $^{206}Pb/^{238}U$	±%	$^{206}Pb/^{238}U$ age ± error (Ma)	
1860-02.1	$1.5E^{-3}$	35	0.0530	4.8	0.227	5.0	0.227	56	35	0.0392	1.9	247	5
1860-03.1	$-1.4E^{-4}$	100	0.0552	4.1	0.203	4.4	0.493	76	44	0.0402	1.8	253	5
1860-04.1	$-4.2E^{-4}$	71	0.0523	5.1	0.168	6.1	0.111	49	26	0.0411	2.5	259	6
1860-05.1	$1.3E^{-5}$	100	0.0515	1.2	0.052	2.6	0.007	789	122	0.0416	1.7	263	5
1860-06.1†	—	—	0.0510	4.5	0.202	7.7	−0.074	61	37	0.0421	2.2	266	6
1860-07.1	$3.3E^{-4}$	58	0.0522	3.7	0.212	3.8	0.135	94	58	0.0392	1.8	248	4
1860-08.1	—	—	0.0493	4.2	0.177	4.8	−0.220	74	42	0.0385	2.1	244	5
1860-09.1	$2.3E^{-4}$	71	0.0479	4.3	0.175	4.3	−0.425	88	51	0.0402	1.9	255	5

†Spots were statistically rejected from mean age determinations.

Mean age of coherent group (N=7)	252.4 Ma
Age error (95% confidence, without error in standard)	3.7 Ma
MSWD	1.91
Probability of fit	0.08
Age error (95% confidence, with error in standard)	5.2 Ma
Final age and error	252.4 ± 5.2 Ma

Table 26. Sensitive high-resolution ion microprobe-reverse geometry (SHRIMP-RG) U-Pb zircon data for sample 17-LM-1992, Lane Mountain area, California.

[Spot designation indicates sample number, crystal number, and spot number for each zircon analysis. Pb, lead; Pb_c, common lead; U, uranium; Th, thorium; ppm, part per million; Ma, mega-annum; MSWD, mean square weighted deviation; N, number of zircon spot analyses; %, percent; —, not applicable. All analyses are from different crystals although some spots in runs 1 and 2 have identical numbers.]

Sample 17-LM-1992 (this report)													
Spot	$^{204}Pb/^{206}Pb$	±%	$^{207}Pb/^{206}Pb$	±%	$^{208}Pb/^{206}Pb$	±%	% $^{206}Pb_c$	ppm U	ppm Th	Total $^{206}Pb/^{238}U$	±%	$^{206}Pb/^{238}U$ age ± error (Ma)	
Run 1													
1992-01.1	$3.7E^{-4}$	58	0.0504	4.1	0.139	7.1	−0.134	61	31	0.0411	2.7	260	7
1992-02.1	$1.9E^{-4}$	71	0.0506	3.6	0.144	6.0	−0.160	88	42	0.0443	4.0	280	11
1992-03.1†	$-2.8E^{-4}$	58	0.0475	3.7	0.250	9.5	−0.433	90	72	0.0378	1.6	240	4
1992-04.1	$-1.3E^{-4}$	100	0.0513	4.4	0.142	7.2	−0.035	59	30	0.0418	2.6	264	7
1992-05.1	$-8.4E^{-5}$	100	0.0483	3.4	0.121	6.1	−0.407	101	44	0.0418	2.7	265	7
Run 2													
1992-01.1	$1.6E^{-4}$	71	0.0496	11.8	15.3	1.2	−0.197	116	60	0.0390	2.0	247	5
1992-02.1	$-3.5E^{-4}$	58	0.0475	3.5	19.0	11.6	−0.457	86	38	0.0391	2.3	249	6
1992-03.1	—	—	0.0512	3.3	24.0	5.2	0.020	89	51	0.0381	2.8	241	7
1992-04.1†	$3.4E^{-4}$	58	0.0526	3.3	17.4	1.7	0.168	70	48	0.0397	28.1	250	70
Run 3													
1992-05.1	$3.0E^{-4}$	94	0.0520	6.2	0.196	6.4	0.115	77	47	0.038	2.4	242	6
1992-06.1	$9.8E^{-5}$	152	0.0506	2.8	0.230	4.5	−0.070	134	97	0.040	2.1	250	5
1992-07.1	$6.6E^{-4}$	95	0.0542	4.4	0.141	9.4	0.384	51	22	0.039	1.8	247	4
1992-08.1	$3.1E^{-4}$	72	0.0512	3.1	0.222	5.0	−0.015	101	69	0.040	2.2	255	5
1992-09.1	$1.7E^{-4}$	146	0.0515	2.8	0.265	4.1	0.064	130	96	0.038	3.5	238	8
1992-10.1	$2.5E^{-4}$	114	0.0531	3.3	0.235	5.4	0.252	91	66	0.039	1.4	247	3
1992-11.1	$3.6E^{-5}$	1,293	0.0536	4.2	0.167	7.9	0.295	60	28	0.040	1.7	250	4
1992-12.1	$1.7E^{-4}$	131	0.0519	2.8	0.244	4.5	0.078	135	97	0.040	2.8	253	7
1992-13.1	$-5.2E^{-5}$	335	0.0503	4.3	0.236	4.0	−0.124	171	124	0.040	3.1	253	8
1992-14.1	$3.3E^{-5}$	1,293	0.0519	4.0	0.212	7.0	0.082	63	40	0.040	3.5	253	9

†Spots were statistically rejected from mean age determinations.

·Run 1

Mean age of coherent group (N=4)	264.7 Ma
Age error (95% confidence, without error in standard)	7.5 Ma
MSWD	0.79
Probability of fit	0.50
Age error (95% confidence, with error in standard)	7.9 Ma

·Run 2

Mean age of coherent group (N=3)	246.2 Ma
Age error (95% confidence, without error in standard)	6.7 Ma
MSWD	0.39
Probability of fit	0.67
Age error (95% confidence, with error in standard)	7.4 Ma

·Run 3

Mean age of coherent group (N=10)	248.6 Ma
Age error (95% confidence, without error in standard)	3.3 Ma
MSWD	0.64
Probability of fit	0.77
Age error (95% confidence, with error in standard)	4.0 Ma
Final age and error (statistical mean of all runs)	252.0 ± 9.5 Ma

Table 27. Sensitive high-resolution ion microprobe-reverse geometry (SHRIMP-RG) U-Pb zircon data for sample 17-LM-2000, Lane Mountain area, California.

[Spot designation indicates sample number, crystal number, and spot number for each zircon analysis. Pb, lead; Pb_c, common lead; U, uranium; Th, thorium; ppm, part per million; Ma, mega-annum; MSWD, mean square weighted deviation; N, number of zircon spot analyses; %, percent. All analyses are from different crystals although some spots in runs 1 and 2 have identical numbers.]

Sample 17-LM-2000 (this report)													
Spot	$^{204}Pb/^{206}Pb$	±%	$^{207}Pb/^{206}Pb$	±%	$^{208}Pb/^{206}Pb$	±%	% $^{206}Pb_c$	ppm U	ppm Th	Total $^{206}Pb/^{238}U$	±%	$^{206}Pb/^{238}U$ age ± error (Ma)	
Run 1													
2000-01.1†	1.7E^{-4}	45	0.0520	4.4	0.321	4.4	0.173	275	277	0.0354	1.8	224	4
2000-02.1	−4.5E^{-5}	100	0.0494	4.1	0.229	3.3	−0.204	199	158	0.0381	2.0	242	5
2000-03.1	5.3E^{-5}	71	0.0515	3.1	0.348	3.2	0.022	312	346	0.0402	2.4	254	6
2000-04.1	5.1E^{-5}	71	0.0518	1.9	0.381	2.0	0.055	340	398	0.0404	2.2	255	6
2000-05.1†	1.6E^{-5}	100	0.0480	2.4	0.036	9.9	−0.141	637	64	0.0241	2.8	154	4
Run 2													
2000-01.1	1.6E^{-4}	110	0.0585	6.7	0.344	3.3	0.914	285	310	0.0121	3.8	249	4
2000-02.1	−3.4E^{-5}	465	0.0550	5.4	0.344	2.9	0.490	356	377	0.0122	3.6	244	5
2000-03.1	1.1E^{-4}	125	0.0546	2.3	0.430	5.7	0.433	388	516	0.0123	6.1	247	4
2000-04.1	1.4E^{-4}	152	0.0559	2.6	0.379	3.0	0.596	334	382	0.0126	3.4	248	4
2000-05.1	3.1E^{-4}	64	0.0551	4.9	0.379	3.0	0.493	291	321	0.0131	3.5	247	4
2000-06.1	2.0E^{-4}	67	0.0529	2.3	0.301	3.3	0.193	397	368	0.0128	3.8	256	5
2000-07.1	−1.4E^{-4}	176	0.0557	6.3	0.183	5.2	0.555	208	127	0.0115	6.9	251	6
2000-08.1†	1.0E^{-3}	32	0.0533	2.9	0.056	8.6	0.502	388	58	0.0091	9.0	159	4
2000-09.1	3.7E^{-4}	69	0.0549	2.8	0.220	4.2	0.486	263	172	0.0125	4.5	241	4
2000-10.1	1.5E^{-4}	110	0.0531	2.7	0.340	3.2	0.255	317	302	0.0133	3.9	244	5
2000-11.1	1.0E^{-4}	125	0.0521	2.3	0.469	2.3	0.124	400	610	0.0116	2.9	247	4
2000-12.1†	1.7E^{-4}	67	0.0549	2.1	0.414	2.3	0.421	447	547	0.0138	2.9	266	4
2000-13.1	9.0E^{-5}	139	0.0529	2.1	0.617	1.9	0.206	471	832	0.0135	2.8	252	5
2000-14.1	1.4E^{-4}	82	0.0526	2.2	0.409	2.4	0.164	413	542	0.0120	3.1	252	5
2000-15.1	5.7E^{-4}	46	0.0545	3.0	0.289	3.9	0.405	250	219	0.0127	4.3	251	4
2000-16.1	3.6E^{-4}	46	0.0531	2.4	0.401	2.6	0.247	355	427	0.0126	3.1	247	4

†Spots were statistically rejected from mean age determinations.

Run 1

Mean age of coherent group (N=3)	249.2 Ma
Age error (95% confidence, without error in standard)	6.3 Ma
MSWD	2.01
Probability of fit	0.13
Age error (95% confidence, with error in standard)	6.7 Ma

Run 2

Mean age of coherent group (N=14)	248.0 Ma
Age error (95% confidence, without error in standard)	2.4 Ma
MSWD	0.72
Probability of fit	0.75
Age error (95% confidence, with error in standard)	3.1 Ma
Final age and error (statistical mean of both runs)	248.2 ± 4.0 Ma

Table 28. Sensitive high-resolution ion microprobe-reverse geometry (SHRIMP-RG) U-Pb zircon data for sample 17-LM-2001, Lane Mountain area, California.

[Spot designation indicates sample number, crystal number, and spot number for each zircon analysis. Pb, lead; Pb_c, common lead; U, uranium; Th, thorium; ppm, part per million; Ma, mega-annum; MSWD, mean square weighted deviation; N, number of zircon spot analyses; %, percent.]

Sample 17-LM-2001 (this report)													
Spot	$^{204}Pb/^{206}Pb$	±%	$^{207}Pb/^{206}Pb$	±%	$^{208}Pb/^{206}Pb$	±%	% $^{206}Pb_c$	ppm U	ppm Th	Total $^{206}Pb/^{238}U$	±%	$^{206}Pb/^{238}U$ age ± error (Ma)	
2001-01.1	$4.2E^{-4}$	26	0.0500	2.0	0.355	4.2	−0.132	373	405	0.0383	2.4	243	6
2001-02.1	$4.0E^{-5}$	100	0.0500	4.7	0.341	6.6	−0.138	234	258	0.0384	2.6	243	6
2001-03.1	$2.0E^{-5}$	71	0.0512	1.1	0.034	7.5	−0.017	878	91	0.0405	1.9	256	5
2001-04.1	$2.2E^{-5}$	100	0.0524	2.8	0.294	2.0	0.139	404	376	0.0404	1.9	255	5
2001-05.1	$-1.2E^{-5}$	100	0.0501	2.6	0.296	2.7	−0.148	670	629	0.0398	2.0	252	5

Mean age of coherent group (N=5)	250.8 Ma
Age error (95% confidence, without error in standard)	4.6 Ma
MSWD	1.34
Probability of fit	0.25
Age error (95% confidence, with error in standard)	5.2 Ma
Final age and error	250.8 ± 5.2 Ma

Table 29. Sensitive high-resolution ion microprobe-reverse geometry (SHRIMP-RG) U-Pb zircon data for sample 17-LM-2002, Lane Mountain area, California.

[Spot designation indicates sample number, crystal number, and spot number for each zircon analysis. Pb, lead; Pb_c, common lead; U, uranium; Th, thorium; ppm, part per million; Ma, mega-annum; MSWD, mean square weighted deviation; N, number of zircon spot analyses; %, percent.]

Sample 17-LM-2002 (this report)													
Spot	$^{204}Pb/^{206}Pb$	±%	$^{207}Pb/^{206}Pb$	±%	$^{208}Pb/^{206}Pb$	±%	% $^{206}Pb_c$	ppm U	ppm Th	Total $^{206}Pb/^{238}U$	±%	$^{206}Pb/^{238}U$ age ± error (Ma)	
2002-01.1	$-3.9E^{-4}$	45	0.056	5.4	0.075	7.4	0.671	169	40	0.0387	1.9	243	5
2002-02.1	$-7.9E^{-5}$	58	0.050	3.2	0.379	4.8	−0.175	534	626	0.0392	1.8	249	5
2002-03.1	$3.3E^{-4}$	33	0.054	2.1	0.374	1.5	0.414	384	427	0.0390	1.8	246	4
2002-04.1	$1.7E^{-4}$	41	0.054	3.0	0.392	1.3	0.394	453	536	0.0392	1.8	247	4
2002-05.1	$3.7E^{-4}$	41	0.050	8.7	0.117	3.5	−0.134	224	72	0.0390	2.5	247	6
2002-06.1	$-1.2E^{-4}$	50	0.051	1.9	0.398	1.3	−0.064	465	567	0.0390	1.8	247	4

Mean age of coherent group (N=6)	246.3 Ma
Age error (95% confidence, without error in standard)	3.8 Ma
MSWD	0.17
Probability of fit	0.97
Age error (95% confidence, with error in standard)	4.4 Ma
Final age and error	246.3 ± 4.4 Ma

Table 30. Sensitive high-resolution ion microprobe-reverse geometry (SHRIMP-RG) U-Pb zircon data for sample 17-LM-2112, Lane Mountain area, California.

[Spot designation indicates sample number, crystal number, and spot number for each zircon analysis. Pb, lead; Pb_c, common lead; U, uranium; Th, thorium; ppm, part per million; Ma, mega-annum; MSWD, mean square weighted deviation; N, number of zircon spot analyses; %, percent. All analyses are from different crystals although some spots in runs 1 and 2 have identical numbers.]

Sample 17-LM-2112 (this report)													
Spot	$^{204}Pb/^{206}Pb$	±%	$^{207}Pb/^{206}Pb$	±%	$^{208}Pb/^{206}Pb$	±%	% $^{206}Pb_c$	ppm U	ppm Th	Total $^{206}Pb/^{238}U$	±%	$^{206}Pb/^{238}U$ age ± error (Ma)	
Run 1													
2112-02.1†	$-2.0E^{-4}$	58	0.0508	5.1	0.372	6.3	0.211	208	246	0.0243	2.2	154	3
2112-03.1	$4.9E^{-4}$	58	0.0454	5.2	0.259	6.0	−0.451	92	70	0.0225	2.0	144	3
2112-04.1	$-8.3E^{-4}$	58	0.0477	6.5	0.102	13.6	−0.135	55	19	0.0216	2.5	138	3
2112-05.1	$1.2E^{-4}$	100	0.0466	9.4	0.283	5.0	−0.292	127	128	0.0224	2.8	143	4
2112-06.1	$4.1E^{-4}$	45	0.0505	3.4	0.357	3.6	0.200	186	221	0.0220	1.9	140	3
Run 2													
2112-01.1	$1.9E^{-5}$	1,067	0.0470	3.2	0.303	4.3	−0.253	195	199	0.023	2.1	148	3
2112-02.1	$9.6E^{-4}$	84	0.0464	12.3	0.144	11.3	−0.347	60	32	0.024	2.0	153	3
2112-03.1	$5.3E^{-4}$	131	0.0449	5.2	0.221	8.0	−0.518	76	49	0.024	1.9	151	3
2112-04.1	$-4.4E^{-4}$	178	0.0726	12.1	0.264	7.4	2.975	77	53	0.023	3.0	142	5
2112-05.1	$-2.2E^{-4}$	139	0.0489	3.6	0.257	5.4	−0.015	150	123	0.024	1.5	150	2
2112-06.1	$-7.0E^{-4}$	120	0.0469	11.0	0.180	9.6	−0.273	66	42	0.024	1.9	154	3
2112-07.1	$-1.0E^{-4}$	225	0.0477	3.6	0.310	9.1	−0.170	156	136	0.024	3.6	150	5
2112-08.1	$3.5E^{-4}$	94	0.0501	4.0	0.219	6.5	0.113	124	101	0.024	2.6	156	4
2112-09.1	$-6.5E^{-4}$	120	0.0461	5.1	0.224	7.9	−0.377	73	49	0.024	3.7	152	6
2112-10.1	$1.6E^{-3}$	95	0.0454	7.8	0.181	13.2	−0.450	38	23	0.023	4.8	149	7

†Spots were statistically rejected from mean age determinations.

Run 1

Mean age of coherent group (N=4)	141.3 Ma
Age error (95% confidence, without error in standard)	3.2 Ma
MSWD	0.79
Probability of fit	0.50
Age error (95% confidence, with error in standard)	3.4 Ma

Run 2

Mean age of coherent group (N=10)	150.9 Ma
Age error (95% confidence, without error in standard)	2.2 Ma
MSWD	0.79
Probability of fit	0.63
Age error (95% confidence, with error in standard)	2.6 Ma
Final age and error (statistical mean of both runs)	148.2 ± 5.2 Ma

Table 31. Sensitive high-resolution ion microprobe-reverse geometry (SHRIMP-RG) U-Pb zircon data for sample 17-LM-2113, Lane Mountain area, California.

[Spot designation indicates sample number, crystal number, and spot number for each zircon analysis. Pb, lead; Pb_c, common lead; U, uranium; Th, thorium; ppm, part per million; Ma, mega-annum; MSWD, mean square weighted deviation; N, number of zircon spot analyses; %, percent.]

Sample 17-LM-2113 (this report)													
Spot	$^{204}Pb/^{206}Pb$	±%	$^{207}Pb/^{206}Pb$	±%	$^{208}Pb/^{206}Pb$	±%	% $^{206}Pb_c$	ppm U	ppm Th	Total $^{206}Pb/^{238}U$	±%	$^{206}Pb/^{238}U$ age ± error (Ma)	
Run 1													
2113-01.1	$6.4E^{-5}$	100	0.048	3.0	0.221	2.4	−0.451	209	147	0.0392	1.9	249	5
2113-02.1	$1.5E^{-4}$	71	0.047	5.5	0.142	3.2	−0.564	180	85	0.0402	1.9	255	5
2113-03.1	$7.3E^{-4}$	32	0.046	5.4	0.155	3.0	−0.691	179	88	0.0403	1.9	256	5
2113-04.1	$2.3E^{-4}$	45	0.051	2.5	0.211	3.8	−0.065	292	185	0.0396	2.0	250	5
2113-05.1	$2.3E^{-4}$	50	0.051	2.7	0.232	5.7	−0.036	223	160	0.0403	2.1	255	5
2113-06.1	$1.4E^{-4}$	38	0.052	1.6	0.149	2.8	0.122	624	292	0.0410	1.9	259	5
Run 2													
2113-07.1	$-1.3E^{-4}$	310	0.0470	5.4	0.194	3.7	−0.542	115	66	0.0400	2.5	254	6
2113-08.1	$-2.1E^{-4}$	139	0.0516	4.0	0.247	2.7	0.063	189	134	0.0383	1.3	242	3
2113-09.1	$1.1E^{-4}$	647	0.0448	7.1	0.143	5.8	−0.772	75	36	0.0375	1.4	239	4
2113-10.1	$5.9E^{-5}$	682	0.0462	5.3	0.248	3.2	−0.613	126	95	0.0385	1.5	245	4
2113-11.1	$-1.3E^{-4}$	183	0.0490	4.0	0.266	2.5	−0.280	208	164	0.0394	1.5	250	4
2113-12.1	$-2.3E^{-5}$	1,158	0.0491	4.3	0.279	2.6	−0.252	185	151	0.0386	1.9	245	5
2113-13.1†	$1.4E^{-4}$	275	0.0572	8.2	0.219	3.3	0.809	147	96	0.0362	1.6	228	4
2113-14.1	$-2.9E^{-5}$	1,226	0.0474	5.0	0.163	3.8	−0.475	139	70	0.0388	1.4	247	3
2113-15.1†	$7.4E^{-5}$	716	0.0471	5.8	0.178	4.3	−0.466	107	58	0.0366	1.8	233	4
2113-16.1	$4.5E^{-4}$	100	0.0483	5.3	0.200	3.7	−0.369	118	73	0.0397	1.4	252	4

†Spots were statistically rejected from mean age determinations.

Run 1

Mean age of coherent group (N=6)	253.9 Ma
Age error (95% confidence, without error in standard)	4.0 Ma
MSWD	0.62
Probability of fit	0.68
Age error (95% confidence, with error in standard)	4.6 Ma

Run 2

Mean age of coherent group (N=8)	245.9 Ma
Age error (95% confidence, without error in standard)	2.7 Ma
MSWD	1.51
Probability of fit	0.16
Age error (95% confidence, with error in standard)	3.4 Ma
Final age and error (statistical mean of both runs)	249.3 ± 5.6 Ma

Table 32. Sensitive high-resolution ion microprobe-reverse geometry (SHRIMP-RG) U-Pb zircon data for sample 17-LM-2127, Lane Mountain area, California.

[Spot designation indicates sample number, crystal number, and spot number for each zircon analysis. Pb, lead; Pb_c, common lead; U, uranium; Th, thorium; ppm, part per million; Ma, mega-annum; MSWD, mean square weighted deviation; N, number of zircon spot analyses; %, percent.]

Sample 17-LM-2127 (this report)													
Spot	$^{204}Pb/^{206}Pb$	±%	$^{207}Pb/^{206}Pb$	±%	$^{208}Pb/^{206}Pb$	±%	% $^{206}Pb_c$	ppm U	ppm Th	Total $^{206}Pb/^{238}U$	±%	$^{206}Pb/^{238}U$ age ± error (Ma)	
2127-01.1	$7.7E^{-4}$	50	0.0435	5.6	0.148	8.6	−0.691	103	57	0.0227	4.0	146	6
2127-02.1	$3.3E^{-4}$	58	0.0485	3.9	0.201	5.6	−0.069	132	94	0.0234	2.0	149	3
2127-03.1	$3.7E^{-4}$	50	0.0522	3.5	0.179	5.5	0.422	147	85	0.0221	3.1	140	4
2127-04.1	$3.9E^{-4}$	50	0.0475	7.3	0.235	8.0	−0.205	142	124	0.0242	5.3	154	8
2127-05.1	$1.3E^{-4}$	71	0.0482	3.0	0.165	4.6	−0.141	235	133	0.0252	5.0	161	8

Mean age of coherent group (N=5)	147.9 Ma
Age error (95% confidence, without error in standard)	4.2 Ma
MSWD	1.65
Probability of fit	0.16
Age error (95% confidence, with error in standard)	4.5 Ma
Final age and error	147.9 ± 4.5 Ma

Table 33. Sensitive high-resolution ion microprobe-reverse geometry (SHRIMP-RG) U-Pb zircon data for sample 17-LM-2128, Lane Mountain area, California.

[Spot designation indicates sample number, crystal number, and spot number for each zircon analysis. Pb, lead; Pb_c, common lead; U, uranium; Th, thorium; ppm, part per million; Ma, mega-annum; MSWD, mean square weighted deviation; N, number of zircon spot analyses; %, percent.]

Sample 17-LM-2128 (this report)													
Spot	$^{204}Pb/^{206}Pb$	±%	$^{207}Pb/^{206}Pb$	±%	$^{208}Pb/^{206}Pb$	±%	% $^{206}Pb_c$	ppm U	ppm Th	Total $^{206}Pb/^{238}U$	±%	$^{206}Pb/^{238}U$ age ± error (Ma)	
2128-01.1	$3.9E^{-3}$	35	0.0494	14.8	0.157	13.2	0.079	32	18	0.0216	3.5	137	5
2128-02.1	$3.1E^{-4}$	58	0.0497	3.9	0.292	4.6	0.082	142	131	0.0232	3.5	148	5
2128-03.1	$1.8E^{-4}$	100	0.0425	5.3	0.152	15.0	−0.817	75	45	0.0232	2.2	149	3
2128-04.1	$3.3E^{-3}$	27	0.0910	6.8	0.229	7.7	5.291	57	28	0.0237	5.0	143	7
2128-05.1	$5.9E^{-4}$	58	0.0470	5.5	0.167	14.5	−0.252	75	39	0.0231	3.1	147	5

Mean age of coherent group (N=5)	146.1 Ma
Age error (95% confidence, without error in standard)	4.1 Ma
MSWD	1.09
Probability of fit	0.36
Age error (95% confidence, with error in standard)	4.3 Ma
Final age and error	146.1 ± 4.3 Ma

Table 34. Sensitive high-resolution ion microprobe-reverse geometry (SHRIMP-RG) U-Pb zircon data for sample 17-LM-2191, Lane Mountain area, California.

[Spot designation indicates sample number, crystal number, and spot number for each zircon analysis. Pb, lead; Pb_c, common lead; U, uranium; Th, thorium; ppm, part per million; Ma, mega-annum; MSWD, mean square weighted deviation; N, number of zircon spot analyses; %, percent; —, not applicable]

Sample 17-LM-2191 (this report)													
Spot	$^{204}Pb/^{206}Pb$	±%	$^{207}Pb/^{206}Pb$	±%	$^{208}Pb/^{206}Pb$	±%	$\%\ ^{206}Pb_c$	ppm U	ppm Th	Total $^{206}Pb/^{238}U$	±%	$^{206}Pb/^{238}U$ age ± error (Ma)	
2191-01.1	—	—	0.0467	5.0	0.234	7.1	−0.285	267	184	0.0226	2.1	145	3
2191-02.1	$-3.6E^{-4}$	41	0.0470	3.0	0.334	3.2	−0.298	253	260	0.0258	9.2	165	15
2191-03.1	$-6.2E^{-5}$	100	0.0471	3.0	0.224	3.9	−0.249	240	190	0.0237	1.9	151	3
2191-04.1	$-8.6E^{-5}$	71	0.0484	2.5	0.170	3.8	−0.079	370	208	0.0233	2.3	148	3
2191-05.1	—	100	0.0493	2.2	0.209	5.4	0.025	419	267	0.0238	2.2	152	3

Mean age of coherent group (N=5)	149.2 Ma
Age error (95% confidence, without error in standard)	3.1 Ma
MSWD	1.17
Probability of fit	0.32
Age error (95% confidence, with error in standard)	3.4 Ma
Final age and error	149.2 ± 3.4 Ma

Table 35. Sensitive high-resolution ion microprobe-reverse geometry (SHRIMP-RG) U-Pb zircon data for sample 17-LM-2203, Lane Mountain area, California.

[Spot designation indicates sample number, crystal number, and spot number for each zircon analysis. Pb, lead; Pb_c, common lead; U, uranium; Th, thorium; ppm, part per million; Ma, mega-annum; MSWD, mean square weighted deviation; N, number of zircon spot analyses; %, percent; —, not applicable]

Sample 17-LM-2203 (this report)													
Spot	$^{204}Pb/^{206}Pb$	±%	$^{207}Pb/^{206}Pb$	±%	$^{208}Pb/^{206}Pb$	±%	$\%\ ^{206}Pb_c$	ppm U	ppm Th	Total $^{206}Pb/^{238}U$	±%	$^{206}Pb/^{238}U$ age ± error (Ma)	
2203-01.1	$2.6E^{-4}$	71	0.0496	3.7	0.151	8.0	0.049	134	73	0.0248	4.2	158	7
2203-02.1	$-8.7E^{-4}$	50	0.0485	4.9	0.129	10.5	−0.073	83	43	0.0237	3.8	151	6
2203-03.1	$2.9E^{-4}$	100	0.0421	13.3	0.106	12.8	−0.878	62	34	0.0236	4.3	152	7
2203-04.1	—	—	0.0515	9.2	0.178	12.7	0.306	129	86	0.0233	4.5	148	7
2203-05.1	$-3.3E^{-4}$	71	0.0422	5.3	0.201	6.9	−0.840	94	54	0.0221	2.2	142	3

Mean age of coherent group (N=5)	146.9 Ma
Age error (95% confidence, without error in standard)	4.4 Ma
MSWD	1.62
Probability of fit	0.16
Age error (95% confidence, with error in standard)	4.6 Ma
Final age and error	146.9 ± 4.6 Ma

Table 36. Sensitive high-resolution ion microprobe-reverse geometry (SHRIMP-RG) U-Pb zircon data for sample 18-LM-2594, Lane Mountain area, California.

[Spot designation indicates sample number, crystal number, and spot number for each zircon analysis. Pb, lead; Pb_c, common lead; U, uranium; Th, thorium; ppm, part per million; Ma, mega-annum; MSWD, mean square weighted deviation; N, number of zircon spot analyses; %, percent.]

Sample 18-LM-2594 (this report)													
Spot	$^{204}Pb/^{206}Pb$	±%	$^{207}Pb/^{206}Pb$	±%	$^{208}Pb/^{206}Pb$	±%	% $^{206}Pb_c$	ppm U	ppm Th	Total $^{206}Pb/^{238}U$	±%	$^{206}Pb/^{238}U$ age ± error (Ma)	
2594-01.1	$2.2E^{-3}$	46	0.1071	11.5	0.308	7.3	7.317	108	59	0.0235	2.4	139	4
2594-02.1	$5.9E^{-3}$	35	0.1316	20.2	0.241	11.4	10.384	56	28	0.0252	2.8	144	7
2594-03.1	$4.5E^{-4}$	231	0.0766	12.4	0.284	8.0	3.462	103	65	0.0240	1.8	147	3
2594-04.1	$5.1E^{-4}$	110	0.0760	12.5	0.297	5.4	3.391	222	151	0.0240	2.1	148	4
2594-05.1	$1.8E^{-3}$	39	0.0657	4.4	0.134	22.2	2.082	173	81	0.0242	3.2	151	5
2594-06.1	$9.7E^{-4}$	39	0.0532	3.4	0.281	4.3	0.521	373	299	0.0239	1.8	151	3

Mean age of coherent group (N=6)	147.6 Ma
Age error (95% confidence, without error in standard)	3.0 Ma
MSWD	1.44
Probability of fit	0.21
Age error (95% confidence, with error in standard)	3.2 Ma
Final age and error	147.6 ± 3.2 Ma

Table 37. Sensitive high-resolution ion microprobe-reverse geometry (SHRIMP-RG) U-Pb zircon data for sample 18-LM-2595, Lane Mountain area, California.

[Spot designation indicates sample number, crystal number, and spot number for each zircon analysis. Pb, lead; Pb_c, common lead; U, uranium; Th, thorium; ppm, part per million; Ma, mega-annum; MSWD, mean square weighted deviation; N, number of zircon spot analyses; %, percent.]

Sample 18-LM-2595 (this report)													
Spot	$^{204}Pb/^{206}Pb$	±%	$^{207}Pb/^{206}Pb$	±%	$^{208}Pb/^{206}Pb$	±%	% $^{206}Pb_c$	ppm U	ppm Th	Total $^{206}Pb/^{238}U$	±%	$^{206}Pb/^{238}U$ age ± error (Ma)	
Run 1													
2595-01.1	$-5.9E^{-5}$	154	0.0531	2.0	0.277	6.2	0.218	534	465	0.0407	1.9	256	5
2595-02.1	$1.7E^{-4}$	56	0.0522	1.8	0.423	1.9	0.122	715	942	0.0395	1.7	250	4
2595-03.1	$7.6E^{-4}$	16	0.0621	1.5	0.477	1.4	1.352	1,169	1,605	0.0405	1.6	253	4
2595-04.1	$4.5E^{-4}$	24	0.0574	2.5	0.418	2.8	0.759	948	1,130	0.0403	1.7	253	4
2595-05.1	$2.0E^{-4}$	37	0.0559	1.5	0.104	6.7	0.580	1,027	332	0.0400	1.7	252	4
2595-06.1†	$3.2E^{-4}$	51	0.0532	2.5	0.043	15.2	0.527	605	65	0.0232	1.6	147	2
Run 2													
2595-07.1†	$-9.6E^{-6}$	1,352	0.0498	2.7	0.109	2.6	−0.119	455	156	0.0361	1.6	229	4
2595-08.1†	$-1.7E^{-5}$	1,291	0.0492	3.7	0.089	3.9	−0.007	415	123	0.0252	1.5	160	2
2595-09.1	$-8.1E^{-6}$	1,158	0.0487	4.3	0.417	1.3	−0.317	521	639	0.0397	1.5	252	4
2595-10.1†	$-3.5E^{-5}$	310	0.0506	2.6	0.296	2.8	−0.039	493	444	0.0370	1.5	234	4
2595-11.1	$-5.1E^{-6}$	1,226	0.0513	2.0	0.403	1.0	0.035	874	1,072	0.0384	1.4	243	3
2595-12.1†	$1.1E^{-3}$	33	0.0635	16.5	0.323	5.6	1.602	211	172	0.0365	2.1	228	6
2595-13.1	$6.2E^{-5}$	136	0.0518	2.1	0.020	4.8	0.093	718	47	0.0382	1.4	242	3
2595-14.1†	$-4.7E^{-6}$	1,291	0.0504	1.9	0.082	2.1	0.167	1,617	402	0.0233	1.7	148	3
2595-15.1†	$-1.1E^{-5}$	1,226	0.0515	2.9	0.350	1.6	0.102	385	422	0.0358	1.4	227	3
2595-16.1	$-5.5E^{-5}$	183	0.0495	4.7	0.527	1.2	−0.221	543	868	0.0395	1.4	250	3
2595-17.1	$-5.4E^{-5}$	173	0.0527	2.5	0.402	1.3	0.196	556	686	0.0391	1.5	247	4

†Spots were statistically rejected from mean age determinations.

Run 1

Mean age of coherent group (N=5)	252.4 Ma
Age error (95% confidence, without error in standard)	3.9 Ma
MSWD	0.29
Probability of fit	0.89
Age error (95% confidence, with error in standard)	4.4 Ma

Run 2

Mean age of coherent group (N=5)	246.2 Ma
Age error (95% confidence, without error in standard)	3.2 Ma
MSWD	1.61
Probability of fit	0.17
Age error (95% confidence, with error in standard)	3.8 Ma
Final age and error (statistical mean of both runs)	249.3 ± 5.1 Ma

Table 38. Sensitive high-resolution ion microprobe-reverse geometry (SHRIMP-RG) U-Pb zircon data for sample 18-LM-2603, Lane Mountain area, California.

[Spot designation indicates sample number, crystal number, and spot number for each zircon analysis. Pb, lead; Pb_c, common lead; U, uranium; Th, thorium; ppm, part per million; Ma, mega-annum; MSWD, mean square weighted deviation; N, number of zircon spot analyses; %, percent.]

Sample 18-LM-2603 (this report)													
Spot	$^{204}Pb/^{206}Pb$	±%	$^{207}Pb/^{206}Pb$	±%	$^{208}Pb/^{206}Pb$	±%	% $^{206}Pb_c$	ppm U	ppm Th	Total $^{206}Pb/^{238}U$	±%	$^{206}Pb/^{238}U$ age ± error (Ma)	
2603-01.1	$4.6E^{-3}$	41	0.1172	17.2	0.292	22.6	8.587	65	40	0.0239	3.9	139	7
2603-02.1	$1.7E^{-3}$	69	0.0783	5.1	0.277	14.7	3.695	112	59	0.0230	1.8	141	3
2603-03.1	$1.8E^{-3}$	110	0.1202	17.4	0.364	11.2	8.921	39	23	0.0267	5.7	155	10
2603-04.1	$4.3E^{-4}$	75	0.0558	3.7	0.303	4.3	0.843	304	266	0.0239	2.1	151	3
2603-05.1	$3.8E^{-3}$	118	0.1091	19.1	0.330	15.3	7.570	29	15	0.0236	2.6	139	5
2603-06.1	$2.5E^{-3}$	58	0.0745	11.0	0.119	16.9	3.203	64	33	0.0242	4.2	149	6

Mean age of coherent group (N=6)	144.6 Ma
Age error (95% confidence, without error in standard)	3.4 Ma
MSWD	1.84
Probability of fit	0.10
Age error (95% confidence, with error in standard)	3.6 Ma
Final age and error	144.6 ± 3.6 Ma

Table 39. Sensitive high-resolution ion microprobe-reverse geometry (SHRIMP-RG) U-Pb zircon data for sample 18-LM-2604, Lane Mountain area, California.

[Spot designation indicates sample number, crystal number, and spot number for each zircon analysis. Pb, lead; Pb_c, common lead; U, uranium; Th, thorium; ppm, part per million; Ma, mega-annum; MSWD, mean square weighted deviation; N, number of zircon spot analyses; %, percent.]

Sample 18-LM-2604 (this report)													
Spot	$^{204}Pb/^{206}Pb$	±%	$^{207}Pb/^{206}Pb$	±%	$^{208}Pb/^{206}Pb$	±%	% $^{206}Pb_c$	ppm U	ppm Th	Total $^{206}Pb/^{238}U$	±%	$^{206}Pb/^{238}U$ age ± error (Ma)	
Run 1													
2604-01.1†	$8.5E^{-5}$	254	0.0524	2.8	0.154	11.9	0.129	331	167	0.0404	0.42	255	4
2604-02.1	$4.0E^{-4}$	75	0.0551	10.1	0.297	4.7	0.504	203	191	0.0388	0.42	244	5
2604-03.1	$4.7E^{-4}$	51	0.0565	2.9	0.293	4.2	0.663	243	185	0.0399	0.45	251	7
2604-04.1†	$3.6E^{-4}$	46	0.0533	4.7	0.413	2.5	0.232	442	538	0.0412	0.26	260	5
2604-05.1	$3.8E^{-4}$	46	0.0534	2.8	0.287	3.2	0.308	429	335	0.0376	0.33	237	5
2604-06.1	$8.0E^{-4}$	35	0.0549	2.9	0.256	6.9	0.481	309	230	0.0382	0.39	241	4
Run 2													
2604-07.1	$-5.9E^{-5}$	1,158	0.0513	6.9	0.191	5.0	0.046	72	39	0.0371	1.9	235	4
2604-08.1	$-2.3E^{-5}$	1,226	0.0512	4.1	0.312	4.0	0.035	182	175	0.0375	1.7	237	4
2604-09.1	$1.1E^{-5}$	749	0.0511	2.1	0.400	1.1	0.001	690	843	0.0383	1.4	242	3
2604-10.1	$1.1E^{-5}$	647	0.0514	2.1	0.367	1.2	0.038	623	710	0.0387	1.5	245	4
2604-11.1	$3.1E^{-5}$	682	0.0496	3.6	0.353	2.0	−0.197	243	254	0.0392	1.3	248	3
2604-12.1	$-3.0E^{-5}$	1,352	0.0430	5.2	0.315	2.9	−0.990	136	130	0.0371	1.6	237	4
2604-13.1	$-6.8E^{-6}$	1,352	0.0526	2.2	0.032	4.1	0.200	593	56	0.0383	1.3	242	3
2604-14.1	$-1.4E^{-4}$	104	0.0539	2.9	0.387	1.6	0.356	352	416	0.0384	1.5	242	4
2604-15.1	$2.0E^{-5}$	275	0.0513	1.8	0.328	1.0	0.031	963	958	0.0386	1.3	244	3
2604-16.1	$9.8E^{-5}$	275	0.0499	4.1	0.320	2.3	−0.140	201	193	0.0380	1.5	241	4

†Spots were statistically rejected from mean age determinations.

Run 1

Mean age of coherent group (N=4)	242.0 Ma
Age error (95% confidence, without error in standard)	5.1 Ma
MSWD	0.91
Probability of fit	0.43
Age error (95% confidence, with error in standard)	5.5 Ma

Run 2

Mean age of coherent group (N=10)	241.9 Ma
Age error (95% confidence, without error in standard)	2.3 Ma
MSWD	1.12
Probability of fit	0.35
Age error (95% confidence, with error in standard)	3.0 Ma
Final age and error (statistical mean of both runs)	241.9 ± 3.9

Table 40. Sensitive high-resolution ion microprobe-reverse geometry (SHRIMP-RG) U-Pb zircon data for sample 18-LM-2607, Lane Mountain area, California.

[Spot designation indicates sample number, crystal number, and spot number for each zircon analysis. Pb, lead; Pb_c, common lead; U, uranium; Th, thorium; ppm, part per million; Ma, mega-annum; MSWD, mean square weighted deviation; N, number of zircon spot analyses; %, percent.]

Sample 18-LM-2607 (this report)													
Spot	$^{204}Pb/^{206}Pb$	±%	$^{207}Pb/^{206}Pb$	±%	$^{208}Pb/^{206}Pb$	±%	$\%\ ^{206}Pb_c$	ppm U	ppm Th	Total $^{206}Pb/^{238}U$	±%	$^{206}Pb/^{238}U$ age ± error (Ma)	
2607-01.1	$-4.1E^{-4}$	195	0.0569	15.6	0.157	21.7	0.984	132	68	0.0239	2.5	151	4
2607-02.1	$4.1E^{-4}$	125	0.0528	4.7	0.298	5.9	0.474	179	154	0.0235	1.7	149	3
2607-03.1	$3.2E^{-3}$	64	0.0758	13.5	0.223	22.8	3.352	52	29	0.0244	2.1	151	4
2607-04.1	$2.0E^{-3}$	125	0.0853	9.3	0.299	22.4	4.570	33	17	0.0233	4.4	142	6
2607-05.1	$4.2E^{-3}$	58	0.1006	12.6	0.289	13.4	6.486	35	23	0.0245	3.8	146	6
2607-06.1	$1.9E^{-3}$	69	0.0581	7.1	0.281	8.5	1.141	85	71	0.0235	1.9	148	3

Mean age of coherent group (N=6)	148.7 Ma
Age error (95% confidence, without error in standard)	3.0 Ma
MSWD	0.41
Probability of fit	0.84
Age error (95% confidence, with error in standard)	3.2 Ma
Final age and error	148.7 ± 3.2 Ma

Table 41. Sensitive high-resolution ion microprobe-reverse geometry (SHRIMP-RG) U-Pb zircon data for sample 18-LM-2725, Lane Mountain area, California.

[Spot designation indicates sample number, crystal number, and spot number for each zircon analysis. Pb, lead; Pb_c, common lead; U, uranium; Th, thorium; ppm, part per million; Ma, mega-annum; MSWD, mean square weighted deviation; N, number of zircon spot analyses; %, percent.]

Sample 18-LM-2725 (this report)													
Spot	$^{204}Pb/^{206}Pb$	±%	$^{207}Pb/^{206}Pb$	±%	$^{208}Pb/^{206}Pb$	±%	$\%\ ^{206}Pb_c$	ppm U	ppm Th	Total $^{206}Pb/^{238}U$	±%	$^{206}Pb/^{238}U$ age ± error (Ma)	
2725-01.1	$-1.1E^{-4}$	354	0.0557	4.3	0.202	12.9	0.842	184	108	0.0234	1.7	148	3
2725-02.1	$2.5E^{-3}$	39	0.0651	5.0	0.197	8.7	2.012	131	71	0.0243	1.7	152	3
2725-03.1	$7.2E^{-4}$	67	0.0639	7.7	0.262	6.0	1.861	193	145	0.0244	1.7	153	3
2725-04.1	$1.1E^{-4}$	871	0.0648	11.0	0.162	10.6	1.989	97	47	0.0236	3.0	147	5
2725-05.1	$2.3E^{-3}$	46	0.0629	5.7	0.157	10.9	1.720	100	47	0.0252	1.9	157	3
2725-06.1	$5.9E^{-4}$	125	0.0723	4.7	0.219	7.9	2.914	123	69	0.0241	3.9	149	6

Mean age of coherent group (N=6)	151.5 Ma
Age error (95% confidence, without error in standard)	2.6 Ma
MSWD	1.36
Probability of fit	0.24
Age error (95% confidence, with error in standard)	2.8 Ma
Final age and error	151.5 ± 2.8 Ma

Table 42. Sensitive high-resolution ion microprobe-reverse geometry (SHRIMP-RG) U-Pb zircon data for sample 18-LM-2744, Lane Mountain area, California.

[Spot designation indicates sample number, crystal number, and spot number for each zircon analysis. Pb, lead; Pb_c, common lead; U, uranium; Th, thorium; ppm, part per million; Ma, mega-annum; MSWD, mean square weighted deviation; N, number of zircon spot analyses; %, percent.]

Sample 18-LM-2744 (this report)													
Spot	$^{204}Pb/^{206}Pb$	±%	$^{207}Pb/^{206}Pb$	±%	$^{208}Pb/^{206}Pb$	±%	$\%\ ^{206}Pb_c$	ppm U	ppm Th	Total $^{206}Pb/^{238}U$	±%	$^{206}Pb/^{238}U$ age ± error (Ma)	
Run 1													
2744-01.1	$1.5E^{-3}$	51	0.0618	8.6	0.270	7.1	1.370	78	63	0.0372	2.7	232	6
2744-02.1	$2.8E^{-4}$	110	0.0641	7.0	0.221	5.5	1.653	159	92	0.0380	1.7	236	4
2744-03.1	$9.6E^{-4}$	44	0.0510	8.5	0.184	5.3	−0.025	198	114	0.0397	2.0	251	5
2744-04.1	$5.5E^{-4}$	75	0.0570	3.8	0.248	5.4	0.712	150	123	0.0402	3.2	252	8
2744-05.1	$6.8E^{-4}$	58	0.0578	3.7	0.180	6.3	0.822	147	87	0.0394	2.1	247	5
2744-06.1	$-1.2E^{-4}$	413	0.0564	4.4	0.261	6.2	0.656	104	77	0.0390	2.4	245	6
Run 2													
2744-07.1	$-3.8E^{-5}$	1,291	0.0488	5.7	0.172	4.2	−0.264	106	57	0.0371	1.6	235	4
2744-08.1†	$2.5E^{-4}$	183	0.0560	4.9	0.185	3.8	0.596	138	76	0.0397	6.0	249	15
2744-09.1	$-1.8E^{-5}$	1,226	0.0489	3.8	0.173	2.9	−0.239	264	147	0.0365	1.4	232	3
2744-10.1	$3.7E^{-4}$	167	0.0462	6.5	0.246	6.9	−0.558	114	81	0.0355	1.4	226	3
2744-11.1†	$-3.5E^{-5}$	1,158	0.0517	5.2	0.142	4.4	0.075	129	55	0.0386	1.6	244	4
2744-12.1	$1.5E^{-4}$	682	0.0566	7.6	0.200	5.9	0.723	60	39	0.0368	1.5	231	4
2744-13.1	$-2.3E^{-5}$	1,352	0.0545	4.1	0.288	5.0	0.454	213	197	0.0373	2.0	235	5
2744-14.1	$-2.0E^{-4}$	183	0.0522	4.8	0.297	2.9	0.175	155	137	0.0367	1.6	232	4
2744-15.1†	$1.2E^{-4}$	261	0.0527	4.3	0.275	5.4	0.191	189	161	0.0392	1.7	248	4
2744-16.1†	$2.7E^{-4}$	261	0.0477	6.9	0.150	5.5	−0.446	79	40	0.0396	2.1	251	5

†Spots were statistically rejected from mean age determinations.

Run 1

Mean age of coherent group (N=6)	243.1 Ma
Age error (95% confidence, without error in standard)	4.4 Ma
MSWD	1.97
Probability of fit	0.08
Age error (95% confidence, with error in standard)	4.9 Ma

Run 2

Mean age of coherent group (N=6)	231.4 Ma
Age error (95% confidence, without error in standard)	3.0 Ma
MSWD	0.85
Probability of fit	0.52
Age error (95% confidence, with error in standard)	3.6 Ma
Final age and error (statistical mean of both runs)	237.3 ± 7.3 Ma

Table 43. Sensitive high-resolution ion microprobe-reverse geometry (SHRIMP-RG) U-Pb zircon data for sample 18-LM-2756, Lane Mountain area, California.

[Spot designation indicates sample number, crystal number, and spot number for each zircon analysis. Pb, lead; Pb_c, common lead; U, uranium; Th, thorium; ppm, part per million; Ma, mega-annum; MSWD, mean square weighted deviation; N, number of zircon spot analyses; %, percent; —, not applicable]

Sample 18-LM-2756 (this report)													
Spot	$^{204}Pb/^{206}Pb$	±%	$^{207}Pb/^{206}Pb$	±%	$^{208}Pb/^{206}Pb$	±%	% $^{206}Pb_c$	ppm U	ppm Th	Total $^{206}Pb/^{238}U$	±%	$^{206}Pb/^{238}U$ age ± error (Ma)	
2756-01.1	$6.5E^{-4}$	41	0.0505	3.7	0.157	7.3	0.173	183	96	0.0237	1.0	150	2
2756-02.1	$3.8E^{-4}$	58	0.0467	4.1	0.119	5.5	−0.301	161	69	0.0234	1.1	150	2
2756-03.1	—	—	0.0472	2.4	0.129	3.1	−0.234	444	176	0.0237	1.6	151	2
2756-04.1	$-1.2E^{-4}$	100	0.0487	4.0	0.192	4.3	−0.049	164	99	0.0240	1.6	153	3
2756-05.1	—	—	0.0484	4.5	0.163	5.2	−0.083	129	59	0.0233	1.7	149	3

Mean age of coherent group (N=5)	150.5
Age error (95% confidence, without error in standard)	1.8
MSWD	0.38
Probability of fit	0.82
Age error (95% confidence, with error in standard)	2.0
Final age and error	150.5 ± 2.0 Ma

Table 44. Sensitive high-resolution ion microprobe-reverse geometry (SHRIMP-RG) U-Pb zircon data for sample 18-LM-2809, Lane Mountain area, California.

[Spot designation indicates sample number, crystal number, and spot number for each zircon analysis. Pb, lead; Pb_c, common lead; U, uranium; Th, thorium; ppm, part per million; Ma, mega-annum; MSWD, mean square weighted deviation; N, number of zircon spot analyses; %, percent; ---, not applicable]

Sample 18-LM-2809 (this report)													
Spot	$^{204}Pb/^{206}Pb$	±%	$^{207}Pb/^{206}Pb$	±%	$^{208}Pb/^{206}Pb$	±%	% $^{206}Pb_c$	ppm U	ppm Th	Total $^{206}Pb/^{238}U$	±%	$^{206}Pb/^{238}U$ age ± error (Ma)	
Run 1													
2809-01.1	$-2.2E^{-5}$	71	0.0506	1.2	0.315	1.0	−0.086	1,074	1,025	0.0402	1.3	254	3
2809-02.1	$4.6E^{-5}$	71	0.0513	1.7	0.228	1.7	0.004	455	311	0.0399	1.6	252	4
2809-03.1†	$-1.3E^{-4}$	71	0.0468	3.0	0.119	4.0	−0.291	294	104	0.0238	1.3	152	2
2809-03.2†	—	—	0.0465	3.6	0.145	4.4	−0.323	185	77	0.0233	1.9	149	3
2809-03.3†	—	—	0.0514	1.9	0.146	2.4	0.291	578	251	0.0239	1.6	152	2
2809-04.1	$3.0E^{-5}$	58	0.0521	1.1	0.294	1.6	0.090	1,173	1,051	0.0408	1.6	257	4
2809-05.1	—	—	0.0525	1.9	0.053	4.0	0.164	369	60	0.0393	1.7	248	4
2809-06.1	$-2.8E^{-5}$	71	0.0518	1.3	0.258	2.2	0.064	777	592	0.0402	1.7	254	4
2809-07.1†	$-8.6E^{-5}$	100	0.0484	3.4	0.150	4.0	−0.091	229	109	0.0236	2.1	151	3
Run 2													
2809-08.1	$1.2E^{-5}$	275	0.0501	1.4	0.345	1.7	−0.155	1,485	1,598	0.0400	1.4	253	3
2809-09.1	$-4.1E^{-5}$	344	0.0483	3.0	0.159	2.3	−0.385	391	193	0.0406	1.4	257	4
2809-10.1	$2.3E^{-5}$	261	0.0505	1.9	0.237	1.3	−0.105	837	600	0.0403	1.3	255	3
2809-11.1	$3.1E^{-5}$	275	0.0514	2.2	0.242	5.9	0.003	601	463	0.0408	1.3	258	3
2809-12.1†	$-7.1E^{-6}$	1,226	0.0510	2.3	0.242	1.5	0.000	606	444	0.0380	1.3	241	3
2809-13.1	$2.7E^{-4}$	76	0.0496	3.3	0.202	2.4	−0.207	297	171	0.0396	1.3	251	3
2809-14.1	$1.4E^{-5}$	682	0.0510	2.4	0.227	1.6	−0.038	549	376	0.0397	1.4	251	4

†Spots were statistically rejected from mean age determinations.

Run 1

Mean age of coherent group (N=5)	253.3 Ma
Age error (95% confidence, without error in standard)	3.5 Ma
MSWD	0.66
Probability of fit	0.62
Age error (95% confidence, with error in standard)	3.8 Ma

Run 2

Mean age of coherent group (N=6)	254.1 Ma
Age error (95% confidence, without error in standard)	2.8 Ma
MSWD	0.75
Probability of fit	0.59
Age error (95% confidence, with error in standard)	3.5 Ma
Final age and error (statistical mean of both runs)	253.7 ± 3.7 Ma

Table 45. Sensitive high-resolution ion microprobe-reverse geometry (SHRIMP-RG) U-Pb zircon data for sample 18-LM-2997, Lane Mountain area, California.

[Spot designation indicates sample number, crystal number, and spot number for each zircon analysis. Pb, lead; Pb_c, common lead; U, uranium; Th, thorium; ppm, part per million; Ma, mega-annum; MSWD, mean square weighted deviation; N, number of zircon spot analyses; %, percent; —, not applicable]

Sample 18-LM-2997 (this report)													
Spot	$^{204}Pb/^{206}Pb$	±%	$^{207}Pb/^{206}Pb$	±%	$^{208}Pb/^{206}Pb$	±%	% $^{206}Pb_c$	ppm U	ppm Th	Total $^{206}Pb/^{238}U$	±%	$^{206}Pb/^{238}U$ age ± error (Ma)	
2997-01.1	$-7.8E^{-5}$	100	0.0498	3.1	0.303	2.7	−0.203	156	140	0.0409	1.1	259	3
2997-02.1	—	—	0.0498	2.8	0.277	2.5	−0.204	188	161	0.0412	2.3	261	6
2997-03.1	$4.1E^{-5}$	71	0.0519	1.6	0.467	1.2	0.067	606	831	0.0405	1.2	256	3
2997-04.1	$-2.4E^{-4}$	100	0.0511	5.5	0.168	6.4	−0.037	49	26	0.0406	3.4	257	9

Mean age of coherent group (N=4)	257.8 Ma
Age error (95% confidence, without error in standard)	3.8 Ma
MSWD	0.25
Probability of fit	0.86
Age error (95% confidence, with error in standard)	4.2 Ma
Final age and error	257.8 ± 4.2 Ma

Table 46. Sensitive high-resolution ion microprobe-reverse geometry (SHRIMP-RG) U-Pb zircon data for sample 18-LM-3042, Lane Mountain area, California.

[Spot designation indicates sample number, crystal number, and spot number for each zircon analysis. Pb, lead; Pb_c, common lead; U, uranium; Th, thorium; ppm, part per million; Ma, mega-annum; MSWD, mean square weighted deviation; N, number of zircon spot analyses; %, percent.]

Sample 18-LM-3042 (this report)													
Spot	$^{204}Pb/^{206}Pb$	±%	$^{207}Pb/^{206}Pb$	±%	$^{208}Pb/^{206}Pb$	±%	% $^{206}Pb_c$	ppm U	ppm Th	Total $^{206}Pb/^{238}U$	±%	$^{206}Pb/^{238}U$ age ± error (Ma)	
Run 1													
3042-01.1	$-5.4E^{-5}$	100	0.0516	2.5	0.290	2.3	0.056	206	173	0.0390	1.4	246	3
3042-02.1	$2.2E^{-4}$	71	0.0526	3.6	0.248	3.6	0.176	99	78	0.0396	1.2	250	3
3042-03.1	$6.7E^{-5}$	100	0.0492	5.9	0.338	2.4	−0.239	180	181	0.0390	2.6	247	7
3042-04.1	$1.1E^{-4}$	71	0.0512	2.7	0.331	2.3	−0.016	189	182	0.0401	1.4	254	4
3042-05.1†	$4.3E^{-5}$	100	0.0516	2.4	0.041	5.7	0.087	330	39	0.0371	1.7	235	4
3042-06.1	$1.8E^{-5}$	100	0.0506	2.4	0.570	1.0	−0.089	596	1024	0.0401	1.2	254	3
Run 2													
3042-07.1	$-2.9E^{-5}$	1,158	0.0503	4.8	0.258	3.1	−0.112	153	123	0.0394	1.8	249	5
3042-08.1	$-2.2E^{-5}$	1,226	0.0498	4.1	0.295	2.5	−0.172	212	200	0.0391	1.6	248	4
3042-09.1	$-4.0E^{-5}$	1,158	0.0515	5.5	0.250	3.7	0.066	113	89	0.0379	1.8	240	4
3042-10.1	$2.1E^{-4}$	88	0.0545	3.1	0.383	1.7	0.427	336	388	0.0389	1.3	245	3
3042-11.1	$-1.4E^{-4}$	292	0.0535	5.6	0.289	3.2	0.293	124	111	0.0392	1.4	247	4
3042-12.1	$-2.6E^{-4}$	173	0.0492	5.5	0.173	4.3	−0.255	121	68	0.0394	1.6	250	4
3042-13.1	$-3.1E^{-5}$	1,158	0.0517	4.8	0.256	5.4	0.078	138	108	0.0384	1.4	243	3
3042-14.1	$6.3E^{-5}$	647	0.0509	5.1	0.241	6.3	−0.037	129	97	0.0394	1.4	249	4
3042-15.1	$-3.2E^{-6}$	1,291	0.0509	1.6	0.265	1.1	−0.039	1,334	1,101	0.0396	1.6	250	4
3042-16.1	$3.9E^{-5}$	647	0.0538	3.9	0.312	2.4	0.309	201	187	0.0405	1.4	255	3

†Spots were statistically rejected from mean age determinations.

Run 1

Mean age of coherent group (N=5)	250.6 Ma
Age error (95% confidence, without error in standard)	3.2 Ma
MSWD	0.88
Probability of fit	0.48
Age error (95% confidence, with error in standard)	3.5 Ma

Run 2

Mean age of coherent group (N=10)	247.7 Ma
Age error (95% confidence, without error in standard)	2.4 Ma
MSWD	1.29
Probability of fit	0.24
Age error (95% confidence, with error in standard)	3.1 Ma
Final age and error (statistical mean of both runs)	248.7 ± 3.5 Ma

Table 47. Sensitive high-resolution ion microprobe-reverse geometry (SHRIMP-RG) U-Pb zircon data for sample 19-LM-3063, Lane Mountain area, California.

[Spot designation indicates sample number, crystal number, and spot number for each zircon analysis. Pb, lead; Pb_c, common lead; U, uranium; Th, thorium; ppm, part per million; Ma, mega-annum; MSWD, mean square weighted deviation; N, number of zircon spot analyses; %, percent.]

Sample 19-LM-3063 (this report)													
Spot	$^{204}Pb/^{206}Pb$	±%	$^{207}Pb/^{206}Pb$	±%	$^{208}Pb/^{206}Pb$	±%	% $^{206}Pb_c$	ppm U	ppm Th	Total $^{206}Pb/^{238}U$	±%	$^{206}Pb/^{238}U$ age ± error (Ma)	
Run 1													
3063-01.1†	$4.9E^{-5}$	100	0.0543	2.5	7.0	21.9	0.526	670	386	0.0313	34.1	198	67
3063-02.1†	$3.9E^{-5}$	50	0.0507	1.0	2.4	0.7	−0.150	1,033	649	0.0443	18.2	280	50
3063-03.1	$1.0E^{-5}$	100	0.0521	1.0	2.4	0.6	0.120	1,061	723	0.0388	2.0	245	5
3063-04.1	$9.7E^{-5}$	58	0.0503	1.8	7.7	0.8	−0.122	341	172	0.0395	2.1	250	5
3063-05.1	$1.4E^{-4}$	71	0.0510	2.7	16.3	1.1	−0.013	141	75	0.0383	2.0	242	5
3063-06.1	$2.7E^{-3}$	16	0.0529	2.2	9.7	1.0	0.183	307	140	0.0410	2.0	258	5
3063-07.1	$1.7E^{-5}$	100	0.0510	1.3	4.1	3.0	0.004	599	450	0.0377	2.1	238	5
Run 2													
3063-08.1	$5.7E^{-4}$	60	0.0527	3.6	0.185	11.9	0.204	74	41	0.039	1.5	245	4
3063-09.1	$2.5E^{-4}$	114	0.0515	3.3	0.173	10.6	0.023	91	57	0.040	2.4	255	6
3063-10.1	$9.4E^{-6}$	1,808	0.0508	2.2	0.220	3.6	−0.056	238	158	0.039	2.4	250	6
3063-11.1	$8.3E^{-5}$	131	0.0510	2.0	0.134	4.0	−0.031	263	113	0.040	5.0	254	12
3063-12.1	$-1.5E^{-5}$	335	0.0512	1.4	0.261	2.1	0.001	558	422	0.039	2.4	249	6
3063-13.1	$6.7E^{-5}$	131	0.0542	1.7	0.223	2.8	0.363	350	240	0.040	3.7	252	9

†Spots were statistically rejected from mean age determinations.

Run 1		Run 2	
Mean age of coherent group (N=5)	246.7 Ma	Mean age of coherent group (N=6)	248.5 Ma
Age error (95% confidence, without error in standard)	9.5 Ma	Age error (95% confidence, without error in standard)	4.8 Ma
MSWD	2.41	MSWD	0.56
Probability of fit	0.05	Probability of fit	0.73
Age error (95% confidence, with error in standard)	10.0 Ma	Age error (95% confidence, with error in standard)	5.3 Ma
		Final age and error (statistical mean of both runs)	247.7 ± 7.8 Ma

Table 48. Sensitive high-resolution ion microprobe-reverse geometry (SHRIMP-RG) U-Pb zircon data for sample 19-LM-3160, Lane Mountain area, California.

[Spot designation indicates sample number, crystal number, and spot number for each zircon analysis. Pb, lead; Pb_c, common lead; U, uranium; Th, thorium; ppm, part per million; Ma, mega-annum; MSWD, mean square weighted deviation; N, number of zircon spot analyses; %, percent; —, not applicable]

Sample 19-LM-3160 (this report)													
Spot	$^{204}Pb/^{206}Pb$	±%	$^{207}Pb/^{206}Pb$	±%	$^{208}Pb/^{206}Pb$	±%	% $^{206}Pb_c$	ppm U	ppm Th	Total $^{206}Pb/^{238}U$	±%	$^{206}Pb/^{238}U$ age ± error (Ma)	
3160-01.1	$1.5E^{-5}$	100	0.0514	1.2	2.7	2.0	0.051	683	854	0.0376	2.0	238	5
3160-02.1	$5.6E^{-5}$	45	0.0515	1.1	3.1	1.5	0.049	817	345	0.0389	2.4	246	6
3160-03.1	$1.9E^{-4}$	50	0.0530	2.2	9.4	1.0	0.261	195	101	0.0373	2.3	236	5
3160-04.1	$4.9E^{-5}$	71	0.0509	1.6	6.4	0.7	0.008	372	196	0.0368	2.2	233	5
3160-05.1	$6.8E^{-5}$	50	0.0520	1.3	3.9	1.2	0.124	549	358	0.0383	2.1	242	5
3160-06.1	$4.6E^{-5}$	50	0.0510	1.1	2.6	2.3	−0.022	801	599	0.0389	2.0	246	5
3160-07.1	—	—	0.0528	2.0	9.3	2.0	0.205	246	113	0.0391	2.3	247	6
3160-08.1	—	—	0.0489	1.5	5.4	0.7	−0.292	413	191	0.0399	2.0	253	5
3160-09.1†	$4.6E^{-5}$	100	0.0512	2.2	12.0	0.9	0.138	225	54	0.0312	2.0	198	4
3160-10.1	$8.1E^{-5}$	58	0.0505	1.8	6.5	2.4	−0.090	327	80	0.0398	2.4	252	6
3160-11.1†	—	—	0.0520	1.6	5.6	0.8	0.150	382	249	0.0364	2.1	230	5
3160-12.1†	$9.0E^{-5}$	41	0.0511	1.2	3.2	1.1	−0.057	591	580	0.0416	2.1	263	5

†Spots were statistically rejected from mean age determinations.

Mean age of coherent group (N=9)	243.1 Ma
Age error (95% confidence, without error in standard)	3.5 Ma
MSWD	1.74
Probability of fit	0.08
Age error (95% confidence, with error in standard)	4.7 Ma
Final age and error	243.1 ± 4.7 Ma

Table 49. Sensitive high-resolution ion microprobe-reverse geometry (SHRIMP-RG) U-Pb zircon data for sample 19-LM-3210, Lane Mountain area, California.

[Spot designation indicates sample number, crystal number, and spot number for each zircon analysis. Pb, lead; Pb_c, common lead; U, uranium; Th, thorium; ppm, part per million; Ma, mega-annum; MSWD, mean square weighted deviation; N, number of zircon spot analyses; %, percent; —, not applicable]

Sample 19-LM-3210 (this report)													
Spot	$^{204}Pb/^{206}Pb$	±%	$^{207}Pb/^{206}Pb$	±%	$^{208}Pb/^{206}Pb$	±%	% $^{206}Pb_c$	ppm U	ppm Th	Total $^{206}Pb/^{238}U$	±%	$^{206}Pb/^{238}U$ age ± error (Ma)	
Run 1													
3210-01.1†	$3.5E^{-4}$	33	0.0521	3.8	7.1	2.4	0.186	238	219	0.0351	4.8	222	11
3210-02.1	$8.0E^{-5}$	100	0.0494	3.1	15.8	3.3	−0.204	131	99	0.0380	3.0	241	7
3210-03.1†	$-7.6E^{-5}$	100	0.0508	2.8	16.1	2.2	0.120	167	91	0.0297	2.6	188	5
3210-04.1	—	—	0.0496	2.6	14.5	1.1	−0.169	161	119	0.0376	2.0	238	5
3210-05.1†	$2.5E^{-4}$	58	0.0546	2.8	20.0	1.2	0.505	136	83	0.0349	2.3	220	5
3210-06.1	$8.0E^{-5}$	58	0.0499	1.7	6.3	0.8	−0.163	349	250	0.0390	2.0	247	5
3210-07.1	—	—	0.0503	2.7	15.2	1.1	−0.090	137	107	0.0382	2.4	242	6
Run 2													
3210-08.1	$1.1E^{-5}$	1,293	0.0537	2.3	0.165	4.4	0.342	169	85	0.038	2.1	241	5
3210-09.1	$-1.8E^{-4}$	109	0.0533	2.5	0.263	3.9	0.267	135	104	0.039	1.1	248	3
3210-10.1	$2.3E^{-4}$	60	0.0509	2.3	0.243	3.6	−0.037	173	133	0.040	1.8	252	5
3210-11.1†	$7.2E^{-4}$	51	0.0515	3.2	0.212	5.3	0.067	97	66	0.038	1.3	239	3
3210-13.1†	$2.0E^{-4}$	122	0.0510	2.5	0.186	8.3	0.019	169	99	0.037	1.2	232	3
3210-14.1†	$2.1E^{-4}$	69	0.0523	3.6	0.204	3.8	0.320	261	131	0.029	3.9	183	7
3210-15.1	$2.1E^{-5}$	1,067	0.0489	3.3	0.217	5.5	−0.298	85	60	0.040	2.4	253	6
3210-16.1	$3.2E^{-4}$	60	0.0500	5.6	0.249	7.6	−0.190	125	98	0.041	2.2	262	6
3210-17.1	$-1.1E^{-4}$	109	0.0505	1.9	0.213	3.3	−0.072	248	162	0.038	3.2	243	8

†Spots were statistically rejected from mean age determinations.

Run 1

Mean age of coherent group (N=4)	242.1 Ma
Age error (95% confidence, without error in standard)	5.4 Ma
MSWD	0.58
Probability of fit	0.63
Age error (95% confidence, with error in standard)	6.2 Ma

Run 2

Mean age of coherent group (N=6)	248.9 Ma
Age error (95% confidence, without error in standard)	3.6 Ma
MSWD	1.90
Probability of fit	0.09
Age error (95% confidence, with error in standard)	4.3 Ma
Final age and error (statistical mean of both runs)	246.2 ± 6.1 Ma

Table 50. ICP-AES-MS (inductively coupled plasma atomic emission spectroscopy-mass spectrometry) geochemical analyses of silicon, titanium, aluminum, iron, magnesium, manganese, calcium, potassium, phosphorus, and sulfur in samples included in this report.

[Numerical values are in weight percent. Si, silicon; Ti, titanium, Al, aluminum; Mg, magnesium; Fe, iron; Mn, manganese, Ca, calcium; K, potassium; P, phosphorus; S, sulfur; —, not measured. Two separate analyses were obtained for sample 17-LM-2203.]

Sample	Si	Ti	Al	Fe	Mg	Mn	Ca	K	P	S
Permian-Triassic										
14-LM-16	—	0.58	10.2	1.77	3.53	0.044	6.23	0.27	0.14	—
14-LM-43*	—	0.54	8.81	1.94	5.5	0.115	4.88	1.98	0.15	—
15-LM-802A	28	0.53	9.27	1.99	5.62	—	4.86	1.89	0.12	<0.1
15-LM-816	28.4	0.49	9.06	1.88	5.22	—	5.21	1.92	0.1	<0.1
17-LM-1562	29.2	0.61	8.19	1.62	2.69	—	3.96	0.41	0.11	0.05
17-LM-1688	26.2	0.56	9.47	1.65	4.36	—	4.51	0.65	0.11	0.06
17-LM-1771	26.4	0.63	8.19	2.1	5.37	—	4.47	2.27	0.15	<0.1
17-LM-1779	26.2	0.54	8.54	2.19	4.97	—	5.15	1.62	0.14	<0.1
17-LM-1792	27.2	0.59	7.93	1.77	4.85	—	4.25	2.45	0.15	<0.1
17-LM-1835	25.3	0.59	7.93	2.38	5.64	—	4.87	2.24	0.15	<0.1
17-LM-1837	25.2	0.61	8.31	2.55	5.94	—	5.31	1.68	0.16	<0.1
17-LM-1860	24.7	0.65	9.31	1.98	4.7	—	5.77	0.78	0.17	<0.1
17-LM-1992	24.7	0.91	9	2.65	6.37	—	5.98	1.05	0.22	0.1
17-LM-2000	27.7	0.76	8.94	2.03	3.99	—	4.74	0.64	0.18	0.1
17-LM-2001	28.9	0.63	8.54	1.56	3.81	—	4	0.89	0.16	0.1
17-LM-2002	26.4	0.83	9.28	2.73	6.61	—	6.41	0.72	0.23	0.2
17-LM-2113	26.6	0.66	8.37	2.09	5.07	—	5.01	2.18	0.15	0.1
18-LM-2595	28.4	0.45	8.37	1.16	3.56	—	3.16	1.9	0.1	<0.1
18-LM-2604	27.4	0.5	8.95	1.86	4.83	—	4.57	0.72	0.12	0.1
18-LM-2744	29.8	0.39	9.2	2.08	2.25	—	4.27	0.42	0.13	<0.1
18-LM-2809	30.9	0.49	9.12	1.19	1.76	—	4.74	1.03	0.1	<0.1
18-LM-2997	28	0.56	9.04	2.24	5.71	—	5.08	0.31	0.08	<0.1
18-LM-3042	30.7	0.45	8.66	1.19	3.43	—	3.32	1.8	0.09	<0.1
19-LM-3063	26.6	0.51	9.58	1.98	3.68	—	4.08	0.6	0.13	<0.1
19-LM-3160	28	0.47	8.32	1.38	3.63	—	3.88	1.01	0.11	<0.1
19-LM-3210	29.2	0.32	8.54	1.68	1.54	—	3.3	1.09	0.09	<0.1
Jurassic										
14-LM-1*	—	0.32	8.19	0.77	2.59	0.06	2.45	2.82	0.05	—
14-LM-106	—	0.49	8.42	4.36	6.3	0.112	7.38	1.03	0.04	—
14-LM-154*	—	0.58	10.1	3.93	4.84	0.09	8.1	0.59	0.09	—
14-LM-468	—	0.49	9.54	1.59	1.67	0.032	5.44	0.31	0.07	—
14-LM-479	—	0.37	9.16	3.29	5.92	0.115	6.52	0.92	0.04	—
14-LM-490*	—	0.46	8.93	1.32	4.21	0.09	3.85	1.73	0.1	—
15-LM-806	—	0.54	10	1.76	2.94	0.054	6.6	0.5	0.16	—
15-LM-810	24	0.77	8.14	3.49	8	—	7.16	0.54	0.08	0.2
17-LM-1385	32.8	0.09	7.73	0.17	0.84	—	0.71	4.47	0.03	<0.01
17-LM-1656	23.9	0.49	9.82	2.58	6.06	—	6.74	0.59	0.07	0.09
17-LM-1748	26.1	0.64	8.93	1.76	5.23	—	4.47	1.42	0.14	0.06
17-LM-1749	26.5	0.59	9.3	1.62	5.04	—	4.15	1.51	0.12	0.05
17-LM-2112	24.9	0.63	10.6	2.7	4.72	—	7.05	1.1	0.12	0.2
17-LM-2127	26.1	0.65	10.4	1.54	4.78	—	5.25	1.18	0.18	0.1
17-LM-2128	26.5	0.66	9.91	1.74	5.23	—	5.27	1.22	0.19	0.1
17-LM-2191	32.5	0.23	8.69	0.41	1.69	—	2.09	3.08	0.06	<0.1
17-LM-2203 (1)	31.7	0.24	8.63	0.67	2.07	—	2.61	1.31	0.13	<0.1
17-LM-2203 (2)	32.6	0.28	8.29	0.89	2.82	—	2.4	1.5	0.08	<0.1
18-LM-2594	26.7	0.68	8.85	2.15	6.99	—	5.1	1.35	0.12	0.1
18-LM-2603	24.7	0.56	10.2	1.91	5.88	—	5.52	1.1	0.15	0.1
18-LM-2607	24.4	0.59	9.96	2.06	5.95	—	5.64	1.12	0.15	0.1
18-LM-2725	25.5	0.62	10.2	1.82	5.49	—	5.2	1.15	0.15	0.1
18-LM-2756	24.6	0.39	10	3.09	5.96	—	7.58	0.55	0.05	<0.1

*Indicates samples reported by Stone and others (2019).

Table 51. ICP-AES-MS (inductively coupled plasma atomic emission spectroscopy-mass spectrometry) geochemical analyses of lithium, beryllium, boron, scandium, vanadium, chromium, manganese, cobalt, nickel, and copper in samples included in this report.

[Numerical values are in parts per million. Li, lithium; Be, beryllium; B, boron; Sc, scandium; V, vanadium; Cr, chromium; Mn, manganese; Co, cobalt; Ni, nickel; Cu, copper; —, not measured. Two separate analyses were obtained for sample 17-LM-2203.]

Sample	Li	Be	B	Sc	V	Cr	Mn	Co	Ni	Cu
Permian-Triassic										
14-LM-16	<10	<5	—	23	215	<10	—	8.7	6	<5
14-LM-43*	20	<5	—	21	229	10	—	22.5	<5	110
15-LM-802A	15	<5	15	20	216	<10	1,100	21.5	9	288
15-LM-816	13	<5	13	20	211	<10	1,010	20	7	135
17-LM-1562	11	<5	<10	20	198	<10	267	10	14	22
17-LM-1688	<10	<5	17	19	188	<10	439	13	10	11
17-LM-1771	11	<5	24	23	218	12	1,160	21.5	13	94
17-LM-1779	11	<5	48	25	199	<10	1,510	21.3	12	138
17-LM-1792	13	<5	27	21	189	11	978	18.7	10	119
17-LM-1835	18	<5	41	24	239	13	1,160	23.8	16	131
17-LM-1837	13	<5	43	27	251	<10	1,290	24.4	14	133
17-LM-1860	<10	<5	19	24	203	<10	928	12.2	13	5
17-LM-1992	13	<5	26	34	278	<10	1,140	26.2	12	49
17-LM-2000	<10	<5	12	27	221	<10	572	13	8	123
17-LM-2001	11	<5	12	21	157	11	955	14.4	9	20
17-LM-2002	10	<5	25	31	278	<10	1,100	25.9	17	108
17-LM-2113	19	<5	26	25	231	12	1,140	25.9	13	187
18-LM-2595	18	<5	11	15	131	<10	716	10.7	13	25
18-LM-2604	23	<5	<10	20	178	14	734	16.2	11	46
18-LM-2744	12	<5	<10	14	193	11	342	13.3	13	35
18-LM-2809	<10	<5	<10	19	98	11	398	4.3	<5	24
18-LM-2997	17	<5	<10	23	226	13	360	8.1	11	99
18-LM-3042	<10	<5	<10	15	119	<10	430	7.7	6	9
19-LM-3063	<10	<5	<10	24	152	18	759	10.3	14	20
19-LM-3160	<10	<5	<10	17	166	13	323	9.7	5	15
19-LM-3210	<10	<5	<10	13	105	14	363	5.8	10	5
Jurassic										
14-LM-1*	20	<5	—	9	70	10	—	8.1	<5	6
14-LM-106	30	<5	—	33	233	170	—	40.8	29	36
14-LM-154*	10	<5	—	31	163	300	—	30.5	74	56
14-LM-468	<10	<5	—	21	103	10	—	4.2	12	<5
14-LM-479	10	<5	—	24	241	70	—	30.2	47	66
14-LM-490*	20	<5	—	15	126	10	—	14.1	18	39
15-LM-806	<10	<5	—	22	114	<10	—	9.6	<5	13
15-LM-810	14	<5	34	43	365	22	1,850	35.5	18	51
17-LM-1385	19	<5	<10	<5	8	<10	251	1.6	8	<5
17-LM-1656	11	<5	29	25	303	36	1,260	27.5	23	68
17-LM-1748	22	<5	20	17	169	13	1,040	19.3	14	26
17-LM-1749	26	<5	22	17	144	15	1,090	15.7	13	26
17-LM-2112	22	<5	18	19	167	57	1,120	18.6	28	15
17-LM-2127	22	<5	18	22	153	11	962	16.9	11	43
17-LM-2128	20	<5	19	23	153	12	1,050	17.9	11	36
17-LM-2191	28	<5	<10	<5	37	<10	390	4.2	7	<5
17-LM-2203 (1)	14	<5	<10	8	68	<10	422	5.9	9	11
17-LM-2203 (2)	15	<5	12	8	84	11	524	6.9	6	14
18-LM-2594	18	<5	<10	28	249	<10	1,370	22.7	10	53
18-LM-2603	23	<5	<10	19	160	<10	1,040	18.2	8	37
18-LM-2607	18	<5	<10	22	182	11	1,150	18.2	9	45
18-LM-2725	21	<5	<10	20	163	<10	1,030	15.6	9	34
18-LM-2756	13	<5	<10	33	320	35	941	29.9	31	107

*Indicates samples reported by Stone and others (2019).

Table 52. ICP-AES-MS (inductively coupled plasma atomic emission spectroscopy-mass spectrometry) geochemical analyses of zinc, gallium, germanium, arsenic, selenium, rubidium, strontium, yttrium, zirconium, and niobium in samples included in this report.

[Numerical values are in parts per million. Zn, zinc; Ga, gallium; Ge, germanium; As, arsenic; Se, selenium; Rb, rubidium; Sr, strontium; Y, yttrium; Zr, zirconium; Nb, niobium; —, not measured. Two separate analyses were obtained for sample 17-LM-2203.]

Sample	Zn	Ga	Ge	As	Se	Rb	Sr	Y	Zr	Nb
Permian-Triassic										
14-LM-16	46	20	2	<30	—	2.4	837	27.2	137	10
14-LM-43*	79	19	2	<30	—	65	634	25.5	132	13
15-LM-802A	71	19.8	2	<5	<5	60.1	597	23.2	255	10.8
15-LM-816	70	19.3	2	<5	<5	63.4	605	20.1	176	9.5
17-LM-1562	14	16.7	2	<5	<5	8.3	472	36	237	17.5
17-LM-1688	25	18.7	2	<5	<5	12.6	635	27.9	164	11.7
17-LM-1771	79	18	2	<5	<5	73.4	472	24	128	16.1
17-LM-1779	75	18.2	2	<5	<5	46.9	588	26.3	103	10.8
17-LM-1792	75	17.4	2	<5	<5	96.6	456	32.4	156	16.8
17-LM-1835	77	18	2	<5	<5	70.1	548	27	103	13.7
17-LM-1837	84	18.2	2	<5	<5	57.3	551	26.5	101	11.1
17-LM-1860	57	20.5	2	<5	<5	16.2	720	29.5	120	10.6
17-LM-1992	55	20.5	2	<5	<5	37.7	584	43.1	101	13.3
17-LM-2000	50	20.5	3	<5	<5	10.9	498	50	375	22
17-LM-2001	36	19	2	<5	<5	13.3	461	34.6	317	15.1
17-LM-2002	65	19.7	2	<5	<5	20.7	633	29.4	130	10.6
17-LM-2113	71	19.8	2	<5	<5	62.6	502	26.9	175	13.4
18-LM-2595	45	18.9	2	<5	<5	53.9	422	25.9	230	12.2
18-LM-2604	34	19	2	<5	<5	11.9	531	24.3	174	8.3
18-LM-2744	14	19.3	2	<5	<5	6.9	508	20.8	144	9.1
18-LM-2809	18	19	2	<5	<5	17.7	401	40.4	266	15.5
18-LM-2997	13	19.7	2	<5	<5	7.4	463	23.9	141	8.3
18-LM-3042	22	19.1	2	<5	<5	42.3	416	28.6	196	12.6
19-LM-3063	26	17.1	1	<5	<5	20.5	846	24.6	119	8.7
19-LM-3160	12	17.6	2	<5	<5	14.6	485	25.9	215	13.8
19-LM-3210	25	16.8	2	<5	<5	25.9	324	19.5	155	11.3
Jurassic										
14-LM-1*	55	18	2	<30	—	110	370	25.5	221	13
14-LM-106	77	18	2	<30	—	38.9	581	19.7	126	6
14-LM-154*	52	17	1	<30	—	16.8	485	17.2	81.2	5
14-LM-468	13	18	2	<30	—	3.9	580	48.3	169	11
14-LM-479	65	18	1	<30	—	22.1	634	17.3	73.5	5
14-LM-490*	70	19	1	<30	—	56	480	23.4	187	10
15-LM-806	21	21	2	<30	—	5.3	829	25.5	84.9	10
15-LM-810	108	19.8	2	<5	<5	14.7	486	27.7	67.2	5.2
17-LM-1385	18	16.3	2	23	<5	242	189	23.6	130	19.3
17-LM-1656	77	19.6	2	<5	<5	18.3	687	15.5	70	3.4
17-LM-1748	85	19.9	2	<5	<5	55.3	592	25.1	191	10.7
17-LM-1749	91	21.1	2	<5	<5	55.6	607	26.9	270	12.3
17-LM-2112	68	20.9	2	<5	<5	35.6	623	26.4	186	8.8
17-LM-2127	77	23.3	2	<5	<5	43.6	744	41.7	367	12.6
17-LM-2128	84	23.9	2	<5	<5	47	726	41.7	416	11.8
17-LM-2191	33	19	2	<5	<5	111	384	24.1	244	13.8
17-LM-2203 (1)	27	17	2	<5	<5	44.9	398	15.8	189	4.2
17-LM-2203 (2)	31	17	1	<5	<5	49.1	376	11.4	210	3.8
18-LM-2594	95	20.8	2	<5	<5	44.2	498	31	152	10.9
18-LM-2603	74	23.4	2	<5	<5	37.6	799	28.2	393	5.9
18-LM-2607	88	22.1	2	<5	<5	39.5	724	29.5	155	6.6
18-LM-2725	70	22.9	2	<5	<5	44.3	690	37.4	411	10
18-LM-2756	54	18.7	1	<5	<5	12.6	558	12.8	51.9	3

*Indicates samples reported by Stone and others (2019).

Table 53. ICP-AES-MS (inductively coupled plasma atomic emission spectroscopy-mass spectrometry) geochemical analyses of molybdemum, silver, cadmium, indium, tin, antimony, tellurium, cesium, barium, and hafnium in samples included in this report.

[Numerical values are in parts per million. Mo, molybdenum; Ag, silver; Cd, cadmium; In, indium; Sn, tin; Sb, antimony; Te, tellurium; Cs, cesium; Ba, barium; Hf, hafnium; —, not measured. Two separate analyses were obtained for sample 17-LM-2203.]

Sample	Mo	Ag	Cd	In	Sn	Sb	Te	Cs	Ba	Hf
Permian-Triassic										
14-LM-16	<2	<1	<0.2	<0.2	2	—	0.3	0.3	381	4
14-LM-43*	2	<1	<0.2	<0.2	1	—	0.6	1.4	613	4
15-LM-802A	3	<1	<0.2	<0.2	1	<0.5	0.4	1.4	671	7
15-LM-816	2	<1	<0.2	<0.2	1	<0.5	<0.1	1.4	656	5
17-LM-1562	<2	<1	<0.2	<0.2	1	<0.5	0.1	0.3	451	6
17-LM-1688	<2	<1	<0.2	<0.2	1	<0.5	0.3	0.7	509	4
17-LM-1771	<2	<1	<0.2	<0.2	1	<0.5	0.2	0.9	729	3
17-LM-1779	2	<1	<0.2	<0.2	<1	<0.5	0.2	1.4	694	3
17-LM-1792	<2	<1	<0.2	<0.2	1	<0.5	0.2	4	700	4
17-LM-1835	2	<1	<0.2	<0.2	1	<0.5	0.3	1.6	851	3
17-LM-1837	<2	<1	<0.2	<0.2	1	<0.5	0.4	1.1	580	3
17-LM-1860	<2	<1	<0.2	<0.2	<1	<0.5	<0.1	0.3	654	3
17-LM-1992	<2	<1	<0.2	<0.2	2	<0.5	0.5	0.9	440	3
17-LM-2000	3	<1	0.3	<0.2	5	<0.5	0.8	0.3	454	10
17-LM-2001	3	<1	<0.2	<0.2	4	<0.5	0.6	0.2	838	8
17-LM-2002	2	<1	<0.2	<0.2	2	<0.5	0.8	0.7	471	4
17-LM-2113	3	<1	<0.2	<0.2	2	<0.5	0.7	0.9	828	5
18-LM-2595	3	<1	<0.2	<0.2	<1	<0.5	<0.1	0.5	882	6
18-LM-2604	<2	<1	<0.2	<0.2	<1	<0.5	<0.1	0.4	504	5
18-LM-2744	<2	<1	<0.2	<0.2	1	<0.5	<0.1	0.2	181	4
18-LM-2809	2	<1	<0.2	<0.2	2	<0.5	0.2	0.2	664	7
18-LM-2997	<2	<1	<0.2	<0.2	2	<0.5	<0.1	0.5	228	4
18-LM-3042	<2	<1	<0.2	<0.2	1	<0.5	1.1	0.6	905	5
19-LM-3063	<2	<1	<0.2	<0.2	<1	<0.5	0.3	0.8	202	4
19-LM-3160	<2	<1	<0.2	<0.2	2	<0.5	0.1	0.2	572	6
19-LM-3210	<2	<1	<0.2	<0.2	<1	<0.5	0.3	0.4	198	4
Jurassic										
14-LM-1*	2	<1	<0.2	<0.2	2	—	0.4	3.3	1,010	6
14-LM-106	<2	<1	<0.2	<0.2	2	—	0.4	2.3	365	4
14-LM-154*	<2	<1	<0.2	<0.2	1	—	0.3	0.6	276	2
14-LM-468	<2	<1	<0.2	<0.2	1	—	<0.1	0.2	239	4
14-LM-479	<2	<1	<0.2	<0.2	1	—	0.1	1.1	345	2
14-LM-490*	<2	<1	<0.2	<0.2	2	—	0.2	1.7	782	5
15-LM-806	4	<1	<0.2	<0.2	2	—	0.3	0.2	665	2
15-LM-810	<2	<1	0.2	<0.2	2	<0.5	0.6	0.3	304	2
17-LM-1385	<2	<1	<0.2	<0.2	2	<0.5	0.6	5.5	941	5
17-LM-1656	<2	<1	<0.2	<0.2	<1	<0.5	0.2	0.7	345	2
17-LM-1748	<2	<1	<0.2	<0.2	1	<0.5	0.1	1.7	613	5
17-LM-1749	<2	<1	0.2	<0.2	1	<0.5	0.3	1.9	1,120	7
17-LM-2112	<2	<1	<0.2	<0.2	4	<0.5	0.4	1.6	482	5
17-LM-2127	<2	<1	<0.2	<0.2	3	<0.5	0.6	1.8	719	9
17-LM-2128	<2	<1	<0.2	<0.2	4	<0.5	0.5	3.8	673	10
17-LM-2191	<2	<1	<0.2	<0.2	3	<0.5	0.5	3	1,290	7
17-LM-2203 (1)	<2	<1	<0.2	<0.2	2	<0.5	0.4	1.5	955	5
17-LM-2203 (2)	<2	<1	<0.2	<0.2	1	<0.5	0.4	1.7	877	5
18-LM-2594	<2	<1	<0.2	<0.2	1	<0.5	0.1	2.3	596	4
18-LM-2603	<2	<1	<0.2	<0.2	<1	<0.5	0.3	2.6	565	9
18-LM-2607	<2	<1	<0.2	<0.2	<1	<0.5	<0.1	2.3	614	4
18-LM-2725	<2	4	<0.2	<0.2	2	<0.5	0.1	3	795	10
18-LM-2756	<2	<1	<0.2	<0.2	<1	<0.5	0.5	0.5	215	2

*Indicates samples reported by Stone and others (2019).

Table 54. ICP-AES-MS (inductively coupled plasma atomic emission spectroscopy-mass spectrometry) geochemical analyses of tantalum, tungsten, thallium, lead, bismuth, thorium, uranium, lanthanum, cerium, and praseodymium in samples included in this report.

[Numerical values are in parts per million. Ta, tantalum; W, tungsten; Tl, thallium; Pb, lead; Bi, bismuth; Th, thorium; U, uranium; La, lanthanum; Ce, cerium; Pr, praseodymium; —, not measured. Two separate analyses were obtained for sample 17-LM-2203.]

Sample	Ta	W	Tl	Pb	Bi	Th	U	La	Ce	Pr
Permian-Triassic										
14-LM-16	<0.5	2	<0.5	<5	<0.1	1.1	0.48	17.4	35.3	4.62
14-LM-43*	0.7	2	<0.5	5	<0.1	5.2	1.95	21	44.9	5.69
15-LM-802A	0.5	<1	0.7	6	<0.1	5.5	1.9	20.2	43	5.5
15-LM-816	1.2	<1	0.8	8	<0.1	6.6	2.17	17	36.4	4.68
17-LM-1562	1	2	<0.5	<5	<0.1	7.7	2.04	19.3	42.7	6.07
17-LM-1688	0.6	<1	<0.5	<5	<0.1	2.6	0.89	21.9	50.9	6.66
17-LM-1771	1	<1	<0.5	5	<0.1	10.8	3.89	27.9	56.7	6.48
17-LM-1779	0.6	<1	<0.5	6	<0.1	9.4	2.07	20.4	46	5.48
17-LM-1792	1	<1	<0.5	6	<0.1	13.6	3.64	28.8	64.7	7.61
17-LM-1835	0.8	<1	<0.5	6	<0.1	9.2	2.62	22.2	49.7	5.98
17-LM-1837	0.7	<1	<0.5	5	0.1	12.5	3.3	21.7	48	5.8
17-LM-1860	0.6	<1	<0.5	<5	<0.1	2.4	0.87	21.1	45.4	5.65
17-LM-1992	0.6	<1	<0.5	<5	<0.1	4.6	1.62	24.4	54.5	7.74
17-LM-2000	1.1	1	<0.5	7	0.2	10.4	4	33.8	79.7	10.2
17-LM-2001	0.6	4	<0.5	<5	<0.1	4.1	2.13	46.1	68.1	7.5
17-LM-2002	<0.5	<1	<0.5	<5	0.1	2.5	0.91	20.6	43.9	5.6
17-LM-2113	0.6	1	<0.5	7	0.1	9	3.7	28	56.3	7.35
18-LM-2595	<0.5	<1	<0.5	5	<0.1	3.9	1.47	22.6	47.9	6
18-LM-2604	<0.5	<1	<0.5	<5	<0.1	2.3	0.83	19.3	42.7	5.42
18-LM-2744	<0.5	<1	1.3	<5	<0.1	6.5	1.46	15.9	35.9	4.58
18-LM-2809	1	<1	1.5	<5	0.2	11.3	3.64	32	71.7	9.29
18-LM-2997	<0.5	<1	1.5	<5	<0.1	4.5	1.56	14.8	31.9	4.19
18-LM-3042	1.1	3	1.1	<5	<0.1	6.8	2.08	20.9	45.5	5.7
19-LM-3063	<0.5	<1	<0.5	16	<0.1	5.7	1.54	17.8	38.8	5.12
19-LM-3160	1.1	<1	<0.5	<5	<0.1	8.2	2.31	21.4	45	5.46
19-LM-3210	<0.5	<1	<0.5	9	<0.1	6.2	2.51	19	40.2	4.92
Jurassic										
14-LM-1*	0.9	2	<0.5	11	<0.1	10.4	2.85	38.4	73.5	8.31
14-LM-106	<0.5	1	<0.5	<5	<0.1	1.9	0.79	11.9	27.2	3.76
14-LM-154*	<0.5	<1	<0.5	5	<0.1	1.1	0.39	10.7	24.4	3.34
14-LM-468	0.7	<1	<0.5	5	<0.1	1.6	0.57	19.4	55.7	8.47
14-LM-479	<0.5	<1	<0.5	<5	<0.1	2.9	0.76	12	26.3	3.52
14-LM-490*	0.5	<1	<0.5	10	<0.1	4.2	1.66	23.6	47.2	5.77
15-LM-806	<0.5	<1	<0.5	8	<0.1	1	0.3	20.2	41.3	5.36
15-LM-810	<0.5	1	<0.5	<5	<0.1	2.2	0.8	10.4	26.3	4.04
17-LM-1385	2	<1	1.1	34	<0.1	28.5	3.92	36.5	63.1	6.94
17-LM-1656	<0.5	<1	<0.5	<5	<0.1	2	0.73	9	20.5	2.95
17-LM-1748	0.6	<1	<0.5	10	<0.1	5.2	1.59	24.9	50.1	6.94
17-LM-1749	0.7	<1	<0.5	11	<0.1	4.3	1.59	28	56.8	7.92
17-LM-2112	<0.5	<1	<0.5	7	0.3	3.2	1.38	20.8	48	6.55
17-LM-2127	<0.5	<1	<0.5	8	<0.1	5.1	1.79	30.2	68.8	10.5
17-LM-2128	<0.5	1	<0.5	8	0.2	5.3	2.01	34.8	73.2	10.6
17-LM-2191	1	1	0.7	17	<0.1	14.2	2.92	46.2	85.2	10.4
17-LM-2203 (1)	<0.5	<1	<0.5	9	<0.1	5.6	1.25	16.7	35.4	4.95
17-LM-2203 (2)	<0.5	<1	<0.5	7	<0.1	8.1	0.99	20.4	40.3	4.82
18-LM-2594	2.2	<1	<0.5	6	<0.1	4.4	0.89	24.8	55	7.25
18-LM-2603	<0.5	<1	<0.5	5	<0.1	3.1	0.95	19.5	44.1	6.05
18-LM-2607	<0.5	<1	<0.5	<5	<0.1	3	1.07	19.5	44.8	6.25
18-LM-2725	<0.5	<1	<0.5	6	<0.1	3.3	1.13	28.7	67.6	9.31
18-LM-2756	<0.5	<1	1.5	<5	<0.1	4.5	1.89	7.9	16.5	2.26

*Indicates samples reported by Stone and others (2019).

Table 55. ICP-AES-MS (inductively coupled plasma atomic emission spectroscopy-mass spectrometry) geochemical analyses of neodymium, samarium, europium, gadolinium, terbium, dysprosium, holmium, erbium, thulium, ytterbium, and lutetium in samples included in this report.

[Numerical values are in parts per million. Nd, neodymium; Sm, samarium; Eu, europium; Gd, gadolinium; Tb, terbium; Dy, dysprosium; Ho, holmium; Er, erbium; Tm, thulium; Yb, ytterbium; Lu, lutetium; —, not measured. Two separate analyses were obtained for sample 17-LM-2203.]

Sample	Nd	Sm	Eu	Gd	Tb	Dy	Ho	Er	Tm	Yb	Lu
Permian-Triassic											
14-LM-16	20	4.6	1.39	4.91	0.74	4.57	0.96	2.71	0.38	2.6	0.41
14-LM-43*	23.4	4.9	1.17	4.78	0.7	4.18	0.88	2.51	0.37	2.3	0.37
15-LM-802A	22.1	4.8	1.33	4.75	0.7	4.15	0.86	2.62	0.4	2.6	0.42
15-LM-816	18.5	4.2	1.18	3.96	0.61	3.7	0.76	2.22	0.35	2.3	0.35
17-LM-1562	25.7	6.1	1.58	6.36	1.02	6.6	1.36	4.09	0.58	3.9	0.57
17-LM-1688	27.9	5.8	1.54	5.63	0.81	4.93	0.99	3.09	0.45	3	0.4
17-LM-1771	26.1	5.1	1.34	5.23	0.7	4.33	0.81	2.54	0.36	2.6	0.36
17-LM-1779	23.3	4.8	1.32	5.19	0.77	4.58	0.91	2.85	0.39	2.9	0.46
17-LM-1792	30.9	6.7	1.45	6.5	0.89	5.66	1.09	3.57	0.52	3.7	0.55
17-LM-1835	24.8	5.4	1.43	5.2	0.77	4.6	0.92	2.93	0.41	2.8	0.45
17-LM-1837	24.2	5.5	1.44	5.34	0.77	4.52	1.01	2.88	0.41	2.9	0.43
17-LM-1860	25.5	6	1.87	6.03	0.86	5.49	1.06	3.16	0.44	2.9	0.44
17-LM-1992	34.5	8.5	2.22	9.27	1.47	8.31	1.69	4.79	0.67	4.4	0.63
17-LM-2000	41.7	8.9	2.32	9.8	1.48	8.69	1.83	5.21	0.81	5.5	0.83
17-LM-2001	30.4	6.4	1.63	6.88	1.08	6.12	1.29	3.9	0.56	3.8	0.59
17-LM-2002	23	5.3	1.45	5.7	0.9	5.36	1.11	3.25	0.49	3.2	0.48
17-LM-2113	29.6	6.2	1.43	6.03	0.89	4.95	1.01	3	0.44	3.1	0.47
18-LM-2595	23.4	4.8	1.16	5.41	0.79	4.75	1.02	2.89	0.42	2.9	0.45
18-LM-2604	21.9	4.6	1.26	5.49	0.77	4.75	0.97	2.84	0.41	2.7	0.43
18-LM-2744	18.1	3.9	1.07	3.93	0.61	3.76	0.77	2.33	0.35	2.4	0.37
18-LM-2809	35.2	7.7	1.74	7.57	1.17	7.24	1.5	4.48	0.69	4.5	0.68
18-LM-2997	17.4	4.1	1.26	4.24	0.66	4.37	0.93	2.73	0.4	2.7	0.41
18-LM-3042	22.3	5	1.47	5.08	0.81	5.16	1.07	3.13	0.5	3.2	0.49
19-LM-3063	21.2	4.6	1.39	5.01	0.82	4.7	0.97	2.86	0.4	2.6	0.41
19-LM-3160	21.9	5	1.18	4.92	0.77	4.67	0.99	3.05	0.47	3.2	0.52
19-LM-3210	19.1	3.7	1.02	3.78	0.63	3.55	0.79	2.14	0.35	2.4	0.39
Jurassic											
14-LM-1*	28.8	5.2	1.11	4.6	0.69	4.09	0.84	2.46	0.38	2.5	0.38
14-LM-106	16.3	3.8	1.04	3.85	0.56	3.37	0.68	1.93	0.27	1.8	0.28
14-LM-154*	14.5	3.4	1.2	3.56	0.53	3.17	0.65	1.84	0.26	1.6	0.23
14-LM-468	37	8.7	1.82	8.62	1.4	8.61	1.79	5.11	0.76	4.8	0.68
14-LM-479	15.1	3.3	0.96	3.3	0.51	3.12	0.65	1.95	0.26	1.8	0.28
14-LM-490*	23.5	4.7	1.41	4.57	0.7	4.05	0.86	2.48	0.38	2.6	0.38
15-LM-806	22.7	5.1	1.41	5.15	0.73	4.37	0.9	2.66	0.37	2.4	0.38
15-LM-810	18.6	5.1	1.7	5.44	0.86	5.21	1.06	3.18	0.46	3	0.46
17-LM-1385	23.1	4.3	0.67	3.68	0.63	3.82	0.79	2.47	0.39	2.8	0.45
17-LM-1656	12.3	3	1.09	3.15	0.49	2.97	0.57	1.74	0.25	1.6	0.25
17-LM-1748	27.4	5.8	1.64	5.63	0.78	4.89	0.96	2.8	0.39	2.5	0.39
17-LM-1749	31.1	6.5	1.96	5.94	0.91	5.35	1.05	3.01	0.4	2.6	0.41
17-LM-2112	27.9	5.9	1.52	6.13	0.91	5.03	1	2.93	0.44	2.9	0.45
17-LM-2127	44.7	10.6	2.28	10.1	1.52	8.56	1.67	4.86	0.67	4.1	0.61
17-LM-2128	44.5	9.7	2.34	9.27	1.41	7.86	1.59	4.74	0.69	4.4	0.65
17-LM-2191	35.8	6.1	1.54	5.31	0.81	4.15	0.88	2.69	0.41	3	0.45
17-LM-2203 (1)	19.5	4	1.12	3.67	0.54	2.87	0.56	1.78	0.28	2	0.3
17-LM-2203 (2)	18.6	3.1	0.91	3.16	0.43	2.27	0.43	1.41	0.21	1.5	0.25
18-LM-2594	30.7	6.8	1.53	7.27	1.06	6.21	1.28	3.51	0.51	3.4	0.48
18-LM-2603	26.3	5.9	1.61	6.28	0.9	5.53	1.12	3.18	0.45	3	0.44
18-LM-2607	27.7	6.6	1.6	6.93	1.02	6.04	1.17	3.43	0.48	2.9	0.44
18-LM-2725	38.5	8.5	1.95	9.03	1.28	7.63	1.57	4.34	0.62	4	0.6
18-LM-2756	9.3	2.4	0.81	2.51	0.4	2.37	0.46	1.4	0.21	1.4	0.2

*Indicates samples reported by Stone and others (2019).

Table 56. WDXRF (wavelength dispersive x-ray fluorescence) geochemical analyses of samples included in this report.

[Numerical values are in weight percent. O, oxygen; Si, silicon; Ti, titanium; Al, aluminum; Mg, magnesium; Fe, iron; Mn, manganese; Ca, calcium; K, potassium; Na, sodium; P, phosphorus; Cr, chromium; V, vanadium; Sr, strontium; Ba, barium;, LOI, loss on ignition; —, not measured. Two separate analyses were obtained for sample 17-LM-2203.]

Sample	SiO_2	TiO_2	Al_2O_3	MgO	Fe_2O_3	MnO	CaO	K_2O	Na_2O	P_2O_5	Cr_2O_3	V_2O_3	SrO	BaO	LOI
Permian-Triassic															
14-LM-16	55.1	1.07	19.1	3.15	5.48	0.04	8.82	0.23	5.56	0.35	<0.01	—	—	—	1.17
14-LM-43*	56.9	0.94	16.7	3.36	8.16	0.14	6.83	2.21	3.46	0.3	0.01	—	—	—	0.676
15-LM-802A	58.5	0.87	17.1	3.18	7.74	0.15	6.63	2.21	3.68	0.27	<0.01	0.04	0.06	0.08	0.54
15-LM-816	58	0.81	17	3.11	7.34	0.14	6.91	2.33	3.58	0.23	<0.01	0.04	0.07	0.08	1.78
17-LM-1562	63.5	1.01	15.8	2.77	3.85	0.03	5.69	0.5	6.12	0.26	<0.01	0.04	0.05	0.06	0.88
17-LM-1688	56.8	0.94	18.1	2.81	6.22	0.06	6.46	0.79	5.68	0.25	<0.01	0.03	0.07	0.06	0.87
17-LM-1771	57.9	1.05	16.2	3.6	7.59	0.16	6.33	2.67	3.51	0.31	<0.01	0.04	0.05	0.08	0.91
17-LM-1779	57.3	0.89	16.6	3.71	7.1	0.16	7.28	1.9	3.49	0.3	<0.01	0.03	0.06	0.08	0.74
17-LM-1792	59.6	0.97	15.6	3.09	6.85	0.14	5.98	2.87	3.26	0.33	<0.01	0.04	0.04	0.07	0.7
17-LM-1835	56.7	0.99	15.8	4.03	8.14	0.16	7.01	2.7	3.11	0.31	<0.01	0.04	0.06	0.1	0.78
17-LM-1837	56.3	0.99	16	4.14	8.3	0.17	7.38	1.96	3.19	0.33	<0.01	0.04	0.05	0.06	0.84
17-LM-1860	54.9	1.08	18.5	3.38	6.74	0.13	8.28	0.93	4.75	0.39	<0.01	0.04	0.09	0.08	0.94
17-LM-1992	52.9	1.55	16.8	4.63	9.46	0.15	7.93	1.27	4.78	0.48	<0.01	0.05	0.07	0.06	0.99
17-LM-2000	58.6	1.29	16.6	3.45	5.87	0.08	6.37	0.79	6.75	0.39	<0.01	0.04	0.05	0.06	0.62
17-LM-2001	61.3	1.06	15.9	2.74	5.63	0.12	5.42	1.08	5.86	0.34	<0.01	0.03	0.05	0.09	0.6
17-LM-2002	53.3	1.34	16.4	4.39	9.42	0.13	7.97	0.83	4.69	0.47	<0.01	0.05	0.06	0.05	0.89
17-LM-2113	57.2	1.12	15.8	3.59	7.66	0.15	6.71	2.57	3.31	0.33	<0.01	0.04	0.05	0.09	1.56
18-LM-2595	63.1	0.82	16.4	1.87	5.32	0.09	4.46	2.26	4.59	0.23	<0.01	0.03	0.04	0.09	0.54
18-LM-2604	58.6	0.87	17	3.01	7	0.09	6.14	0.82	5.46	0.26	<0.01	0.04	0.06	0.06	0.44
18-LM-2744	62.6	0.64	16.9	3.26	3.08	0.05	5.8	0.46	6.74	0.28	<0.01	0.03	0.05	0.02	0.98
18-LM-2809	64	0.8	16.6	1.88	2.38	0.05	6.37	1.17	5.53	0.22	<0.01	0.02	0.04	0.08	0.92
18-LM-2997	57.6	0.94	16.8	3.61	8	0.05	6.79	0.36	5.18	0.18	<0.01	0.04	0.05	0.03	0.71
18-LM-3042	63.7	0.74	16.3	1.92	4.83	0.07	4.52	2.12	5.01	0.2	<0.01	0.02	0.04	0.1	1.13
19-LM-3063	57.7	0.9	18.6	3.41	5.34	0.11	5.67	0.67	6.67	0.3	<0.01	0.03	0.1	0.02	0.6
19-LM-3160	61.4	0.85	16.9	2.45	5.45	0.05	5.49	1.23	5.8	0.25	<0.01	0.03	0.06	0.07	0.54
19-LM-3210	64.8	0.55	16.5	2.92	2.22	0.05	4.68	1.31	6.84	0.2	<0.01	0.02	0.04	0.02	0.35
Jurassic															
14-LM-1*	66.8	0.56	15.7	1.33	3.92	0.06	3.3	3.42	3.72	0.16	<0.01	—	—	—	0.891
14-LM-106	51.3	0.84	15.8	7.59	9.43	0.14	10.2	1.2	1.83	0.13	0.01	—	—	—	1.16
14-LM-154*	49.5	1.05	18.7	6.98	7.42	0.11	11.9	0.6	2.54	0.22	0.05	—	—	—	1.94
14-LM-468	59.7	0.85	18.4	2.91	2.53	0.04	7.97	0.31	6.88	0.17	<0.01	—	—	—	0.545

Table 56.—Continued

Sample	SiO_2	TiO_2	Al_2O_3	MgO	Fe_2O_3	MnO	CaO	K_2O	Na_2O	P_2O_5	Cr_2O_3	V_2O_3	SrO	BaO	LOI
14-LM-479	52	0.68	17.4	6.14	9.26	0.16	9.87	0.97	2.44	0.09	0.02	—	—	—	1.04
14-LM-490*	61.1	0.81	17.1	2.41	6.49	0.12	5.65	2.03	4.04	0.24	0.05	—	—	—	0.755
15-LM-806	55.9	0.99	20.7	3.09	4.2	0.07	8.87	0.56	5.41	0.38	<0.01	—	—	—	0.837
15-LM-810	50.8	1.3	15	5.86	11.9	0.25	9.5	0.66	2.59	0.17	<0.01	0.07	0.06	0.03	1.61
17-LM-1385	71.9	0.15	15.2	0.28	1.21	0.03	1.02	5.45	3.74	0.07	<0.01	<0.01	0.02	0.12	0.91
17-LM-1656	52.3	0.8	18.9	4.55	8.9	0.16	9.68	0.69	3.16	0.16	0.01	0.06	0.08	0.04	0.67
17-LM-1748	57.4	1.09	17.3	3.13	7.71	0.13	6.41	1.73	3.83	0.32	<0.01	0.03	0.06	0.07	0.47
17-LM-1749	57.6	0.98	17.7	2.8	7.15	0.15	5.91	1.77	4.15	0.28	<0.01	0.03	0.06	0.13	0.59
17-LM-2112	52.3	1.06	19.3	4.55	6.84	0.15	9.37	1.29	3.31	0.26	<0.01	0.03	0.07	0.06	1.28
17-LM-2127	55.4	1.11	19.2	2.65	6.91	0.13	7.17	1.43	4.26	0.4	<0.01	0.02	0.08	0.09	0.86
17-LM-2128	55.6	1.11	18.2	2.93	7.37	0.14	6.96	1.43	4.14	0.41	<0.01	0.03	0.08	0.07	0.74
17-LM-2191	68.7	0.39	16.1	0.74	2.42	0.05	2.82	3.65	4.2	0.14	<0.01	<0.01	0.05	0.15	0.53
17-LM-2203 (1)	68	0.41	16.2	1.18	2.97	0.05	3.55	1.59	4.48	0.28	<0.01	<0.01	0.03	0.1	1.07
17-LM-2203 (2)	67.4	0.48	15.4	1.39	3.93	0.07	3.22	1.71	3.85	0.18	<0.01	0.02	0.04	0.1	1.06
18-LM-2594	56.2	1.17	16.4	3.4	10.2	0.17	6.79	1.48	3.56	0.27	<0.01	0.05	0.05	0.07	0.71
18-LM-2603	53.2	0.98	19.3	3.14	8.58	0.14	7.65	1.26	3.78	0.35	<0.01	0.03	0.09	0.07	0.5
18-LM-2607	53.2	1.06	19.3	3.43	8.8	0.16	7.84	1.29	3.79	0.34	<0.01	0.03	0.08	0.07	0.71
18-LM-2725	54.6	1.05	19.3	2.94	7.91	0.13	7.28	1.3	4.22	0.33	<0.01	0.03	0.08	0.1	0.73
18-LM-2756	51.6	0.65	18.7	4.97	8.35	0.14	10.4	0.62	2.82	0.12	<0.01	0.06	0.07	0.02	1.49

* Indicates samples reported by Stone and others (2019)

Table 57. Normalized (volatile-free) wavelength dispersive x-ray fluorescence data for samples included in this report.

[Numerical values are in normalized weight percent. O, oxygen; Si, silicon; Ti, titanium; Al, aluminum; Mg, magnesium; Fe, iron; Mn, manganese; Ca, calcium; K, potassium; Na, sodium; P, phosphorus. Two separate analyses were obtained for sample 17-LM-2203. The oxides Cr_2O_3, V_2O_5, SrO, and BaO were excluded from the normalization.]

Sample	SiO_2	TiO_2	Al_2O_3	MgO	Fe_2O_3	MnO	CaO	K_2O	Na_2O	P_2O_5	Total	K_2O+Na_2O
Permian–Triassic												
14-LM-16	55.7	1.08	19.3	3.19	5.54	0.04	8.92	0.23	5.62	0.35	100	5.85
14-LM-43*	57.5	0.95	16.9	3.39	8.24	0.14	6.90	2.23	3.49	0.30	100	5.72
15-LM-802A	58.3	0.87	17.0	3.17	7.71	0.15	6.61	2.20	3.67	0.27	100	5.87
15-LM-816	58.3	0.81	17.1	3.13	7.38	0.14	6.95	2.34	3.60	0.23	100	5.94
17-LM-1562	63.8	1.01	15.9	2.78	3.87	0.03	5.72	0.50	6.15	0.26	100	6.65
17-LM-1688	57.9	0.96	18.4	2.86	6.34	0.06	6.58	0.81	5.79	0.25	100	6.6
17-LM-1771	58.3	1.06	16.3	3.62	7.64	0.16	6.37	2.69	3.53	0.31	100	6.22
17-LM-1779	58.0	0.90	16.8	3.76	7.19	0.16	7.37	1.92	3.53	0.30	100	5.45
17-LM-1792	60.4	0.98	15.8	3.13	6.94	0.14	6.06	2.91	3.30	0.33	100	6.21
17-LM-1835	57.3	1.00	16.0	4.07	8.23	0.16	7.08	2.73	3.14	0.31	100	5.87
17-LM-1837	57.0	1.00	16.2	4.19	8.40	0.17	7.47	1.98	3.23	0.33	100	5.21
17-LM-1860	55.4	1.09	18.7	3.41	6.80	0.13	8.36	0.94	4.79	0.39	100	5.73
17-LM-1992	52.9	1.55	16.8	4.63	9.46	0.15	7.93	1.27	4.78	0.48	100	6.05
17-LM-2000	58.5	1.29	16.6	3.44	5.86	0.08	6.36	0.79	6.74	0.39	100	7.53
17-LM-2001	61.6	1.07	16.0	2.76	5.66	0.12	5.45	1.09	5.89	0.34	100	6.98
17-LM-2002	53.9	1.35	16.6	4.44	9.52	0.13	8.06	0.84	4.74	0.48	100	5.58
17-LM-2113	58.1	1.14	16.1	3.65	7.78	0.15	6.82	2.61	3.36	0.34	100	5.97
18-LM-2595	63.6	0.83	16.5	1.89	5.37	0.09	4.50	2.28	4.63	0.23	100	6.91
18-LM-2604	59.0	0.88	17.1	3.03	7.05	0.09	6.19	0.83	5.50	0.26	100	6.33
18-LM-2744	62.7	0.64	16.9	3.27	3.09	0.05	5.81	0.46	6.75	0.28	100	7.21
18-LM-2809	64.6	0.81	16.8	1.90	2.40	0.05	6.43	1.18	5.59	0.22	100	6.77
18-LM-2997	57.9	0.94	16.9	3.63	8.04	0.05	6.82	0.36	5.21	0.18	100	5.57
18-LM-3042	64.1	0.74	16.4	1.93	4.86	0.07	4.55	2.13	5.04	0.20	100	7.17
19-LM-3063	58.1	0.91	18.7	3.43	5.37	0.11	5.71	0.67	6.71	0.30	100	7.38
19-LM-3160	61.5	0.85	16.9	2.45	5.46	0.05	5.50	1.23	5.81	0.25	100	7.04
19-LM-3210	64.8	0.55	16.5	2.92	2.22	0.05	4.68	1.31	6.84	0.20	100	8.15
Jurassic												
14-LM-1*	67.5	0.57	15.9	1.34	3.96	0.06	3.33	3.46	3.76	0.16	100	7.21
14-LM-106	52.1	0.85	16.0	7.71	9.58	0.14	10.36	1.22	1.86	0.13	100	3.08
14-LM-154*	50.0	1.06	18.9	7.05	7.49	0.11	12.02	0.61	2.57	0.22	100	3.18
14-LM-468	59.8	0.85	18.4	2.92	2.54	0.04	7.99	0.31	6.90	0.17	100	7.21
14-LM-479	52.5	0.69	17.6	6.20	9.35	0.16	9.97	0.98	2.46	0.09	100	3.44
14-LM-490*	61.1	0.81	17.1	2.41	6.49	0.12	5.65	2.03	4.04	0.24	100	6.07
15-LM-806	55.8	0.99	20.7	3.08	4.19	0.07	8.85	0.56	5.40	0.38	100	5.96
15-LM-810	51.8	1.33	15.3	5.98	12.14	0.26	9.69	0.67	2.64	0.17	100	3.31
17-LM-1385	72.6	0.15	15.3	0.28	1.22	0.03	1.03	5.50	3.78	0.07	100	9.28
17-LM-1656	52.7	0.81	19.0	4.58	8.96	0.16	9.75	0.69	3.18	0.16	100	3.87
17-LM-1748	58.0	1.10	17.5	3.16	7.78	0.13	6.47	1.75	3.87	0.32	100	5.62
17-LM-1749	58.5	1.00	18.0	2.84	7.26	0.15	6.00	1.80	4.21	0.28	100	6.01
17-LM-2112	53.1	1.08	19.6	4.62	6.95	0.15	9.52	1.31	3.36	0.26	100	4.67
17-LM-2127	56.2	1.13	19.5	2.69	7.00	0.13	7.27	1.45	4.32	0.41	100	5.77
17-LM-2128	56.6	1.13	18.5	2.98	7.50	0.14	7.08	1.45	4.21	0.42	100	5.66
17-LM-2191	69.2	0.39	16.2	0.75	2.44	0.05	2.84	3.68	4.23	0.14	100	7.91
17-LM-2203 (1)	68.9	0.42	16.4	1.20	3.01	0.05	3.60	1.61	4.54	0.28	100	6.51
17-LM-2203 (2)	69.0	0.49	15.8	1.42	4.03	0.07	3.30	1.75	3.94	0.18	100	5.69
18-LM-2594	56.4	1.17	16.5	3.41	10.24	0.17	6.81	1.49	3.57	0.27	100	5.06
18-LM-2603	54.1	1.00	19.6	3.19	8.72	0.14	7.78	1.28	3.84	0.36	100	5.12
18-LM-2607	53.6	1.07	19.5	3.46	8.87	0.16	7.90	1.30	3.82	0.34	100	5.12
18-LM-2725	55.1	1.06	19.5	2.97	7.99	0.13	7.35	1.31	4.26	0.33	100	5.57
18-LM-2756	52.5	0.66	19.0	5.05	8.49	0.14	10.57	0.63	2.87	0.12	100	3.5

* Indicates samples reported by Stone and others (2019)

Table 58. Whole-rock rubidium-strontium isotopic data for 13 samples analyzed for this report and 4 samples reported by Stone and others (2019).

[Ma, mega-annum; ppm, part per million, Sr_i, calculated initial $^{87}Sr/^{86}Sr$ ratio]

Sample	Age (Ma)	Rb(ppm)	Sr(ppm)	$^{87}Sr/^{86}Sr$	$^{87}Rb/^{86}Sr$	Sr_i
14-LM-1*	151	110	370	0.70772	0.86016	0.70590
14-LM-43*	253	65	634	0.70501	0.29655	0.70396
14-LM-106	151	38.9	581	0.70531	0.19367	0.70490
14-LM-154*	146	16.8	485	0.70573	0.10020	0.70553
14-LM-490*	149	56	480	0.70581	0.33748	0.70511
17-LM-1385	151	242	189	0.71278	3.70643	0.70495
17-LM-1562	245	8.3	472	0.70504	0.05086	0.70487
17-LM-1656	151	18.3	687	0.70487	0.07705	0.70471
17-LM-1688	242	12.6	635	0.70470	0.05739	0.70450
17-LM-1749	151	55.6	607	0.70638	0.26498	0.70582
17-LM-1779	248	46.9	588	0.70446	0.23070	0.70366
17-LM-1992	252	37.7	584	0.70462	0.18672	0.70396
17-LM-2191	149	111	384	0.70900	0.83644	0.70725
18-LM-2603	145	37.6	799	0.70527	0.13612	0.70500
19-LM-3063	248	20.5	846	0.70535	0.07009	0.70511
19-LM-3160	243	14.6	485	0.70481	0.08707	0.70451
19-LM-3210	246	25.9	324	0.70592	0.23134	0.70512

*Indicates samples reported by Stone and others (2019).

Moffett Field Publishing Service Center, California
Manuscript approved September 17, 2021
Edited by Mitchell Phillips
Layout by Cory Hurd

USGS

Stone and others—Geochronologic, Isotopic, and Geochemical Data from Pre-Cretaceous Plutonic Rocks in the Lane Mountain Area, California—Open-File Report 2021–1094

ISSN 2331-1238 (online)
https://doi.org/10.3133/ofr20211094